

**NATURAL RUBBER COMPOSITES FROM
AGRICULTURAL WASTE**



Preeyaporn Injorhor

**A Thesis Submitted in Partial Fulfillment of the Requirements for the
Degree of Master of Engineering in Materials Engineering**

Suranaree University of Technology

Academic Year 2019

วัสดุเชิงประกอบยางธรรมชาติจากวัสดุเหลือทิ้งทางการเกษตร



นางสาวปรียาภรณ์ อินทร์จ่อหอ

วิทยานิพนธ์นี้เป็นส่วนหนึ่งของการศึกษาตามหลักสูตรปริญญาวิศวกรรมศาสตรมหาบัณฑิต

สาขาวิชาวิศวกรรมวัสดุ

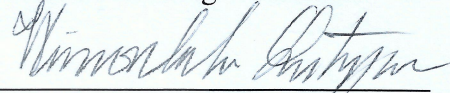
มหาวิทยาลัยเทคโนโลยีสุรนารี

ปีการศึกษา 2562

**NATURAL RUBBER COMPOSITES FROM
AGRICULTURAL WASTE**

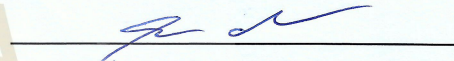
Suranaree University of Technology has approved this thesis submitted in partial fulfillment of the requirements for a Master's Degree.

Thesis Examining Committee



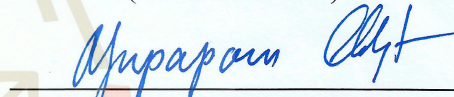
(Assoc. Prof. Dr. Wimonlak Sutapun)

Chairperson



(Assoc. Prof. Dr. Chaiwat Ruksakulpiwat)

Member (Thesis Advisor)



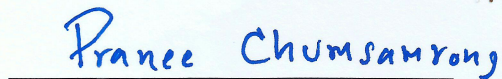
(Assoc. Prof. Dr. Yupaporn Ruksakulpiwat)

Member (Thesis Co-Advisor)



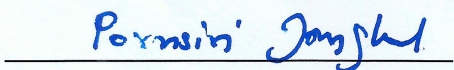
(Assoc. Prof. Dr. Sittipong Amnuaypanich)

Member



(Asst. Prof. Dr. Pranee Chumsamrong)

Member



(Assoc. Prof. Flt.Lt. Dr. Kontorn Chamniprasart) (Assoc. Prof. Dr. Pornsiri Jongkol)

Vice Rector for Academic Affairs
and Internationalization

Dean of Institute of Engineering

ปริยากรณ์ อินทร์จ้อหอ : วัสดุเชิงประกอบยางธรรมชาติจากวัสดุเหลือทิ้งทางการเกษตร
(NATURAL RUBBER COMPOSITES FROM AGRICULTURAL WASTE)

อาจารย์ที่ปรึกษา : รองศาสตราจารย์ ดร.ไชยวัฒน์ รักสกุลพิวัฒน์

อาจารย์ที่ปรึกษาร่วม : รองศาสตราจารย์ ดร.ยุพาพร รักสกุลพิวัฒน์, 90 หน้า.

สำหรับการศึกษานี้ แกลบข้าวและเปลือกกุ้งซึ่งเป็นวัสดุเหลือทิ้งทางการเกษตรถูกนำมาผ่านกระบวนการเพื่อใช้เป็นสารตัวเติมและสารตัวเติมลูกผสมในวัสดุเชิงประกอบยางธรรมชาติ สำหรับแกลบข้าวถูกเตรียมให้อยู่ในรูปสารละลายโซเดียมซิลิเกต โดยผ่านการชะล้างด้วยกรดเพื่อกำจัดออกไซด์ของโลหะร่วมกับการเผาที่อุณหภูมิ 650 องศาเซลเซียสจนกลายเป็นเถ้าแกลบที่มีองค์ประกอบหลักเป็นซิลิกาในรูปอสัณฐานที่มีความบริสุทธิ์สูงร้อยละ 86.12 แล้วจึงนำมาสกัดด้วยโซเดียมไฮดรอกไซด์ ส่วนเปลือกกุ้งถูกเตรียมให้อยู่ในรูปของโคลโคซานที่สามารถละลายได้ในสารละลายกรด โดยผ่านกระบวนการกำจัดแร่ธาตุด้วยกรด ตามด้วยกระบวนการกำจัดโปรตีนด้วยสารละลายด่าง ในขั้นนี้จะได้ผลิตภัณฑ์ที่เรียกว่า โคลดิน แล้วจึงกำจัดหมู่อะซิทิลด้วยสารละลายด่าง ความเข้มข้นสูงจนกลายเป็นโคลโคซานที่มีระดับการกำจัดหมู่อะซิทิลเท่ากับร้อยละ 65 และมีน้ำหนักโมเลกุลเฉลี่ย 642,000 ดาลตัน สารตัวเติมทั้ง 2 ชนิด ถูกนำมาเตรียมร่วมกับน้ำยางชั้นในรูปแบบของสารละลาย แล้วระเหยน้ำออกด้วยความร้อน ก่อนนำมาผสมกับสารเคมีสำหรับคงรูปร่างด้วยเครื่องผสม 2 ลูกกลิ้ง แล้วขึ้นรูปเป็นแผ่นด้วยเครื่องกดอัดที่ความร้อน 150 องศาเซลเซียส

โดยในขั้นต้น สารตัวเติมทั้ง 2 ชนิด ถูกนำมาเตรียมเป็นวัสดุลูกผสมในอัตราส่วนซิลิกาต่อโคลโคซานเป็น 1:1, 2:1, และ 3:1 เพื่อศึกษาสมบัติและความเหมาะสมที่จะสามารถใช้เป็นสารตัวเติมลูกผสมในวัสดุเชิงประกอบยางธรรมชาติ จากผลการศึกษาพบว่าที่อัตราส่วน 2:1 เหมาะสมที่สุดที่จะถูกนำมาใช้เป็นสารตัวเติม เนื่องจากเป็นอัตราส่วนที่ทำให้ได้วัสดุที่มีพื้นที่ผิวมากที่สุด เท่ากับ 441 ตารางเมตรต่อกรัม และมีขนาดอนุภาคเฉลี่ย 14 นาโนเมตร

ในงานวิจัยนี้ยังได้ศึกษา ผลของปริมาณอิน-ซิฟูซิลิกาต่อสมบัติการคงรูป สมบัติทางกล และสัณฐานวิทยาของวัสดุเชิงประกอบระหว่างซิลิกากับยางธรรมชาติ จากผลการศึกษาเมื่อเทียบกับยางธรรมชาติที่ปราศจากสารตัวเติมพบว่า ค่ามอดุลัสที่ร้อยละ 100 และร้อยละ 300 ของการยืด และค่าความแข็งของวัสดุเชิงประกอบยางธรรมชาติเพิ่มขึ้น เมื่อเพิ่มปริมาณอิน-ซิฟูซิลิกา ในขณะที่ค่าร้อยละของการยืดก่อนขาดลดลง เมื่อมีการเติมซิลิกา ค่าความต้านทานต่อแรงดึง และความต้านทานการฉีกขาดเพิ่มขึ้น เมื่อเพิ่มปริมาณอิน-ซิฟูซิลิกาถึง 10 ส่วนต่อเนื้อยาง 100 ส่วนโดยน้ำหนัก

แต่อย่างไรก็ตามตามวัสดุเชิงประกอบที่มีปริมาณสารตัวเติม 20 ส่วนต่อเนื้อยาง 100 ส่วนโดยน้ำหนัก แม้จะมีสมบัติที่ดีกว่าที่ปริมาณ 5 และ 10 ส่วนต่อเนื้อยาง 100 ส่วนโดยน้ำหนัก แต่ยังคงแสดงสมบัติทางกลที่เหนือกว่ายางธรรมชาติที่ปราศจากสารตัวเติมดังกล่าว การเติมอิน-ซิฟู

PREEYAPORN INJORHOR : NATURAL RUBBER COMPOSITES FROM
AGRICULTURAL WASTE. THESIS ADVISOR : ASSOC. PROF. CHAIWAT
RUKSAKULPIWAT, Ph.D. CO-THESIS ADVISOR : ASSOC. PROF.
YUPAPORN RUKSAKULPIWAT, Ph.D. 90 PP.

RICE HUSK/ RICE HUSK SILICA ASH/ SHRIMP SHELL WASTE /CHITOSAN/
NATURAL RUBBER COMPOSITES/ IN-SITU SILICA/ HYBRID FILLER/SOL-GEL/
CURE CHARACTERISTICS/ MECHANICAL PROPERTIES/ ANTIMICROBIAL
ACTIVITY.

In this study, agricultural wastes including rice husk (RH) and shrimp shells were prepared for use as a hybrid filler in natural rubber (NR) composites. RH was synthesized into rice husk ash (RHA) by acid leaching and burning at 650°C. The obtained RHA was 86.12% of silica (SiO₂) with amorphous structure. Then it was extracted by sodium hydroxide (NaOH) to obtain sodium silicate (Na₂SiO₃). Na₂SiO₃ was used as SiO₂ precursor. In addition, the shrimp shells were extracted into chitosan (CS) by removal of minerals, proteins, and acetyl groups. The obtained CS was 65% of degree of acetylation and average molecular weight was 642,000 Da.

The hybrid fillers between SiO₂ and CS at the ratios of 1:1, 2:1, and 3:1 were prepared and investigated. The optimum ratio between SiO₂ and CS was 2:1 which gave the material with the highest BET surface area and the smallest average particle size.

To study the effect of *in situ* SiO₂ content on cure characteristics, mechanical properties, and morphological properties of *in situ* SiO₂/NR composites and *in situ* SiO₂-CS/NR composites., NR composites with *in situ* SiO₂ at contents of 0, 5, 10, and 20 phr and NR composites with *in situ* SiO₂-CS at 5-5, 10-5, and 20-5 phr were prepared

by latex solution and sol-gel method. Then, it was compounded by using a two-roll mill and formed a sheet by compression molding at temperature of 150°C.

Modulus at 100% elongation (M100), Modulus at 300% elongation (M300), and hardness were increased with increasing *in situ* SiO₂ content while elongation at break of *in situ* SiO₂/NR composites and *in situ* SiO₂-CS/NR composites was decreased by the addition of *in situ* SiO₂. Tensile strength and tear strength increased with increasing *in situ* SiO₂ content up to 10 phr for *in situ* SiO₂-CS, up to 5 and 10 phr, respectively. However, the composites with *in situ* SiO₂ content at 20 phr without CS exhibits higher tensile strength, tear strength, and hardness than NR. The scorch time and cure time of *in situ* SiO₂/NR composites and *in situ* SiO₂-CS/NR composites were decreased by the addition of *in situ* SiO₂. Scanning Electron Microscope (SEM) micrographs of *in situ* SiO₂/NR composites and *in situ* SiO₂-CS/NR composites showed rough surface and many layers. The agglomerate of SiO₂ particles was observed from *in situ* SiO₂/NR composites at 5 phr only.

Effect of SiO₂-CS hybrid filler at CS contents of 0, 3, 5 and 10 phr with constant of 10 phr *in situ* SiO₂ on the antimicrobial activity and absorption properties of *in situ* SiO₂-CS/NR composites were investigated. All of the NR composites with the addition of CS show clear zone of *E. coli* inhibition. The optimum CS content was 5 phr which gave NR composite with the highest antimicrobial efficacy. The addition of CS can improve the water absorption of NR composites.

School of Polymer Engineering

Academic Year 2019

Student's Signature Preyaporn Injorhor

Advisor's Signature [Signature]

Co-Advisor's Signature [Signature]

ACKNOWLEDGEMENTS

I gratefully acknowledge Suranaree University of Technology and Center of Excellence on Petrochemical and Materials Technology for their financial support.

I would like to express my deep gratitude to my thesis advisor and co-advisor, Assoc. Prof. Dr. Chaiwat Ruksakulpiwat and Assoc. Prof. Dr. Yupaporn Ruksakulpiwat, for their guidance, enthusiastic encouragement, and useful critiques of this research work. I am also grateful to Assoc. Prof. Dr. Sittipong Amnuaypanich, Assoc. Prof. Dr. Wimonlak Sutapun, and Asst. Prof. Dr. Pranee Chumsamrong for their valuable suggestion and guidance given as committee members.

In addition, my grateful thanks are also extended to Mr. Prakardsak Maogrood and members of the Medical Laboratory of Sirindhorn Hospital, Bangkok Medical Service Department for their help and suggestion in the bacteria analysis. I am grateful to Ms. Pornvenus Watada for her useful suggestion and support. I also thank all faculty, staff members, and friends of School of Polymer Engineering for their support and help.

Finally, I would like to especially thanks to my parents for their support and encouragement throughout my study at Suranaree University of Technology.

Preeyaporn Injorhor

TABLE OF CONTENTS

	Page
ABSTRACT(THAI).....	I
ABSTRACT (ENGLISH).....	III
ACKNOWLEDGEMENTS.....	V
TABLE OF CONTENTS.....	VI
LIST OF TABLES.....	X
LIST OF FIGURES.....	XI
SYMBOLS AND ABBREVIATIONS.....	XV
CHAPTER	
I INTRODUCTION.....	1
1.1 General background.....	1
1.2 Research objectives.....	3
1.3 Scope and limitation of the study.....	4
II LITERATURE REVIEW.....	6
2.1 Natural rubber (NR).....	6
2.2 Silica (SiO ₂).....	8
2.3 Rice Husk (RH).....	9
2.3.1 Composition of RH.....	9
2.3.2 Preparation of RH SiO ₂	9
2.4 Utilization of RHA and RH SiO ₂ in NR composites.....	13

TABLE OF CONTENTS (Continued)

	Page
2.5 Shrimp shells	15
2.5.1 Composition of shrimp shells	15
2.5.2 Shrimp shell chitosan preparation	16
2.6 Utilization of chitosan in NR composites.....	18
2.7 SiO ₂ -CS hybrid materials	19
III EXPERIMENTAL	23
3.1 Materials	23
3.2 Experimental.....	23
3.2.1 Preparation of RHA and sodium silicate (Na ₂ SiO ₃) solution.....	23
3.2.2 Characterization of RHA.....	24
3.2.3 Preparation of CS from shrimp shells	26
3.2.4 Characterization of CS from shrimp shells	27
3.2.5 Preparation of SiO ₂ -CS hybrid filler	29
3.2.6 Characterization of SiO ₂ -CS hybrid filler	29
3.2.7 Preparation of NR composites.....	30
3.2.8 Characterization of NR composites.....	32
3.2.9 Preparation of vulcanized NR composites.....	32
3.2.10 Characterization of vulcanized NR composites.....	34
IV RESULTS AND DISCUSSION	35
4.1 Characteristics of RHA.....	35

TABLE OF CONTENTS (Continued)

	Page
4.2 Characteristics of CS from shrimp shells	37
4.3 Characterization of SiO ₂ -CS hybrid filler	40
4.4 Effect of <i>in situ</i> SiO ₂ content on the properties of NR composites	46
4.4.1 The SiO ₂ content in <i>in situ</i> SiO ₂ /NR composites	46
4.4.2 Cure characteristics	47
4.4.3 Mechanical properties.....	51
4.4.4 Morphological properties	51
4.5 Effect of <i>in situ</i> SiO ₂ -CS hybrid filler at various SiO ₂ content on the properties of NR omposites	58
4.5.1 The SiO ₂ content in <i>in situ</i> SiO ₂ -CS/NR composites	58
4.5.2 Cure characteristics	59
4.5.3 Mechanical properties.....	63
4.5.4 Morphological properties	69
4.6 Effect of SiO ₂ -CS hybrid filler at various CS contents on the antimicrobial activity and absorption properties of <i>in situ</i> SiO ₂ -CS/NR composites	71
4.6.1 Antimicrobial activity.....	71
4.6.2 Absorption properties	73
V CONCLUSIONS	75
REFERENCES	77

TABLE OF CONTENTS (Continued)

	Page
APPENDIX A	84
BIOGRAPHY	90



LIST OF TABLES

Table	Page
2.1 SiO ₂ content of RHA was reported by various research works	10
3.1 The ratio of hybrid filler	29
3.2 Formulation of unvulcanized NR composites.....	31
3.3 Compounding formulations	33
4.1 Chemical composition of RHA.....	35
4.2 Chemical composition of CS	38
4.3 The surface characteristics of SiO ₂ -CS hybrid materials.....	45
4.4 Thermal decomposition temperatures of NR and <i>in situ</i> SiO ₂ /NR composites	47
4.5 Cure characteristics of NR and <i>in situ</i> SiO ₂ /NR composites	50
4.6 Mechanical properties of NR and <i>in situ</i> SiO ₂ /NR composites	56
4.7 Thermal decomposition temperatures of NR and <i>in situ</i> SiO ₂ -CS/NR composites	59
4.8 Cure characteristics of NR and <i>in situ</i> SiO ₂ -CS/NR composites.....	62
4.9 Mechanical properties of NR and <i>in situ</i> SiO ₂ -CS/NR composites.....	68
4.10 The diameter of inhibition zone of NR and NR composites.....	72

LIST OF FIGURES

Figure	Page
2.1	Structure of rubber particle.....6
2.2	Network of sulfur vulcanization..... 7
2.3	Formation of silanol groups on the silica surface.....8
2.4	Structure of rice grain..... 9
2.5	Common procedures for producing SiO ₂ from RH..... 11
2.6	Acid leaching-thermal treatment extraction of RH SiO ₂ 11
2.7	Composition of shrimp shells..... 16
2.8	Preparation process of shrimp shell chitosan..... 17
2.9	FT-IR of CS and hybrid materials. (a) CS, (b) TES, (c) CS/TES, (d) CS/TEOS, and (e) CS/TES-TEOS.....20
2.10	¹³ C NMR of CS and hybrid materials. (a) CS, (b) CS/TEOS, (c) CS/TES, and (d) CS/TES-TEOS.....20
2.11	The scheme of synthesis of CS-SiO ₂ composite.....21
2.12	The schematic presentation of in situ SiO ₂ enhanced PA/CS biodegradable films by hydrolysis of sodium metasilicate.....22
3.1	The process to produce sodium silicate solution from rice husk.....25
3.2	The process to produce CS solution from shrimp shells..... 28
4.1	The X-ray diffraction pattern of RHA.....36
4.2	The FTIR spectra of RHA.....37
4.3	SEM micrographs of (a) RHA and (b) SiO ₂ powder from RHA.....37

LIST OF FIGURES (Continued)

Figure	Page
4.4 The FTIR spectrum of chitin and CS.....	39
4.5 The X-ray diffraction pattern of CS.....	39
4.6 SEM micrographs of CS at (a)100 and (b) 1500 magnification.....	40
4.7 The FTIR spectrums of RHA, CS, and hybrid materials at various ratios.....	41
4.8 The X-ray diffraction pattern of RHA, CS, and hybrid materials at various ratios.....	42
4.9 FE-SEM images of the SiO ₂ -CS hybrid materials.....	43
4.10 EDX Spectra of the SiO ₂ -CS hybrid materials.....	44
4.11 The Brunauer-Emmett-Teller (BET) isotherm for the SiO ₂ -CS hybrid materials.....	45
4.12 TGA cure of NR and <i>in situ</i> SiO ₂ /NR composites at various SiO ₂ contents.....	46
4.13 Effect of <i>in situ</i> SiO ₂ content on maximum, minimum torque, and torque difference of <i>in situ</i> SiO ₂ /NR composites.....	49
4.14 Effect of <i>in situ</i> SiO ₂ content on cure time and scorch time of <i>in situ</i> SiO ₂ /NR composites.....	49
4.15 Effect of <i>in situ</i> SiO ₂ content on cure rate index of <i>in situ</i> SiO ₂ /NR composites.....	50
4.16 Stress-Strain curves of NR and <i>in situ</i> SiO ₂ /NR composites at various SiO ₂ contents.....	52

LIST OF FIGURES (Continued)

Figure	Page
4.17 Effect of <i>in situ</i> SiO ₂ content on tensile strength of <i>in situ</i> SiO ₂ /NR composites.....	53
4.18 Effect of <i>in situ</i> SiO ₂ content on elongation at break of <i>in situ</i> SiO ₂ /NR composites.....	53
4.19 Effect of <i>in situ</i> SiO ₂ content on M100 of <i>in situ</i> SiO ₂ /NR composites.....	54
4.20 Effect of <i>in situ</i> SiO ₂ content on M300 of <i>in situ</i> SiO ₂ /NR composites.....	54
4.21 Effect of <i>in situ</i> SiO ₂ content on tear strength of <i>in situ</i> SiO ₂ /NR composites.....	55
4.22 Effect of <i>in situ</i> SiO ₂ content on hardness of <i>in situ</i> SiO ₂ /NR composites.....	55
4.23 SEM micrographs of NR and <i>in situ</i> SiO ₂ NR composite fractured surface at 150 (left) and 1000 (right) magnification.....	57
4.24 TGA cure of NR and <i>in situ</i> SiO ₂ -CS/NR composites at various SiO ₂ contents.....	59
4.25 Effect of <i>in situ</i> SiO ₂ content on maimum, minimum torque, and torque difference of <i>in situ</i> SiO ₂ -CS/NR composites.....	61
4.26 Effect of <i>in situ</i> SiO ₂ content on cure time and scorch time of <i>in situ</i> SiO ₂ -CS/NR composites.....	61
4.27 Effect of <i>in situ</i> SiO ₂ content on CRI of <i>in situ</i> SiO ₂ -CS/NR composites.....	62

LIST OF FIGURES (Continued)

Figure	Page
4.28 Stress-Strain curves of NR and <i>in situ</i> SiO ₂ -CS/NR composites at various SiO ₂ contents.....	64
4.29 Effect of <i>in situ</i> SiO ₂ content on tensile strength of <i>in situ</i> SiO ₂ -CS/NR composites.....	64
4.30 Effect of <i>in situ</i> SiO ₂ content on elongation at break of <i>in situ</i> SiO ₂ -CS/NR composites.....	65
4.31 Effect of <i>in situ</i> SiO ₂ content on M100 of <i>in situ</i> SiO ₂ -CS/NR composites.....	65
4.32 Effect of <i>in situ</i> SiO ₂ content on M300 of <i>in situ</i> SiO ₂ -CS/NR composites.....	66
4.33 Effect of <i>in situ</i> SiO ₂ content on tear strength of <i>in situ</i> SiO ₂ -CS/NR composites.....	66
4.34 Effect of <i>in situ</i> SiO ₂ content on hardness of <i>in situ</i> SiO ₂ -CS/NR composites.....	67
4.35 SEM micrographs of NR and SEM micrographs and their EDX mapping of <i>in situ</i> SiO ₂ -CS/NR composites.....	70
4.36 Effect of CS content on antimicrobial activity of <i>in situ</i> SiO ₂ -CS/NR composite films.....	72
4.37 Effect of CS content on water absorption of NR composites.....	74
4.38 The FTIR spectrum of NR and the NR composites.....	74

SYMBOLS AND ABBREVIATIONS

%	=	Percent
N	=	Normality
M	=	Molarity
°C	=	Degree Celsius
K	=	Kelvin
Da	=	Dalton
DI	=	Deionized
min	=	Minute
g	=	Gram
ml	=	Milliliter
m ²	=	Square Meter
nm	=	Nanometer
phr	=	Parts per hundred of rubber
h	=	Hour(s)
kN	=	Kilonewtons
kV	=	Kilovolt
mA	=	Milliampere
rpm	=	Revolutions per minute
MPa	=	Megapascal
<i>in situ</i>	=	In the reaction mixture

CHAPTER I

INTRODUCTION

1.1 General background

Thailand is predominantly an agriculture-based country. More than half of Thai agricultural is occupied by crops related activities following by fishery cause the topography and climate which are significantly opportune to cultivation. Thailand is one of the top three rubber producers representing 75% of the global rubber output with approximately 33,000 million square meters is the rubber plantation area over the country especially the southern part of Thailand. Since the early 20th century, Thailand has become the largest exporter and producer of the world where is processing high quality rubber products such as tires, rubber gloves, and condoms (Thailand Convention and Exhibition Bureau, 2019).

Natural rubber (NR) or cis 1,4- polyisoprene is an elastomeric material derived from the sap of rubber tree also known as NR latex that contains the NR hydrocarbon in a fine emulsion form in an aqueous serum. It is an important economic crop that can be cultivated in every region of the country. NR is renewable materials which have the advantage such as low cost, flexibility, resistant to water, and use in a variety of application (Kawahara, 2018) (Thongpin et al., 2011).

However, the slowdown in the global economy causes the demand for NR and rubber prices to decrease. To increase demand and utilization of NR, NR composites has been developed various functions. Songsaeng et al., (2019) produced NR/reduced grapheneoxide composite materials which as a green sorbent material for the treatment

of oil spills. Chen and Qiu, (2020) developed the ultraviolet resistance and flame retardant properties of NR by reinforced with basic magnesium oxysulfate whiskers. Intom et al., (2020) developed NR/ Bi₂O₃ composites which as lead-free and flexible radiation shielding materials.

In addition to NR, rice is also Thailand's most important crop and the primary agricultural export. Thailand is one of the world's largest rice exporters. Consequently, the waste from rice cultivation occurred extremely in the country. Rice husk (RH) is the waste from rice milling process. It was used in several applications such as adsorbent for removing heavy metals from wastewater, biomass feedstock for bioethanol production, a coating over the molten metal in steel industries, and blended with cement as a replacement of silica fume (Kumar et al., 2013). Moreover, a product from RH burning process is rice husk ash (RHA) was used as silica (SiO₂) source that contained amorphous SiO₂ around 85-95% (Todkar et al., 2016). Preparation of RH SiO₂ has various methods namely thermal treatment, hydrothermal treatment, biological treatment, and chemical treatment (Shen, 2017). Yuvakkumar et al., (2012) prepared high-purity nano SiO₂ powder from RH by using a simple chemical method which is alkali extraction and followed by an acid precipitation. They obtained the high purity of SiO₂ around 99.9% at 2.5 N of sodium hydroxide in the alkali extraction process. A lot of research used RH SiO₂ as a reinforcement in polymer matrix. Moosa and Saddam, (2017) used RH SiO₂ in the form of nano-SiO₂ as a nanofiller in epoxy-SiO₂ nanocomposites. They found that the nano-SiO₂ can improve the tensile strength of epoxy resin. Jembere and Fanta, (2017) studied on the synthesis of SiO₂ powder from RHA as reinforcement filler in rubber tire tread part for replacement of commercial precipitated SiO₂. They found that the RH SiO₂ can be used as a replacement filler in

NR compound since the RH SiO_2 can enhance properties of modulus, hardness, and abrasion resistance.

In addition, the waste from fishery like shrimp shells, crab shells, and cuttlefish bones are the source of chitin. Chitin is the second widespread biopolymer available in nature after cellulose. The source of chitin namely crustaceans, insects, and microorganism. Chitosan (CS) is a carbohydrate polymer produced by the deacetylation of chitin. The properties of CS namely biocompatibility, biodegradability and antibacterial (Hajji et al., 2014). Moreover, (Rao and Johns, 2008) studied on the mechanical properties of CS and NR blend. They succeeded to prepare CS-NR latex blend by solution casting method and found that the obtained materials have a good adhesion between CS and NR thus, tensile strength of materials improved when compared with neat NR. The CS can be used as a reinforcement filler.

In this research work, SiO_2 from RH and CS from shrimp shells were used as hybrid filler in NR composites. The improvement of NR properties with this filler was expected.

1.2 Research objectives

To produce multifunctional NR composites that can be antimicrobial, eco-friendly, and more strength is my goal. NR composites were expected to use as a rubber wound dressing in medical applications.

Specific objectives of this research work are as follows:

- (1) To study physical and chemical properties of SiO_2 -CS hybrid material which is derived from RH and shrimp shells.
- (2) To study cure characteristics, mechanical properties, morphological properties of *in situ* SiO_2 /NR composites and *in situ* SiO_2 -CS/NR composites.

(3) To study the effect of *in situ* SiO₂ content on cure characteristics, mechanical properties, and morphological properties of *in situ* SiO₂/NR composites and *in situ* SiO₂-CS/NR composites.

(4) To study the effect of CS content on antimicrobial activity and absorption properties of *in situ* SiO₂-CS/NR composites.

1.3 Scope and limitation of the study

NR composites reinforced with *in situ* SiO₂ and *in situ* SiO₂-CS were prepared by a latex solution method. To prepare the hybrid material, the Na₂SiO₃ solution and CS solution were mixed with various ratios of 3:1, 2:1, and 1:1. The effect of *in situ* SiO₂ and *in situ* SiO₂-CS hybrid filler content on cure characteristics, mechanical properties, and morphological properties of NR composites were studied. *In situ* SiO₂/NR composites and *in situ* SiO₂-CS /NR composites were prepared at various *in situ* SiO₂ contents (0, 5, 10, and 20 phr). *In situ* SiO₂-CS /NR composites were added CS at 5 phr. Antimicrobial activity of *in situ* SiO₂-CS /NR composites at various CS contents 3, 5, and 10 phr with constant *in situ* SiO₂ at 10 phr were also studied. Sodium silicate (Na₂SiO₃) was used for *in situ* SiO₂ which was prepared by dissolving RHA with sodium hydroxide. The preparation of Na₂SiO₃ from RH was adapted from (Moosa and Saddam, 2017). CS from shrimp shells was prepared follow (El Knidri et al., 2016).

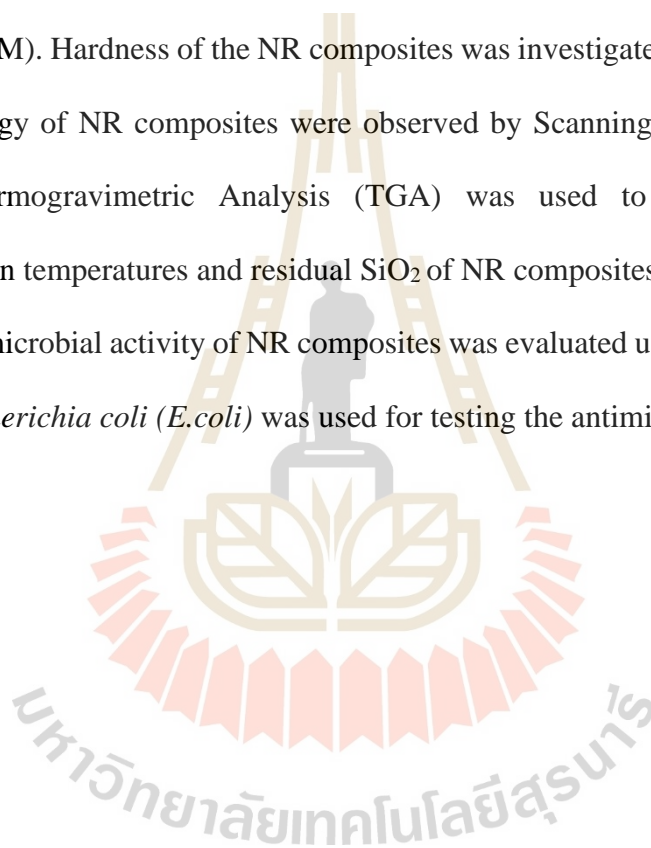
Fourier Transform Infrared Spectroscopy (FTIR) was used to confirm the functional groups of RHA and CS and also used to determine the degree of deacetylation of CS. X-ray Diffraction (XRD) was used to confirm the amorphous structure of RHA and also used to confirm characteristic peak of CS. Molecular weight of CS was measured by Zetasizer Nano ZS.

High ammonia NR latex (HA Latex) with 60% Dry Rubber Content (DRC) and

0.7% ammonia was used. NR and filler were mixed together before mixed with the vulcanizing chemicals by a two-roll mill. A conventional vulcanization system was used.

Mechanical properties of NR composites were investigated. Cure characteristics of NR composites were determined using a moving die rheometer (MDR). Tensile properties and tear properties of NR composites were investigated by a universal testing machine (UTM). Hardness of the NR composites was investigated by Durometer shore A. Morphology of NR composites were observed by Scanning Electron Microscope (SEM). Thermogravimetric Analysis (TGA) was used to obtain the thermal decomposition temperatures and residual SiO₂ of NR composites.

Antimicrobial activity of NR composites was evaluated using the agar diffusion method. *Escherichia coli* (*E.coli*) was used for testing the antimicrobial activity.



CHAPTER II

LITERATURE REVIEW

2.1 Natural rubber (NR)

Natural rubber is biopolymers extracted from the Para rubber (*Hevea brasiliensis*). It consists of the cis-1,4-polyisoprene molecule which composed carbon and hydrogen atoms. NR latex is a colloidal suspension which collected from the sap of rubber trees. Fresh NR latex is composed of 94% rubber hydrocarbon and 6% nonrubber constituents (*i.e.*, proteins, phospholipids, glycolipids, fatty acids) (Wei et al.,2017).

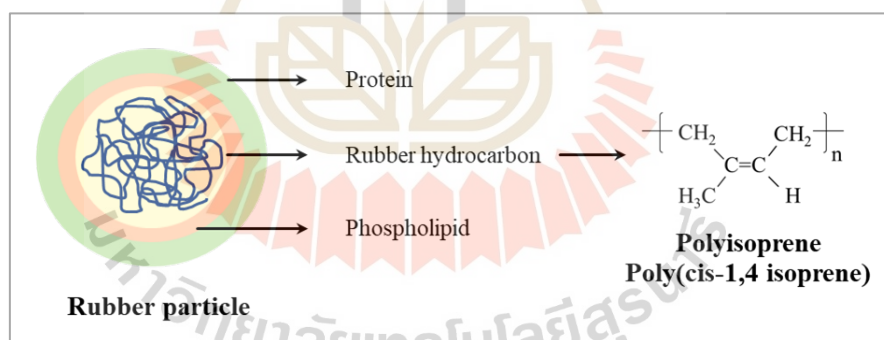


Figure 2.1 Structure of rubber particle.

NR has a variety of properties such as good elasticity and flexibility, biodegradability and renewability, good formability, and antivirus permeation. It has been used in a wide application: engineering, sports, and medical application as well. However, it also has disadvantages such as oxidative and thermal degradation.

Virgin NR is very soft and sticky. It requires vulcanization and any modification for its good properties like mechanical properties, thermal stability, and others (Chen et al.,2014).

Sulfur vulcanization is usually used for vulcanized NR. In the process, NR was compounded with activators, accelerators, fillers, and sulfur before it was shaped. It is also known as NR composites. The filler is an important ingredient which usually filled in the NR compound especially reinforcement fillers. Reinforcement filler is filled to improve tensile strength, tear strengths and abrasion resistance of the NR composites. The popular fillers such as carbon black (CB), silica (SiO_2), and calcium carbonate.

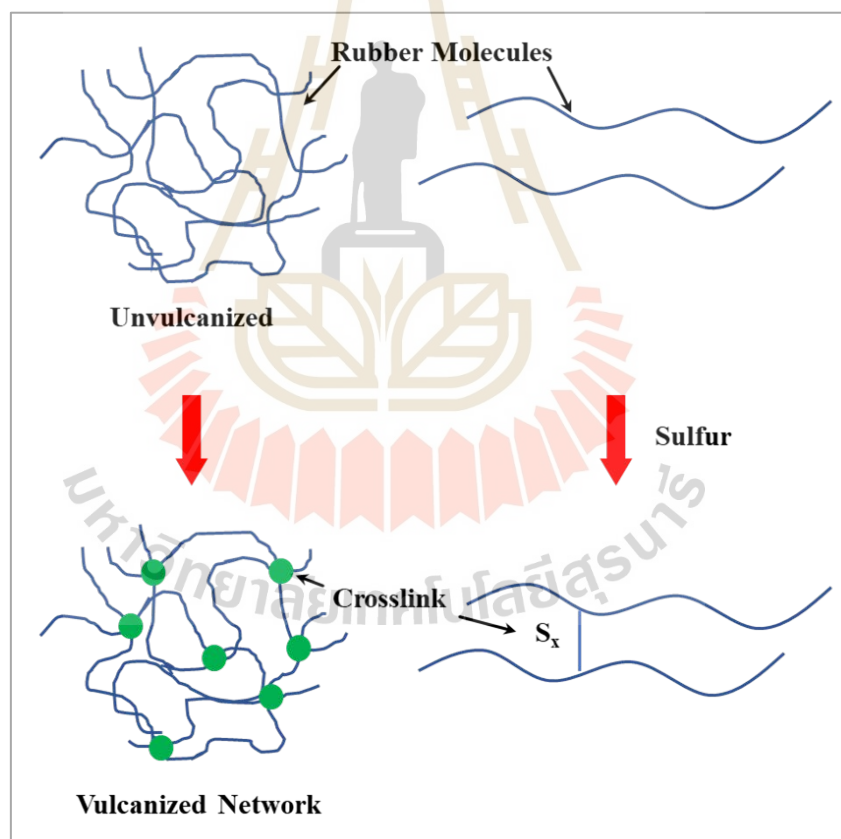


Figure 2.2 Network of sulfur vulcanization.

2.2 Silica (SiO₂)

Silica (SiO₂) is a white filler in amorphous form for use as a reinforcement in NR. It consists of silicon and oxygen in the tetrahedral structure which has silanol groups (Si-OH) on the silica surface. The formation of silanol groups on the SiO₂ surface shown in Figure 2.3. The number of silanol groups leads to high polarity and hydrophilic due to the formation of aggregates, agglomerates of SiO₂. Its hydrophilic affects the compatibility with the NR matrix leads to poor mechanical properties of NR composites. This is a problem to use SiO₂ with NR. Silane coupling agents were used to solve the problem that it can improve compatibility. However, the good distribution of SiO₂ in the NR matrix such as the use of nano-SiO₂ form or *in situ* SiO₂ form also solve this problem since it decreases the interaction between hydroxyl groups on the SiO₂ surface (Zhuralev, 2000).

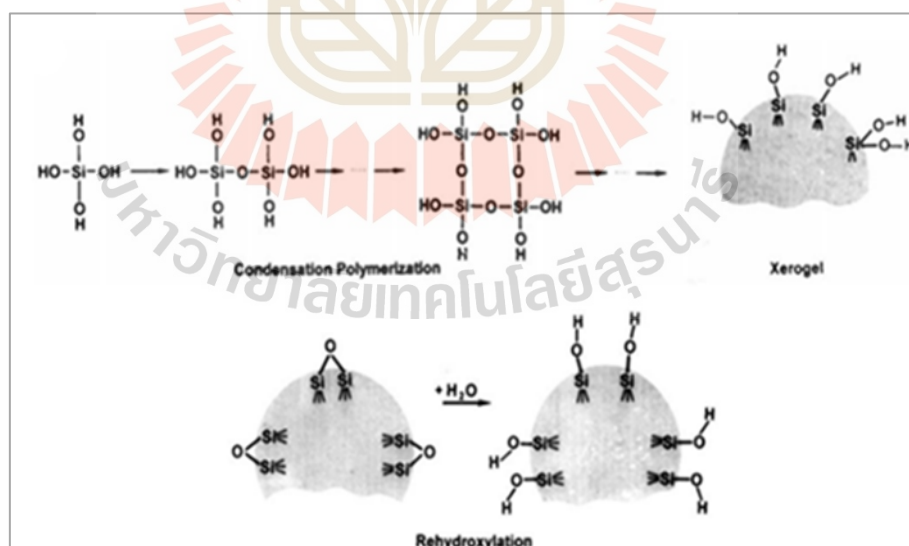


Figure 2.3 Formation of silanol groups on the silica surface (Zhuralev, 2000).

2.3 Rice Husk (RH)

2.3.1 Composition of RH

Rice husk (RH) is the hard-outer cover on rice grain which protects the rice grain from damage during the growing period. The structure of rice gain is shown in Figure 2.4. RH has about 20% of rice gain. The composition of RH consists of organic and inorganic constituents. The organic constituent (cellulose, hemicellulose, lignin, other protein, and vitamin) which can be removed by the burning process. The important inorganic component is silica (SiO_2) that has content more than 80% of the inorganic constituents (Oyelaran and Tuunwada, 2014).

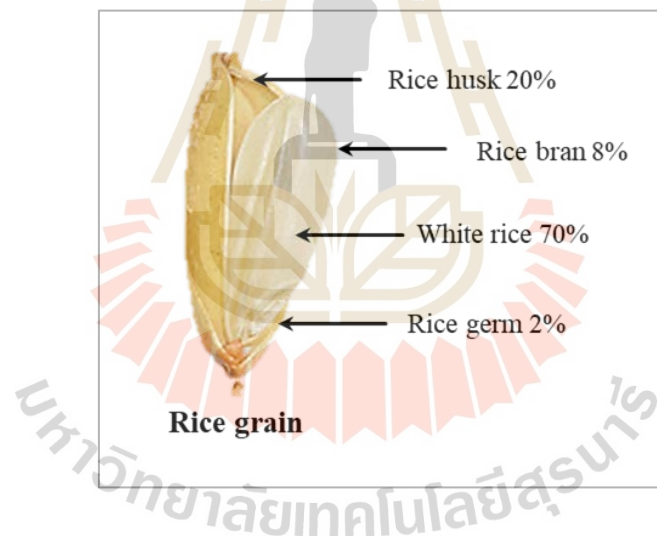


Figure 2.4 Structure of rice grain.

2.3.2 Preparation of RH SiO_2

Rice husk ash (RHA) is produced by burning RH at elevated temperatures. It will become amorphous SiO_2 at $550\text{-}800^\circ\text{C}$ and will become crystalline SiO_2 at a temperature greater than 800°C . Table 2.1 shows the SiO_2 content of RHA was reported by various research works.

Table 2.1 SiO₂ content of RHA was reported by various research works.

SiO ₂ Content (wt%)	References
93.4	Korotkova et al. (2016)
82.1	Raheem and Kareem (2017)
91.4	Rambo et al. (2011)
91.6	Alaneme and Olubambi (2013)
90.5	Todkar et al. (2016)

However, RH also has other elements and impurities thus before or after thermal processes. The impurities were eliminated by acid leaching or alkaline treatment. The common procedures for producing SiO₂ from RH in Figure 2.5.

Acid leaching, RH was treated by acid solution such as a solution of hydrochloric acid or sulfuric acid in Figure 2.6.

Alkaline treatment, RH was treated by a base solution like sodium hydroxide solution. The obtained SiO₂ with white-color SiO₂ and high specific surface area (Shen, 2017).

Liou, (2004) studied the effect of heating rate on the preparation of nano SiO₂ from RH. In his experiment, the RH was refluxed with HCl at 373 K for 1 h. The refluxed RH was dried at 373 K for 24 h before heated with various heating rates (*i.e.*, 5, 10, 15, and 20 K/min) at a temperature between 300 to 1000 K in the air atmosphere. The results found that the impurities about 95% were eliminated by thermal decomposition. The highest specific surface area of SiO₂ powder was 235 m²/g with 5.4 nm of the average pore diameter and the average particle size was 60 nm which gave from the heating rate of 5 K/min. All product which obtain from various heating rates

were amorphous structure. The slower heating rate can reduce metallic ingredients in RH better.

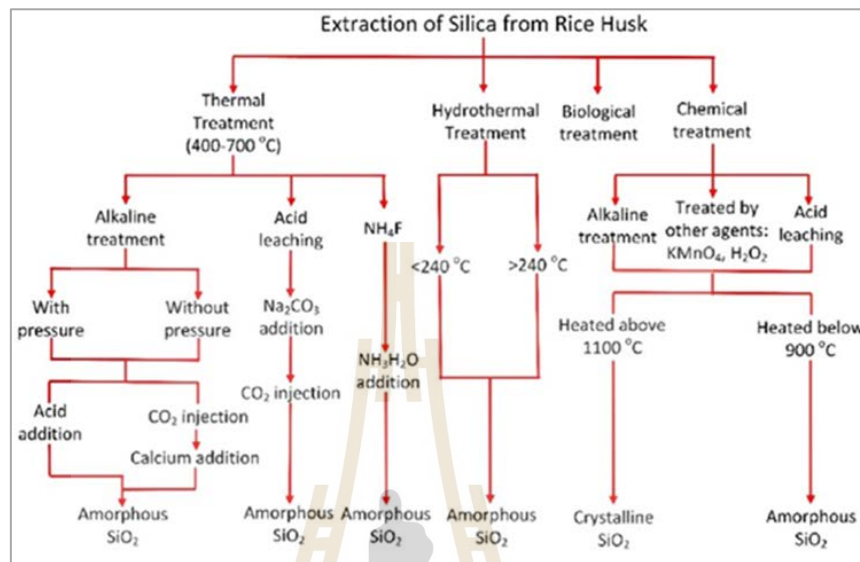


Figure 2.5 Common procedures for producing SiO_2 from RH (Shen, 2017).

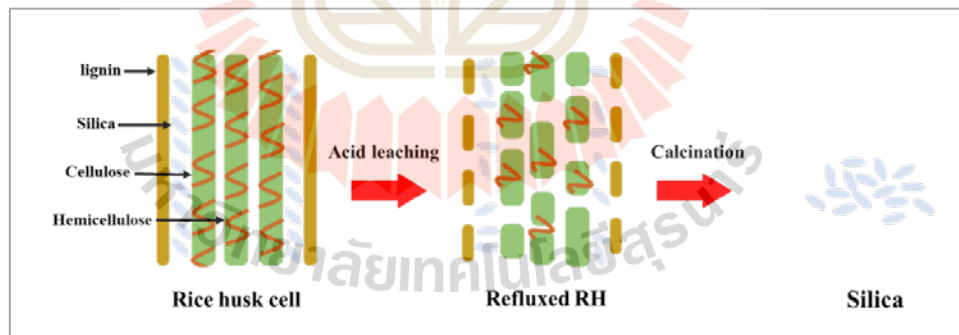


Figure 2.6 Acid leaching and thermal treatment extraction of RH SiO_2 (Salim et al., 2018).

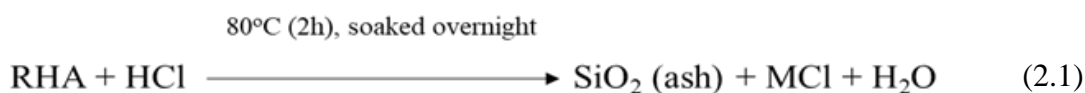
Afterward, Liou and Yang, (2011) prepared SiO_2 from RH and studied on the effect of acid types that use for precipitation. They produced silica from sodium silicate (Na_2SiO_3) and precipitated by different acid types, (*i.e.*, HCl , H_2SO_4 , $\text{C}_6\text{H}_8\text{O}_7$, and $\text{C}_2\text{H}_2\text{O}_4$). The results found that the highest specific surface area of SiO_2 was

636 m²/g with the average particle size was 5-30 nm which gave by using HCl.

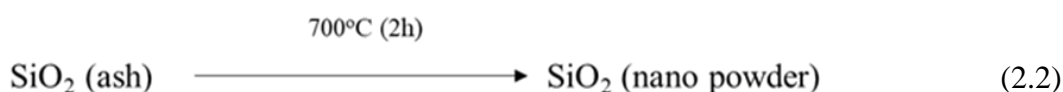
Yuvakkumar et al., (2012) prepared high purity nano SiO₂ powder from RH. They studied the effect of NaOH concentration on the purity of SiO₂ and investigated the optimum condition of alkali extraction. The RH was burned at 973 K for 3 h under inert atmosphere before refluxed with 6 N HCl for 1.5 h. The refluxed RH was boiled with various concentrations of NaOH (*i.e.*, 0.5, 1, 1.5, 2, and 2.5 N) until becoming Na₂SiO₃ solution. The precipitate was washed, filtered, and dried before sintered at 973 and 1373 K for 3 h. After that, the nano SiO₂ powder was obtained. The results found that the optimum concentration of NaOH is 2.5 N which gave the purity of 99.9 wt% with an average particle size of 25 nm and a high specific surface area of 274 m²/g.

Tuan et al., (2017) prepared and characterized nano SiO₂ from RHA by using the combination of chemical treatment and calcination. They presented two steps for synthesizing nano SiO₂ from RHA. The first step is acid treatment another is calcination at 700°C.

The chemical reaction can be shown as follows:



Where M :Na, K, Ca, Fe, Al, Mg,



The chemical composition, functional groups, crystallinity, and particle size of SiO₂ were determined by EDX, FT-IR, XRD, and DLS respectively. The results showed that the composition of nano SiO₂ has only silicon and oxygen which confirm the high purity. The functional groups showed the peaks of SiO₂ structure and hydroxyl of adsorbed water. The obtained nano SiO₂ was amorphous structure with the average diameter of about 45.5±7.2 nm.

2.4 Utilization of RHA and RH SiO₂ in NR composites

The preparation and characterization of NR composites with RH have been reported by several researchers, Da Costa, (2002) prepared NR composites filled RHA. The composites were incorporated by a two-roll mill and used a conventional system for curing. Cure characteristics were studied by using a Monsanto rheometer. They investigated the effect of RHA filled NR composites on mechanical and dynamic mechanical properties. In the experiment, white RHA (WRHA), black RHA (BRHA), carbon black (CB), and commercial SiO₂ were filled in NR for comparing their properties. The results showed that WRHA, BRHA, CB, and commercial SiO₂ filled NR composites gave similar results of the tear strengths and hardness when they were filled at low filler loading. For tensile strength, BRHA not efficient but WRHA still efficient, despite similar the particle size. However, WRHA can not substitute the commercial fillers due to its performance was not enough for use as reinforcing filler in case of dynamic mechanical improvement.

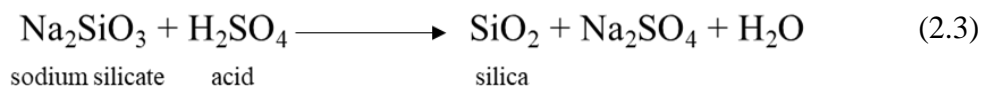
Similar work has been reported by Arayaprane, (2005). They studied the effect of RHA loading on cure characteristics and mechanical properties. RHA was filled in NR compound with various loadings (*i.e.*, 0, 10, 20, 30, and 40 phr) by using the internal mixer.

The results showed that the cure time decreases but Mooney viscosity increases when increasing of RHA loading. Tensile strength and tear strength of the composites decrease slightly with increasing RHA loading but the hardness increases slightly.

Dominic et al., (2013) synthesized nano-SiO₂ from rice husk for use as a reinforcement filler in NR composites. The rice husk nano-SiO₂ (RHNS) was synthesized by acid precipitation. Rice husks were prepared into WRHA by acid leaching followed by calcination. After that, WRHA was refluxed with NaOH. The resulting solution is a sodium silicate solution. RH SiO₂ gel was produced by acid precipitation. Then, the obtained gel was dried into xerogel and grounded to become RHNS. RHNS was filled in the NR compound by a two-roll mill. Commercial SiO₂ was also filled for comparison with RHNS. The results found that the particle size and surface area of RHNS were 10 nm and 252 m²/g, respectively. Both characteristics better than commercial SiO₂. The increasing of tensile strength, tear strength, abrasion resistance, and rebound resilience were given by the addition of RHNS.

During the process of rubber production, SiO₂ dust cause problems like air pollution, energy consumption, and machine abrasion. *In situ* SiO₂ formation in the rubber matrix was used to solve these problems. Suwandittakul et al., (2018) presented the preparation of *in situ* SiO₂ in NR latex by sol-gel of sodium silicate solution. They studied and compared the cure characteristics and mechanical properties of NR composites reinforced with *in situ* SiO₂ and *ex situ* SiO₂. The NR latex was filled *in situ* SiO₂ by the sol-gel reaction of sodium silicate which was precipitated turn to SiO₂ by acid solution.

The chemical reaction can be shown as follows:



The results found that the NR composites filled *in situ* SiO₂ not only solve the problem of SiO₂ dust but also the distribution of SiO₂ particles in NR matrix is better than *ex situ* SiO₂. However, the optimum cure time of *in situ* SiO₂ shorter than *ex situ* SiO₂ but similar mechanical properties.

2.5 Shrimp shells

2.5.1 Composition of shrimp shells

Shrimp shell is one of the crustacean shell wastes which composed three major constituents as chitin, protein, and calcium carbonate. Depending on the origins, seasons, ages, and other factors, the percentage of each constituent varies significantly. However, the structures remain similar.

Chitin is the linear amino-polysaccharide which consists of N-acetyl glucosamine units. It has a strong hydrogen bonding network therefore it is insoluble in organic and inorganic solvents. Nevertheless, chitosan is produced by the deacetylation of chitin which has multiple functional groups (hydroxyl and amino groups). The functional groups can take on a positive charge which gave solubility and antimicrobial properties.

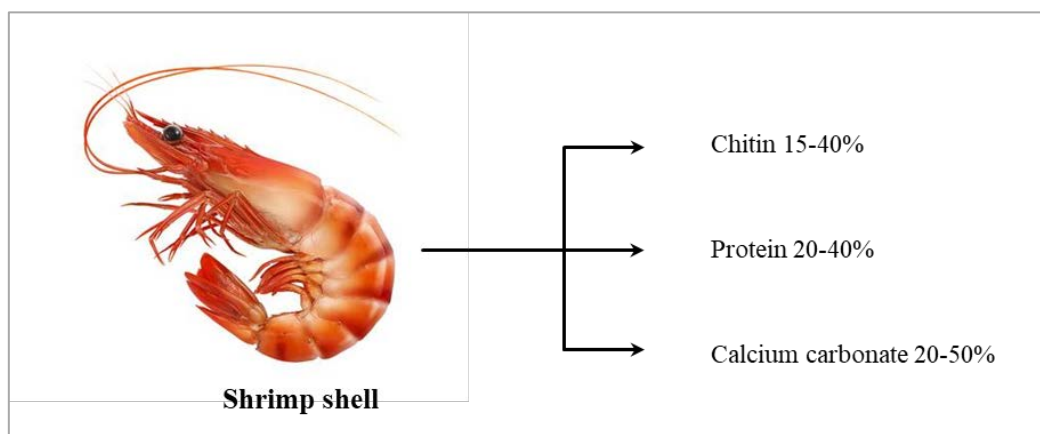


Figure 2.7 Composition of shrimp shells.

The degree of deacetylation (DD) and molecular weight (MW) are the important characteristics of chitosan. The DD indicates the presence of amino groups on the chitosan chains. %DD of chitosan is more than 50% but chitin is less than 50% (Knidri et al., 2018).

2.5.2 Shrimp shell chitosan preparation

Chitin and chitosan are prepared by using 2 processes of extraction which are chemical and biological methods. The biological method is an environmentally friendly method due to the treatments are carried out bacteria and enzymes but long processing time. On the other hand, the chemical method can reduce the processing time by using the acidic treatment and the alkali treatment with a high concentration. Despite the environmentally unfriendly but it is commonly used commercially (Knidri et al., 2018).

Many researchers prepared chitosan from shrimp shells using the chemical extraction method and the combination of two extraction methods which consist of three steps namely, demineralization, deproteinization, and deacetylation.

Hajji et al., (2014) prepared chitin and chitosan from three different sources (shrimp shells, crab shells, and fish bones). To demineralize, using 0.55 M of HCl at room temperature for 15-60 min depending on the source. Deproteinization was carried out using *B. mojavensis* A21 crude enzyme for 3 h and then become chitin. Chitosan was prepared by alkali treatment using 12.5 M of NaOH at 140°C for 4 h.

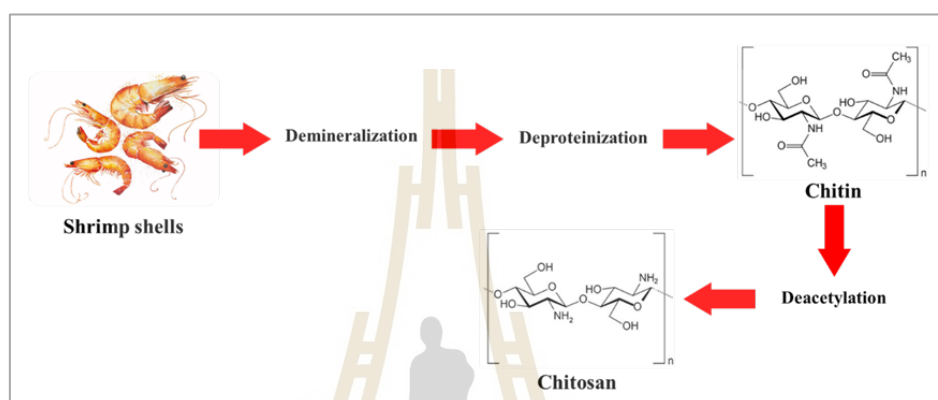


Figure 2.8 Preparation process of shrimp shell chitosan.

Islam et al., (2016) prepared chitin and chitosan from shrimp shell wastes. The shell was treated with 1.25 N of HCl for 3 h and overnight. Then, deproteinized by 5% NaOH (w/w) at 70-75°C for 1 h. Chitin was prepared into chitosan by using 40% NaOH at 100°C for 5-6 h.

To reduce the processing time of the chitosan extraction, (Knidri et al., 2016) extracted chitosan from shrimp shells via microwave irradiation. The demineralization was carried out with 3 M HCl for 8 min in the microwave oven at 500 W. The deproteinization, the remaining material was treated 10% NaOH for 5 min at 160 W, then 3 min at 350 W. The remaining is chitin. To deacetylated, chitin was treated with 50% NaOH for 8 min at 350 W. The final remaining is chitosan.

2.6 Utilization of chitosan in NR composites

Rao and John, (2008) prepared NR/CS blends with the various ratios of compositions *i.e.*, NR100/CS0, NR90/CS10, NR85/CS15, NR80/CS20, NR65/CS35, NR50/CS50, and NR90/CS10 (vulcanizate) by solution casting. They also investigated the effect of the ratio, crosslinking, and thermal aging on the mechanical properties of the blends. The results found that the optimum NR/CS ratio was 65/35 which gave the maximum tensile strength. Moreover, the aging of NR/CS blend at 55°C for 10 days increases the tensile strength of the blend due to crosslinking of the NR phase by thermal.

Ming-zhe et al., (2017) prepared the blends of NR/CS and investigated the effect of CS loading on the mechanical and antimicrobial properties of NR/CS blends. The blends were prepared by blending the CS microsphere suspension with NR latex. The antimicrobial properties were evaluated according to the Chinese standard QB/T 2591-2003. *Escherichia coli* (*E.coli*) bacteria was used for testing the antimicrobial efficacy. The results found that the mechanical properties and thermal stability of the blends were enhanced by taking CS microspheres. The hydrophobic NR was induced into hydrophilic material by blending with CS. The excellent antimicrobial properties were presented by using 10% w/w of CS microsphere in the blend.

Similar work has been reported by Boonrasri et al., (2018). They studied effect the of CS contents on antimicrobial properties of NR/CS composites. The NR/CS composites were prepared by the latex mixing method. The CS with various contents (*i.e.*, 0.0, 0.5, 1.0, 2.0, 4.0, and 8.0 phr) in suspension form were filled. The antimicrobial activity was tested using the agar diffusion method. The test was carried out by using *S.aureus* bacteria. The results found that at 300% modulus of

the composites was increased when CS contents increasing from 0.5-8.0 phr. but tensile strength and elongation at break were decreased. Adding CS has slightly enhanced the antimicrobial efficacy of the composites compared with unfilled CS.

2.7 SiO₂-CS hybrid materials

Due to this research work intend to prepare and characterize natural rubber composites reinforced with hybrid filler (silica-chitosan) which not sure that have been reported by other the researcher. However, several of the researchers reported the synthesis of silica-chitosan composites and silica-chitosan hybrid materials.

Yeh et al., (2007) have been reported the synthesis and properties of CS-SiO₂ hybrid materials. They studied the strength and thermal properties of tetrathoxysilane /vinylthoxysilane (TEOS-VTES) and CS in different ratios. TEOS and VTES are a precursor that produces SiO₂ via the sol-gel process and can form hybrid materials with CS with a hydrogen bond between the hydroxyl group of SiO₂ and the amino group of CS. The ratios of TEOS-VTES and CS (*i.e.*, 0/0/4, 0/0.8/4, 0.8/0.8/4, 0.8/1.6/4, 0.8/2.4/4, 0.8/3.2/4, 0.8/3.2/4, and 1.2/0/4). The results found that the formation of hydrogen bond between SiO₂ and CS was revealed from the results of FT-IR and NMR analysis which are shown in Figure.2.9 and Figure 2.10. The thermostability and mechanical properties of hybrid materials are better than pure CS and improved with increased TEOS content until the ratio of 0.8/1.6/4. However, when up to 0.8/2.4/4 the mechanical properties depend on VTES content. In the case of excessive TEOS, the mechanical performance deteriorates.

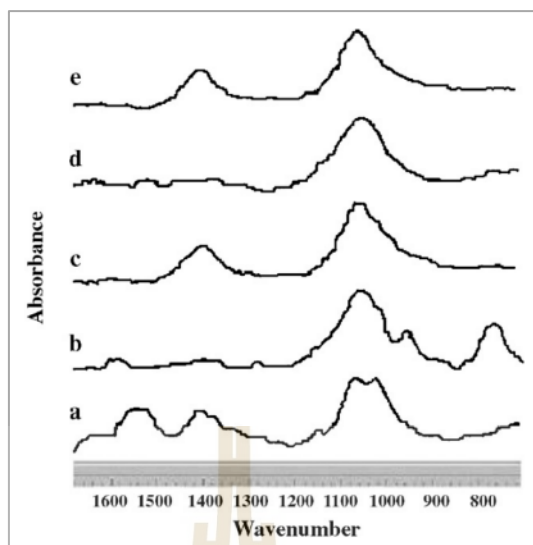


Figure 2.9 FT-IR of CS and hybrid materials. (a) CS, (b) VTES, (c) CS/VTES, (d) CS/TEOS, and (e) CS/VTES-TEOS.

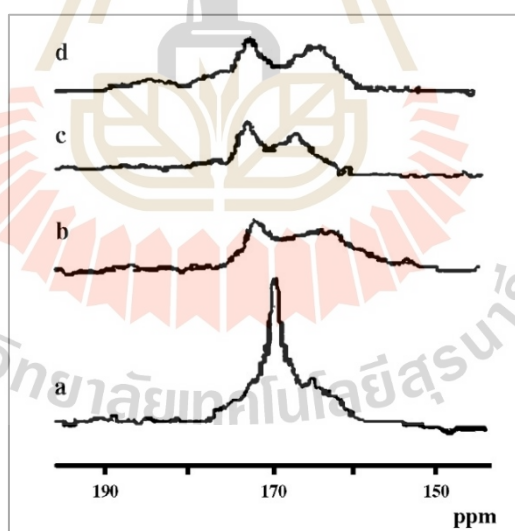


Figure 2.10 ¹³C NMR of CS and hybrid materials. (a) CS, (b) CS/TEOS, (c) CS/VTES, and (d) CS/VTES-TEOS.

Budnyak et al., (2015) studied the synthesis of adsorbent from CS-SiO₂ nanocomposites and investigated the properties. The scheme of synthesis of CS-SiO₂ composites in Figure 2.11. CS-SiO₂ nanocomposites were prepared by the sol-gel method via the hydrolysis TEOS in the CS solution. In the process of preparation, 1 g of *in situ* SiO₂ in the form of TEOS was added in 38-100 g of CS.

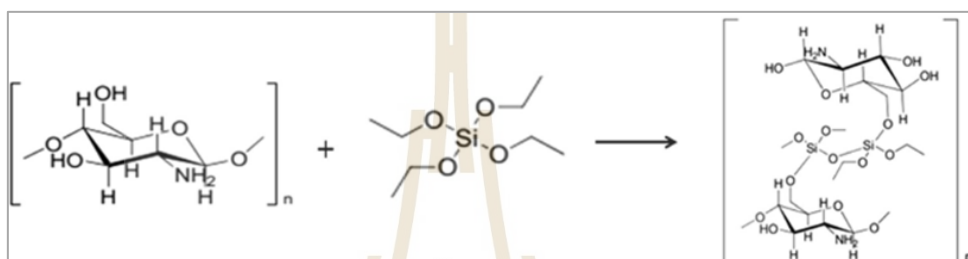


Figure 2.11 The scheme of synthesis of CS-SiO₂ composite (Tetyana et al., 2015).

The interactions between CS and SiO₂ were determined by using FT-IR spectroscopy. The results found that the composites show the peak of Si-O stretching vibrations and a shift of the peak of -NH₂ deformation vibrations. It represents the interactions between each other.

Furthermore, (Yu et al., 2018) studied the preparation of *in situ* SiO₂ with polyvinyl alcohol (PVA) and CS to improve mechanical properties for food packaging films. The *in situ* SiO₂ was used as a reinforcement in PVA-CS by hydrolysis of sodium metasilicate (Na₂SiO₃) under the acid condition. The schematic presentation of *in situ* SiO₂ enhanced PVA/CS biodegradable films is shown in Figure 2.12. The composite films were prepared with different weight ratios of PVA and CS (*i.e.*, PVA/CS=0/100, PVA/CS=20/80, (c) PVA/CS=40/60, PVA/CS=50/50, PVA/CS=60/40, PVA/CS=80/20, and PVA/CS=100/0. In addition, the content of *in situ* SiO₂ in PVA/CS biodegradable films

was 0, 0.3, 0.6 and 0.9 wt.%, respectively. The tensile strength of the composite with 0.6 wt% of *in situ* SiO₂ every ratio of PVA/CS as highest as 44.12 MPa due to improved hydrogen bonds between SiO₂ and CS or PVA.

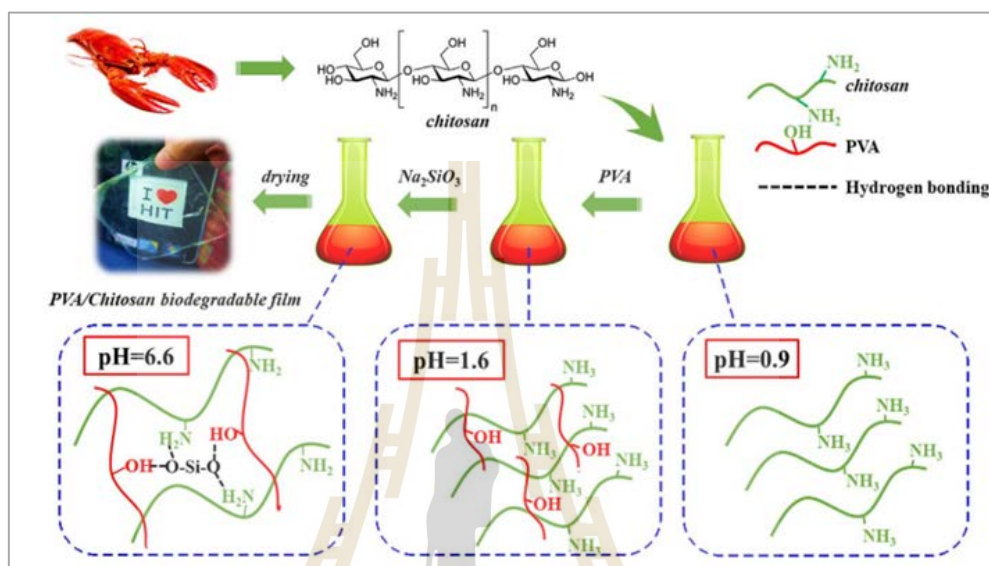


Figure 2.12 The schematic presentation of *in situ* SiO₂ enhanced PVA/CS biodegradable films by hydrolysis of sodium metasilicate (Yu et al., 2018).

Definition of hybrid material is “A hybrid material is a material that includes two moieties blended on the molecular scale.” (Kickelbick, 2007). In my work, the obtained hybrid materials were expected that the possible hydrogen bonding between inorganic (SiO₂) and organic (CS) species or electrostatic interactions. It can be concluded that the material from my work is a hybrid material according to this definition.

CHAPTER III

EXPERIMENTAL

3.1 Materials

High ammonia natural rubber latex (HA Latex) was purchased from Viroonkit Industry Co., Ltd. (Thailand). It contains 60% Dry Rubber Content (DRC) and 0.7% ammonia. Shrimp shells were obtained from local seafood Market. Rice husk (RH) was obtained from local rice mill in Nakhon Ratchasima, Thailand. Hydrochloric Acid (HCl, 37% v/v), Acetic Acid 99.98%, Sodium Hydroxide (NaOH) were purchased from ITALMAR (Thailand) Co., Ltd. Other chemicals for rubber compounding such as stearic acid, zinc oxide (ZnO), N-cyclohexyl-2-benzothiazole-2-sulfenamide (CBS) and Sulfur (S) were supported by Innovation Group (Thailand) Co., Ltd.

3.2 Experimental

3.2.1 Preparation of RHA and sodium silicate (Na_2SiO_3) solution

RH was washed with tap water to eliminate any impurities. The washed RH was oven-dried at 50°C overnight, and then refluxed with HCl 6 N at 65°C for 3 h. When the reaction was completed, refluxed RH was filtered and rinsed with DI water several times to remove the residual acid from the refluxed RH, and then oven dried at 50°C 6 h. After that, dried RH was burned at 650°C for 3 h. White silica ash (SiO_2 ash) was obtained. To prepare 10% Na_2SiO_3 solution, 325.18 g of RHA which compose of 280 g of SiO_2 was stirred with 2800 ml of 2.5 N NaOH solution for 14 h. Then, the suspension was filtered through a filter paper (Whatman No.93) to remove residual of solid. 10% Na_2SiO_3 solution was obtained.

3.2.2 Characterization of RHA

The chemical composition and SiO₂ content of RH SiO₂ ash was analyzed by using Wavelength dispersive X-ray fluorescence spectrometer (WDXRF, Rigaku - ZSXPrimusII).

The structure of SiO₂ ash was identified by The X-ray Diffractometer (XRD, Bruker D2 PHASER) with Ceramic Cu X-ray source at a 30 kV and 10 mA. A setting 2θ within the range of 2θ = 10°– 60° at a scan rate of 2° per min.

Functional group that is present on surface of RH SiO₂ ash was identified by Fourier transform infrared spectrometer (FTIR, Bruker Tensor27) which carried out at resolution of 4 cm⁻¹ in the range 400 - 4000 cm⁻¹. Sample was oven-dried at 60°C for 24 h. The sample was mixed with KBr with ratio 1:8. The sample was made in pellet form before analyzed.

RH SiO₂ ash surface morphology was observed by using Scanning Electron Microscope (SEM, JEOL JSM-6010LV). The sample was grounded, dried, and coated with gold by a sputter coater.

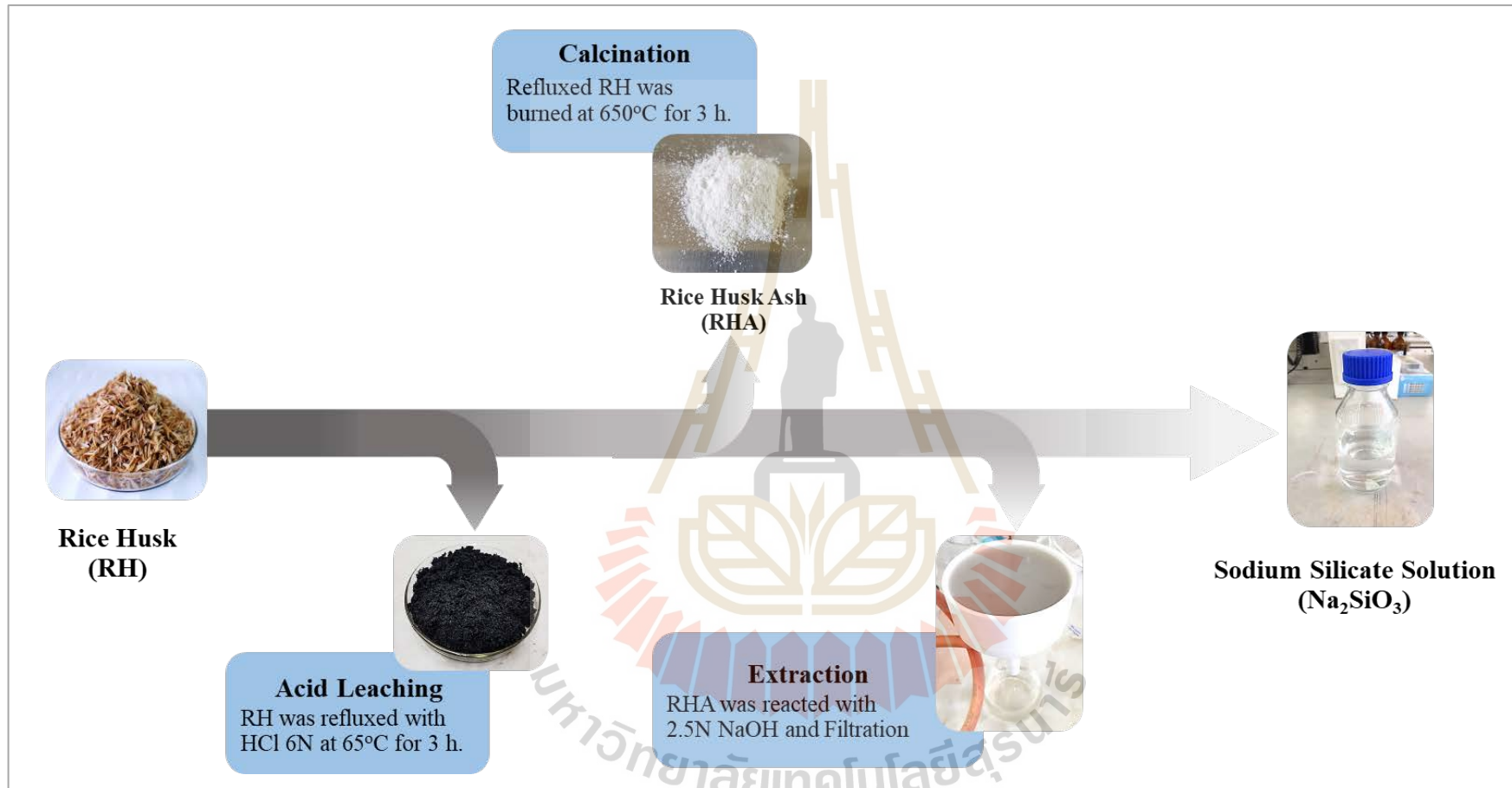


Figure 3.1 The process to produce sodium silicate solution from rice husk.

3.2.3 Preparation of CS from shrimp shells

Before preparation of CS, shrimp shells were rinsed with boiling water several times to eliminate impurities, then washed with DI water and oven-dried at 80°C overnight.

Preparation steps were as follows:

(i) Demineralization

The dried shrimp shells were demineralized by 3 M HCl solution at 75°C for 2 h under constant stirring of 150 rpm to remove calcium carbonate (CaCO₃).

(ii) Deproteinization

The demineralized shrimp shells were deproteinized by 10% NaOH solution at 80°C for 2 h to remove proteins. The resulting material is chitin.

(iii) Deacetylation

The chitin was deacetylated with 50% NaOH solution at an elevated temperature of 100°C for 2 h 30 min. The obtained material is a chitosan (CS).

To prepare 2% CS solution, 50 g of CS were dissolved with 2500 ml of 2% acetic acid.

3.2.4 Characterization of CS from shrimp shells

Chemical composition of CS was analyzed by using Wavelength dispersive X-ray fluorescence spectrometer (WDXRF, Rigaku - ZSXPrimusII).

CS characteristic peaks were detected by using X-ray diffractometer (XRD, Bruker D2 PHASER) with Ceramic Cu X-ray source at a 30 kV and 10 mA. A setting 2θ within the range of 5° - 40° at a scan rate of 2° per min.

Functional groups and degree of deacetylation of Shrimp shell chitosan was identified by using Fourier transform infrared spectrometer (FTIR, Bruker Tensor27) which carried out at resolution of 4 cm^{-1} in the range $400 - 4000\text{ cm}^{-1}$. Shrimp shell chitosan was oven-dried at 60°C for 24 h. Then, it was mixed with KBr with ratio 1:8. The sample was made in pellet form before analyzed. The degree of deacetylation of the chitosan was calculated using Equation (3.1).

$$\text{Degree of deacetylation (\%DD)} = 100 \left[\frac{A_{1655}}{A_{3450}} \times \frac{100}{1.33} \right] \quad (3.1)$$

Where A_{1655} is the absorbance of the amide I at 1655 cm^{-1} and A_{3450} is the absorbance of the hydroxyl at 3450 cm^{-1} .

Average molecular weight (MW) of CS was measured by using Dynamic light scattering analyzer (Malvern, Zetasizer-ZS) with various concentration of shrimp shell CS solution (*i.e.*, 0.1, 1, and 10 g/L).

Surface morphology of shrimp shell chitosan was observed by using Scanning Electron Microscope (SEM, JEOL JSM-6010LV). The sample was grounded, dried, and coated with gold by a sputter coater.

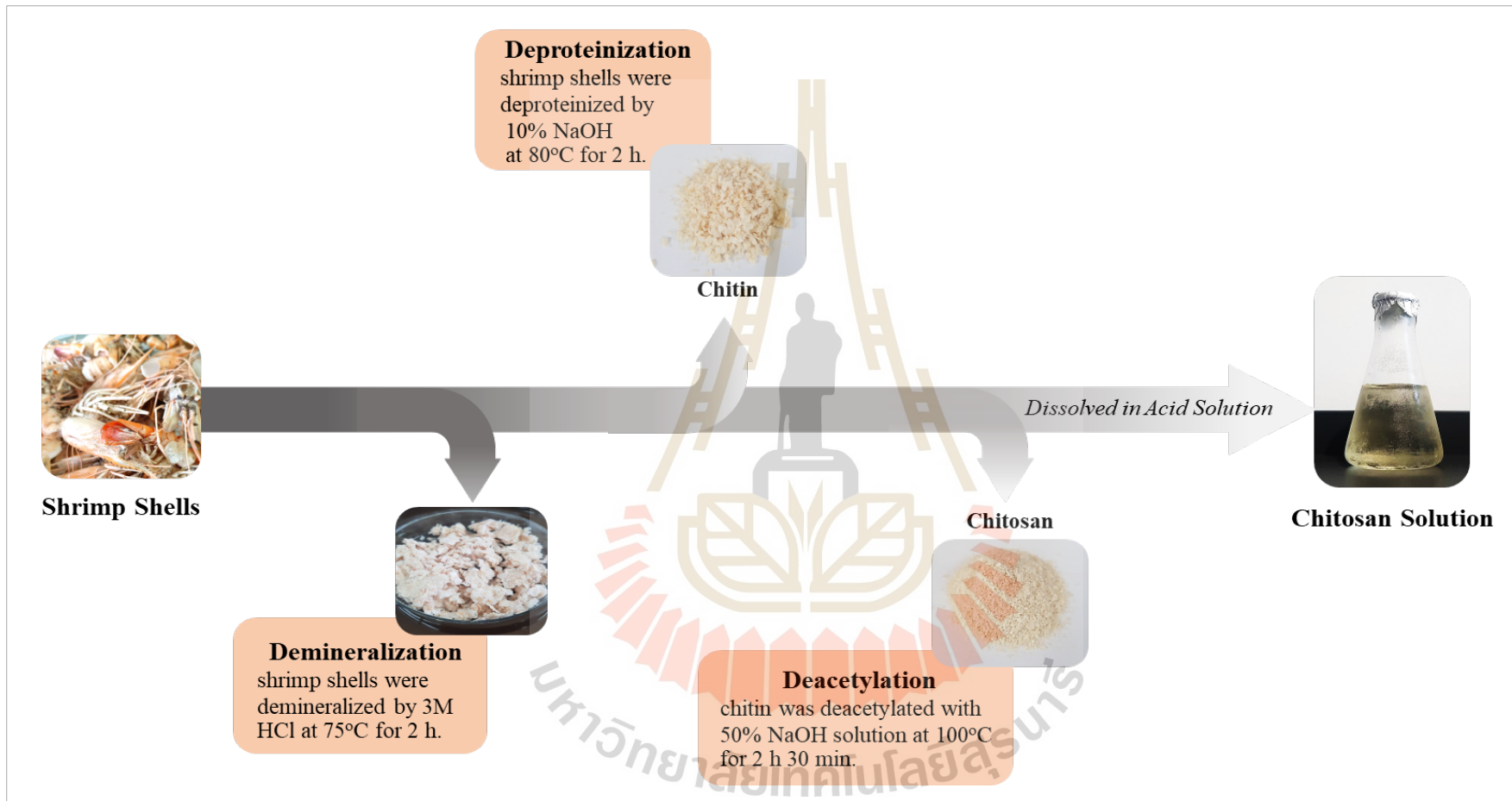


Figure 3.2 The process to produce CS solution from shrimp shells.

3.2.5 Preparation of SiO₂-CS hybrid filler

10% Na₂SiO₃ solution and 2% CS solution were prepared to be the hybrid filler by sol-gel method. The 10% Na₂SiO₃ solution and 2% CS solution were mixed with ratio of SiO₂-CS (*i.e.*, 1:1, 2:1, and 3:1). The pH of the mixture was adjusted to 7 by using 2% acetic acid and kept in 24 h to form SiO₂-CS hybrid gel. The hybrid gel was washed several times to eliminate the excess of sodium acetate and oven-dried at 80°C overnight. The obtained material was SiO₂-CS hybrid material.

Table 3.1 The ratio of hybrid filler

Sample	SiO ₂ (part)	CS (part)
SiO ₂ -CS 1:1	1	1
SiO ₂ -CS 2:1	2	1
SiO ₂ -CS 3:1	3	1

3.2.6 Characterization of SiO₂-CS hybrid filler

X-ray diffractometry was applied to confirm and detect peaks of the SiO₂ and CS. X-ray diffractometer (XRD, Bruker D2 PHASER) with Ceramic Cu X-ray source at a 30 kV and 10 mA was used. A setting 2θ within the range of 5°- 40° at a scan rate of 2° per min. FTIR spectra of the samples were performed by using Fourier transform infrared spectrometer (FTIR, Bruker Tensor 27) in the frequency range of 400 - 4000 cm⁻¹ at a resolution of 4 cm⁻¹. Sample was oven-dried at 60°C for 24h. The sample was mixed with KBr with ratio 1:8. The sample was made in pellet form before analyzed. The surface morphology and elements of hybrid materials were observed using Field emission scanning electron microscope (FE-SEM, Zeiss AURIGA FE-SEM/FIB/ Energy Dispersive X-Ray Analysis EDX).

The surface area, the total pore volume, the average pore volume, and the average particle size of hybrid materials were measured using Surface Area Analyzer, (BET, 3Flex Micromeritics, USA) with a degas temperature at 250°C.

3.2.7 Preparation of NR composites

Preparation of *in situ* SiO₂/ NR composites

The various contents (*i.e.*, 0, 5, 10, and 20 phr) of SiO₂ in the form of 10% Na₂SiO₃ solution was added into NR latex that was diluted into 30% of DRC by DI water. Each solution was stirred for 12 h until obtaining a homogeneous mixture. The pH of the mixture was adjusted to 7 by using 2% acetic acid in order to precipitate SiO₂ in NR latex. The mixtures were stirred for 6 h and cast into aluminum trays. Then, oven-dried at 60°C for 4 days to obtain composite sheets.

Preparation of *in-situ* SiO₂ - CS/ NR composites

To study the effect of hybrid filler contents on the properties of NR composites, the various contents (*i.e.*, 0, 5, 10, and 20 phr) of SiO₂ in the form of 10% Na₂SiO₃ solution was added into NR latex that was diluted into 30% of DRC by DI water. Each mixture was stirred for 12 h until obtaining a homogeneous mixture. 5 phr of CS in the form of 2% CS solution was added into the mixture. The pH of the mixture was adjusted to 7 by using 2% acetic acid in order to precipitate SiO₂ in NR latex. The mixtures were stirred for 6 h and cast into aluminum trays. Then, they were oven-dried at 60°C for 4 days to obtain composite sheets.

To study the effect of CS contents on the antimicrobial activity of NR composites, 10 phr of SiO₂ in the form of 10% Na₂SiO₃ solution was added into NR latex that was diluted into 30% of DRC by DI water. Each mixture was stirred for 12 h until obtaining a homogeneous mixture. The various contents (*i.e.*, 0, 3, 5, and 10 phr) of CS

in the form of 2% CS solution was added into the mixture. The pH of the mixture was adjusted to 7 by using 2% acetic acid. in order to precipitate SiO₂ in NR latex. The mixtures were stirred for 6 h and cast into aluminum trays. Then, they were oven-dried at 60°C for 4 days to obtain composite sheets.

Table 3.2 Formulation of unvulcanized NR composites

Sample	Ingredient (phr)*		
	NR	SiO ₂	CS
NR	100	-	-
To study the effect of <i>in situ</i> SiO ₂ content on mechanical properties of NR composites			
NR/5SiO ₂	100	5	-
NR/10SiO ₂	100	10	-
NR/20SiO ₂	100	20	-
To study the effect of hybrid filler at various <i>in situ</i> SiO ₂ contents on mechanical properties of NR composites			
NR/5SiO ₂ -5CS	100	5	5
NR/10SiO ₂ -5CS	100	10	5
NR/20SiO ₂ -5CS	100	20	5
To study the effect of CS content on antimicrobial and adsorption properties of NR composites			
NR/10SiO ₂ -3CS	100	10	3
NR/10SiO ₂ -5CS	100	10	5
NR/10SiO ₂ -10CS	100	10	10

*phr refer to parts per hundred rubber.

3.2.8 Characterization of NR composites

Thermal decomposition patterns and residual SiO₂ of NR composites were characterized by a thermogravimetric analyzer (TGA, Mettler Toledo TGA/DSC1). TGA thermograms of NR composites were obtained by heating a sample from 50 to 650°C (30°C/min, heating rate) under N₂ atmosphere and from 650 to 850°C under O₂ atmosphere.

The antimicrobial activity of NR, 10SiO₂/NR composite, and *in situ* SiO₂-CS/NR composites with various CS content were evaluated using the agar diffusion method. *Escherichia coli* (*E.coli*) bacteria was used for testing the antimicrobial activity. The composite sheets were placed on Mueller Hinton agar medium that had been seeded with 10⁵ cfu/ml (Colony Forming Units/mL) of the *E.coli*. Each sample was incubated at 37°C for 24 h. The antimicrobial properties of the composite sheets were observed from an inhibitory effect of microbial growth by measure the diameter of the inhibition zone around NR and NR composite sheets.

3.2.9 Preparation of vulcanized NR composites

NR composites were compounded by a two-roll mill machine. The ingredients for compounding were shown in Table 3.3. The compounding was started by mastication of NR composite before adding stearic acid, ZnO, CBS and sulfur. After mixing 15 min, the compound was stored for 24 h in room temperature. Curing time of the compound was determined by Moving Die Rheometer (MDR, GOTECH/GT-M200F) at 150°C. The compounds were vulcanized in a hydraulic press at 150°C with a pressure of 100 kg/cm² with the curing time from MDR testing.

Table 3.3 Compounding formulations

Sample	Ingredient (phr)*						
	NR	SiO ₂	CS	Stearic acid	ZnO	CBS	Sulfur
NR	100	-	-	1	5	1.2	3
NR/5SiO ₂	100	5	-	1	5	1.2	3
NR/10SiO ₂	100	10	-	1	5	1.2	3
NR/20SiO ₂	100	20	-	1	5	1.2	3
NR/5SiO ₂ -5CS	100	5	5	1	5	1.2	3
NR/10SiO ₂ -5CS	100	10	5	1	5	1.2	3
NR/20SiO ₂ -5CS	100	20	5	1	5	1.2	3

*phr refer to parts per hundred rubber

Minimum torque (ML), maximum torque (MH), scorch time (t_{s1}), and cure time (t_{c90}) of NR and NR composite compounds were determined by Moving Die Rheometer (MDR, GOTECH/GT-M200F) at 150°C. Cure rate index (CRI) of NR and NR composite compounds was calculated by following equation.

$$CRI = 100 / (t_{c90} - t_{s1}) \quad (3.2)$$

Moreover, the reinforcing potential of the filler of the NR composites were evaluated by the α_f -value, given by following equation.

$$\alpha_f = \left[(\Delta M_f / \Delta M_g) - 1 \right] / w \quad (3.3)$$

where ΔM_f and ΔM_g denote the torque difference $\Delta M = (MH-ML)$ during vulcanization for the filled and unfilled rubber, respectively, and “w” represent the weigh fraction of the filler in the compound.

3.2.10 Characterization of vulcanized NR composites

To study mechanical properties of NR and NR composites, the vulcanized composite sheet was cut into dumbbell shape specimens with die cutters (Type C). Tensile properties were determined according to ASTM D412-06a using a universal testing machine (UTM, INSTRON/5565) with a load cell of 5 kN and a crosshead speed of 500 mm/min. Tear properties were determined according to ASTM D624 using a universal testing machine (UTM, INSTRON/5565) the rate of jaw separation is 500 mm/min. Hardness of the vulcanized NR composites was determined according to ASTM D2240 using a shore A durometer (Bar Eiss, Type BS61 II).

To study morphological properties of NR and NR composites Fractured surface of NR and NR composites were observed using a scanning electron microscope (SEM, JEOL JSM-6010LV) at 5 keV. The samples were coated with gold before observation.

To study absorption properties of NR, 10SiO₂/NR composite and *in situ* SiO₂-CS/NR composites with various CS contents were cut into 10x10 mm square. Each sample was oven dried at 80°C and cooled in desiccator before weighing (W_1), then the samples were placed in Erlenmeyer flasks of DI water for 2 days at a temperature of 37°C in oven. Every 12 h, the samples were taken out from the oven and wiped with a tissue paper before weighing (W_2).

The water absorption was calculated as follows:

$$\% \text{ Absorption} = \frac{W_2 - W_1}{W_1} \times 100 \quad (3.4)$$

CHAPTER IV

RESULTS AND DISCUSSION

4.1 Characteristics of RHA

In this section, RHA was obtained from the process of acid leaching and calcination. Chemical composition of RHA was analyzed using WD-XRF. RHA chemical composition is shown in Table 4.1. The RHA is composed of SiO₂ as a major component and C, other minor components such as SO₃, Al₂O₃, Na₂O, CaO, etc. Yield of RH SiO₂ was around 10.42 g per 100 g of RH with 86.12% of SiO₂ purity.

Table 4.1 Chemical composition of RHA.

Chemical Compound	Weight (%)
SiO ₂	86.12
C	13.43
SO ₃	0.12
Al ₂ O ₃	0.11
Na ₂ O	0.11
CaO	0.10
Others	0.01

Amorphous structure of RHA was confirmed using XRD. X-ray diffraction pattern of RHA in Figure 4.1 that showed the broad peak at $2\theta \sim 22^\circ$ which confirmed a pattern of amorphous SiO_2 . A small sharp peak at $2\theta \sim 26^\circ$ which was attributed to the crystalline SiO_2 (Quartz) (Adams et al., 2014) (Yuvakkumar et al., 2012).

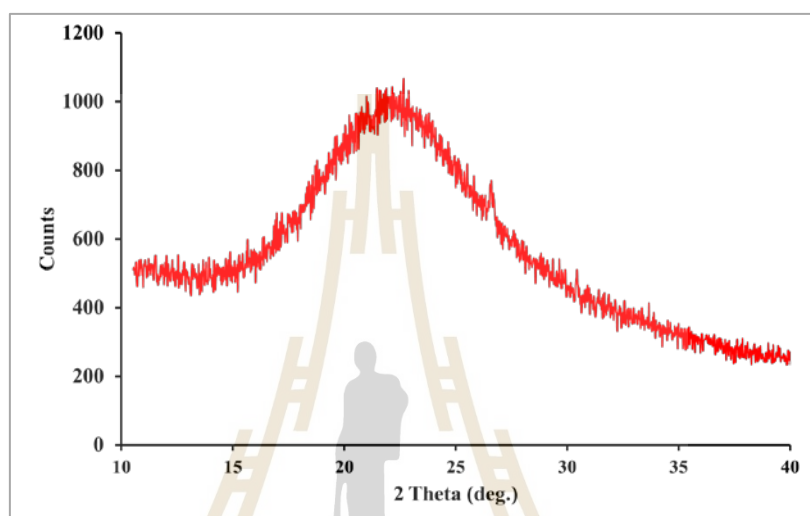


Figure 4.1 The X-ray diffraction pattern of RH.

FTIR spectra of RHA was given in Figure 4.2. FT-IR spectrum of RHA showed peaks at the wavenumbers of 462, 798, 1068, 1637, and 3460 cm^{-1} . The peak at 462, 798, and 1068 cm^{-1} were assigned to the bond rocking of the Si-O, symmetric Si-OH bending (silanol), and asymmetric Si-O-Si stretching, respectively (Tuan et al., 2017).

SEM micrographs of RHA and SiO_2 powder which precipitated from RHA sodium silicate by acetic acid are shown in Figure 4.3. The outer surface micrograph of RHA is shown in Figure 4.3(a) and the SiO_2 powder is shown in Figure 4.3(b). The particle size of RHA and SiO_2 were about $34 \mu\text{m}$ and 18 nm , respectively. The comparison of both was confirmed that the sol-gel method can produce the SiO_2 became a small size.

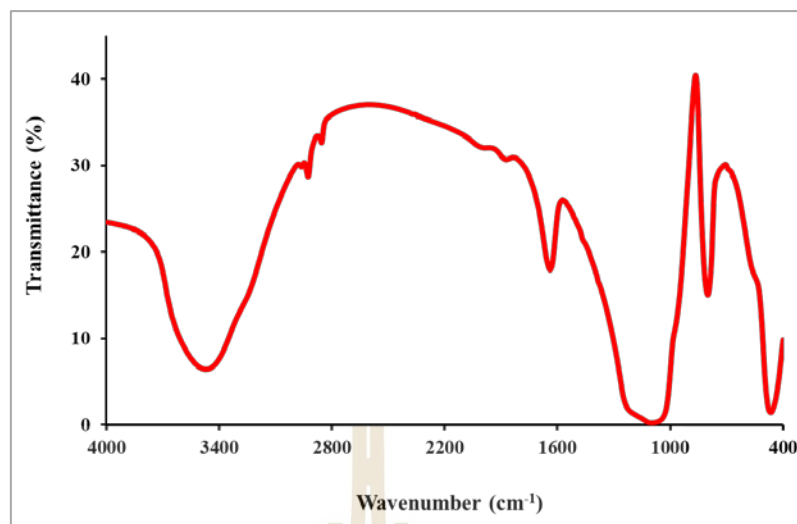


Figure 4.2 The FTIR spectra of RHA.

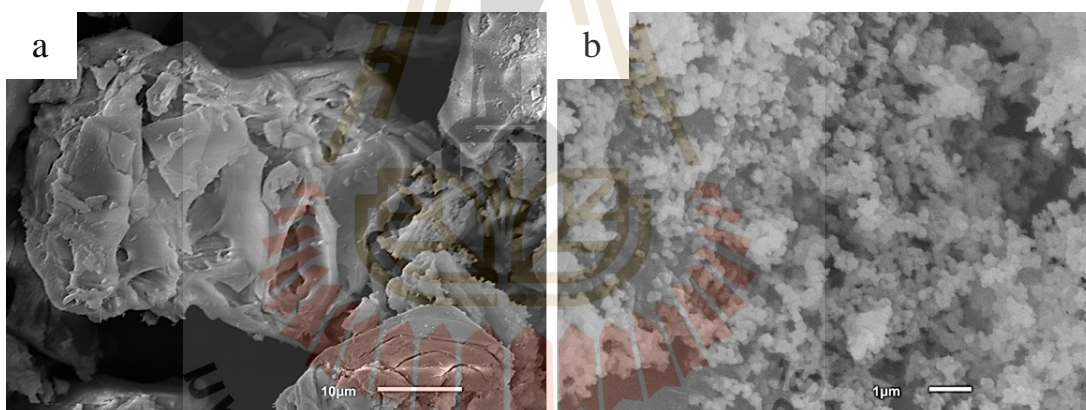


Figure 4.3 SEM micrographs of (a) RHA and (b) SiO₂ powder from RHA.

4.2 Characteristics of CS from shrimp shells

CS was obtained from the deacetylation of shrimp shell chitin. Yield of chitin was around 29.34 g per 100 g of shrimp shells. Yield of CS was around 48.50 g per 100 g of chitin. Chemical composition of CS is shown in Table 4.2 which shows the heavy presence of carbon and oxygen. Minor is nitrogen.

Table 4.2 Chemical composition of CS.

Chemical Elements	Weight (%)
C	45.81
O	45.12
N	8.92
Others	0.15

The FTIR spectrum of shrimp shell chitin and CS are shown in Figure 4.4. The CS spectrum includes absorbance bands around 3476 and 2925 cm^{-1} were assigned to the stretching vibrations of -OH bond and the stretching vibrations of C-H bond. The peaks at 1658, 1421 and 1382 cm^{-1} were assigned to the C=O stretching of the amide I, C-H bending and OH bending, respectively. The peaks at 1155 and 1028 cm^{-1} were assigned to asymmetric stretching of C-O-C bridge and C-O stretching (Yasmeen et al., 2016). The degree of deacetylation of shrimp shell CS was calculated by using the absorbance of -OH band and amide I band. Chitosan's degree of deacetylation ~ 65%.

The X-ray diffraction pattern of CS is shown in Figure 4.5 which showed the diffraction peak at $2\theta \sim 10^\circ$ and 21° indicated that are fingerprints of α -chitosan and γ -chitosan (Ameh et al., 2015).

The average molecular weight (MW) of CS which obtained from the experiment was 642,000 Da. The molecular weight of CS depends on the methods of preparation and the origin of raw materials (Benhabiles et al., 2012).

The morphology of CS is shown in Figure 4.6. The SEM micrographs showed the surface morphology of CS at 100X and 1500X magnification. The small flakes of CS were observed in Figure 4.6(a). The flakes size of CS was about 300 μm .

In higher magnification, some areas showed porous surface and crumbling flakes that were observed in Figure 4.6(b).

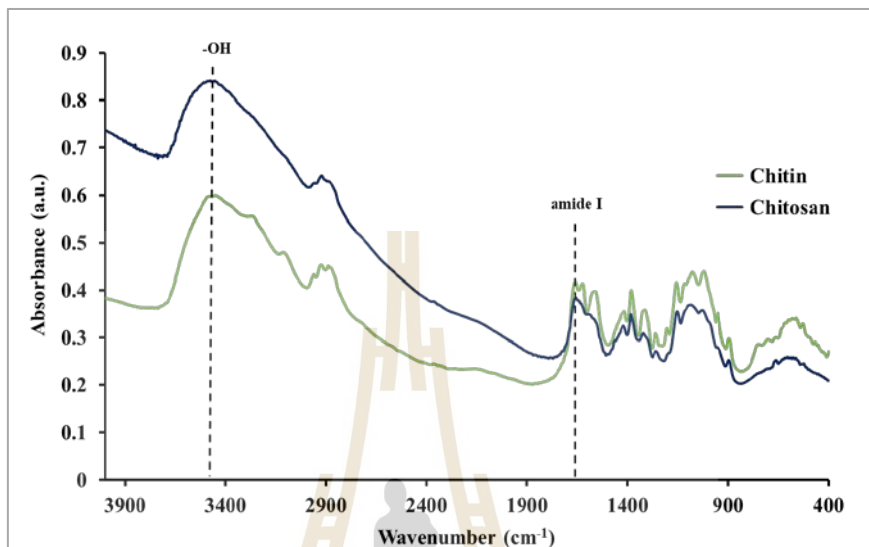


Figure 4.4 The FTIR spectrum of chitin and CS.

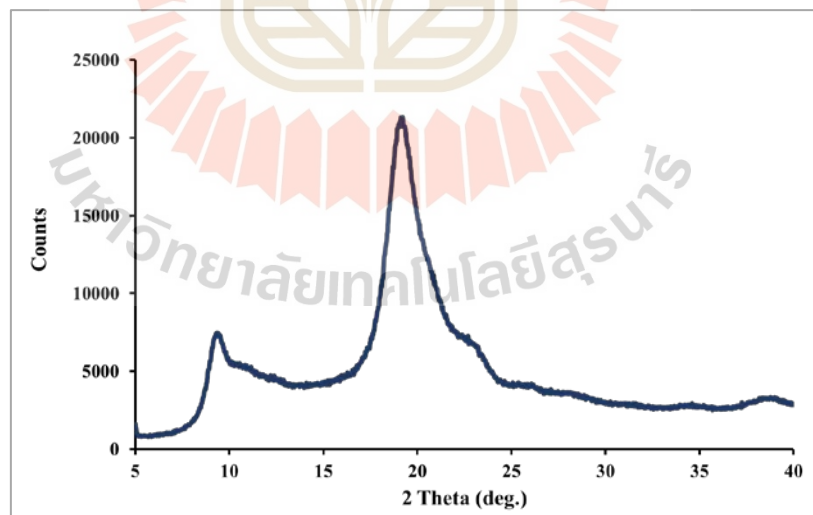


Figure 4.5 The X-ray diffraction pattern of CS.

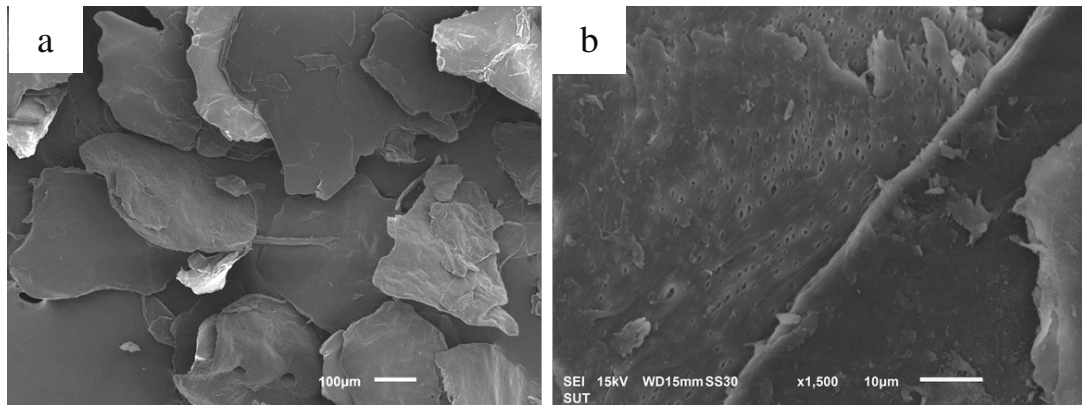


Figure 4.6 SEM micrographs of CS at (a)100X and (b) 1500X magnification.

4.3 Characterization of SiO₂-CS hybrid filler

The FTIR spectrum of SiO₂-CS hybrid materials at various ratios are shown in Figure 4.7. All spectrum showed the same peaks that included the peaks of SiO₂ and the peaks of CS. It indicated that the hybrid material has both constituents.

The X-ray diffraction pattern of SiO₂-CS hybrid materials at various ratios are shown in Figure 4.8. Each ratio of hybrid material showed the diffraction peaks at $2\theta \sim 10^\circ$, 21° , 22° , and 29° corresponding to the characteristics of SiO₂ and CS. However, at $2\theta \sim 29^\circ$ shows the crystalline phase of SiO₂ (Ebisike et al., 2018).

FE-SEM images showed morphology of the SiO₂-CS hybrid materials and their EDX spectra in Figure 4.9 and Figure 4.10, respectively. The hybrid materials have an irregular and too rough surface which indicated that it has a high surface area in comparison with RHA and CS in Figure 4.3 and Figure 4.6 before it was prepared as hybrid material. The EDX spectra showed the elements of hybrid material. At the ratio of 2:1 showed the highest content of Si following the ratio of 3:1 and 1:1, respectively. The EDX spectra of each ratio of the hybrid material were observed the consist of

Si, O, C, and N that are SiO_2 and CS constituent whereas at the ratio of 3:1 was observed Na element from sodium acetate residue.

A strong physical contact between filler and polymer matrix was promoted by using a high surface area material as a filler (Conradi, 2013). In this study, the obtained hybrid material was expected that has a high surface area for use as a filler in composites. The Brunauer-Emmett-Teller (BET) isotherm for the SiO_2 -CS hybrid materials is shown in Figure 4.11 which can be concluded that the SiO_2 -CS hybrid materials are microporous according to the IUPAC classification of adsorption isotherms (Allothman, 2012). The characteristics of SiO_2 -CS hybrid materials are given in Table 4.3. At the ratio of 2:1 (SiO_2 -CS) presents the highest surface area and total pore volume according to the smallest average particle size that is the suitable ratio to produces the hybrid material for use as a filler.

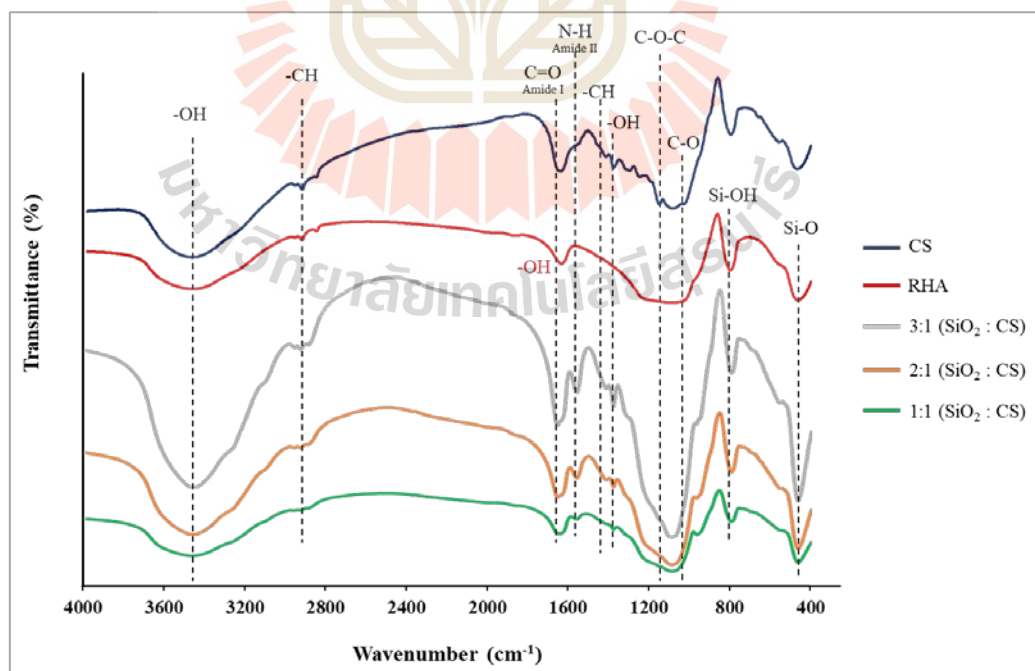


Figure 4.7 The FTIR spectrums of RHA, CS, and hybrid materials at various ratios.

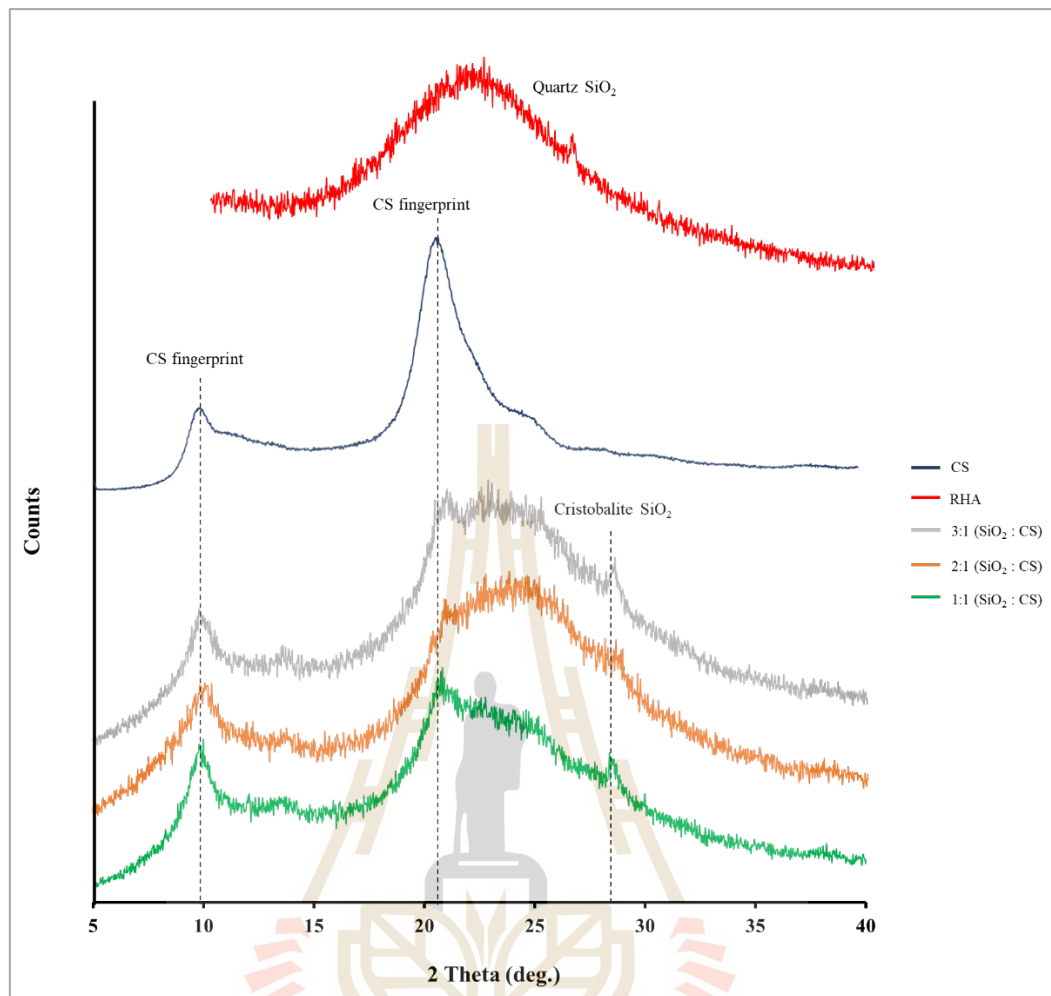


Figure 4.8 The X-ray diffraction patterns of RHA, CS, and hybrid materials at various ratios.

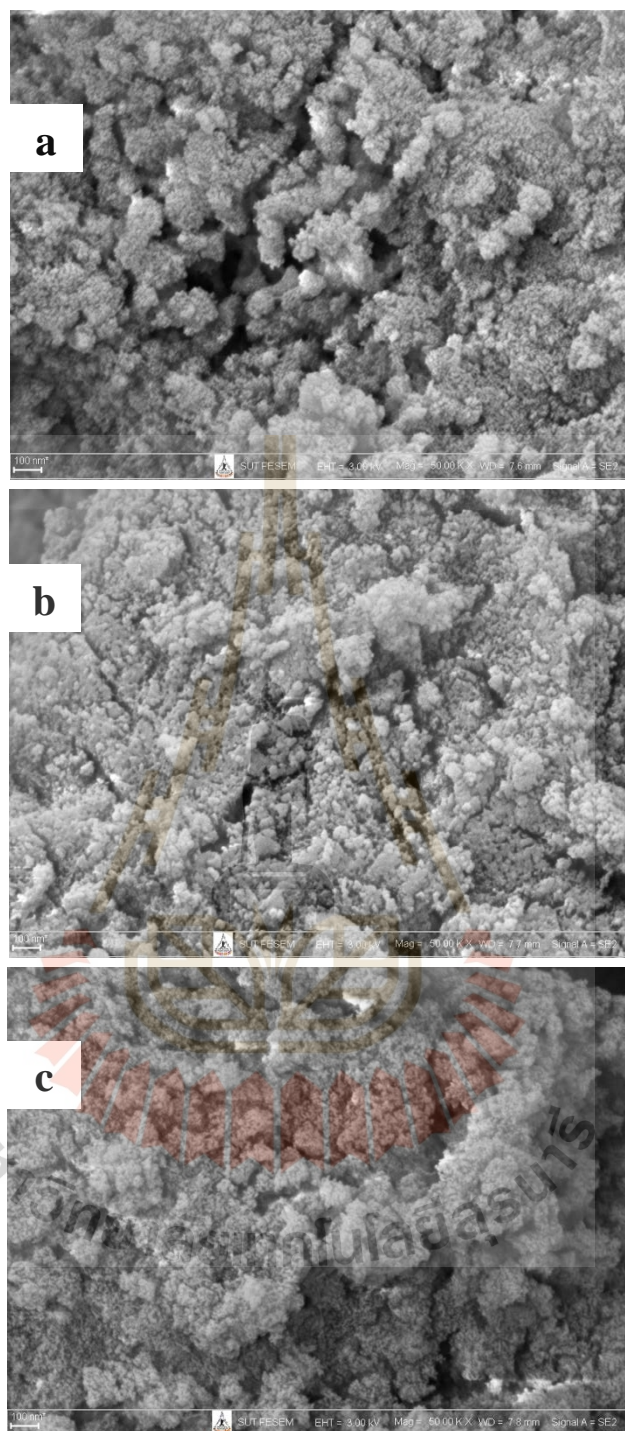


Figure 4.9 FE-SEM images of the SiO₂-CS hybrid materials (a) 1:1, (b) 2:1, and (c) 3:1.

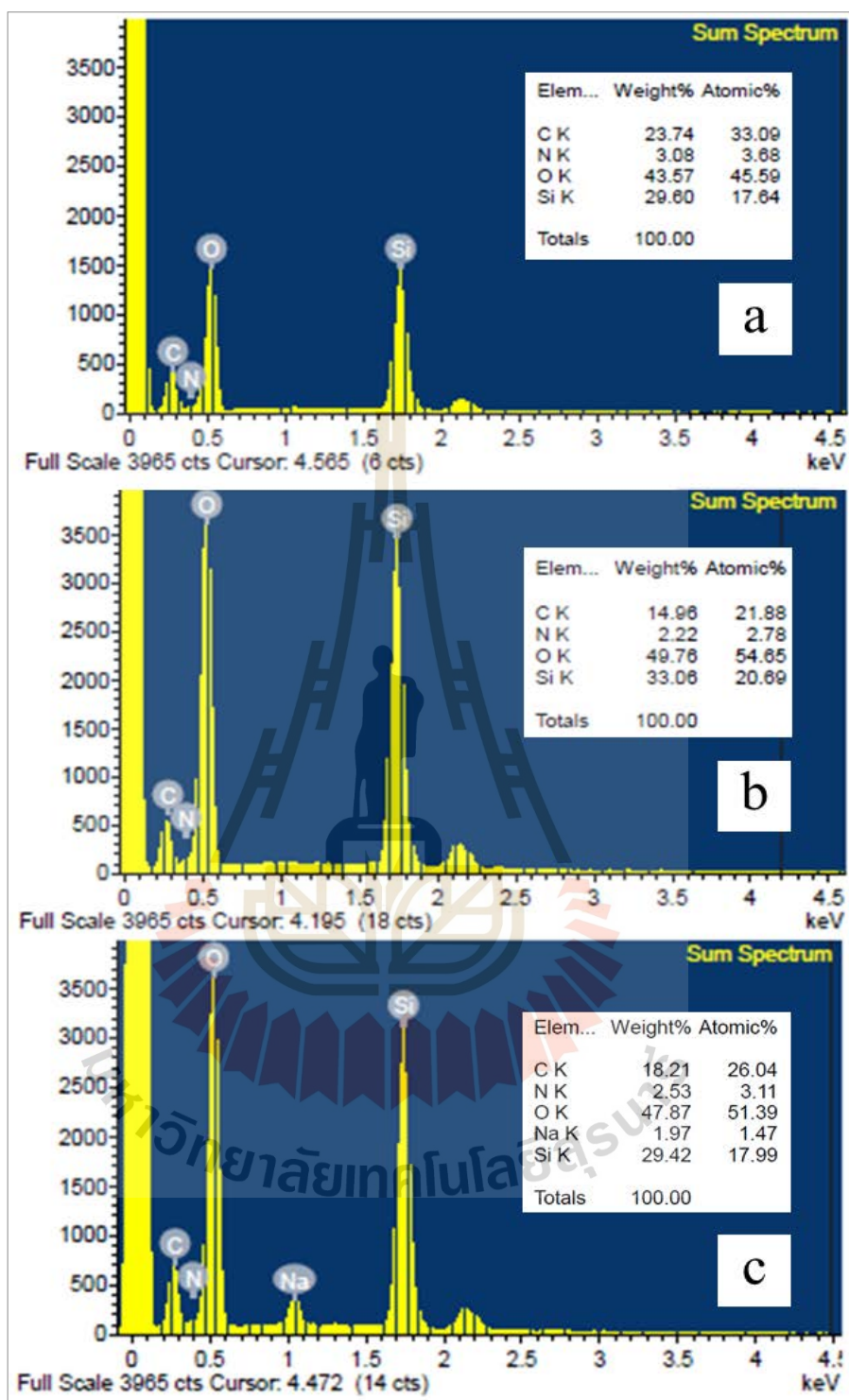


Figure 4.10. EDX Spectra of the SiO₂-CS hybrid materials (a) 1:1, (b) 2:1, and (c)3:1.

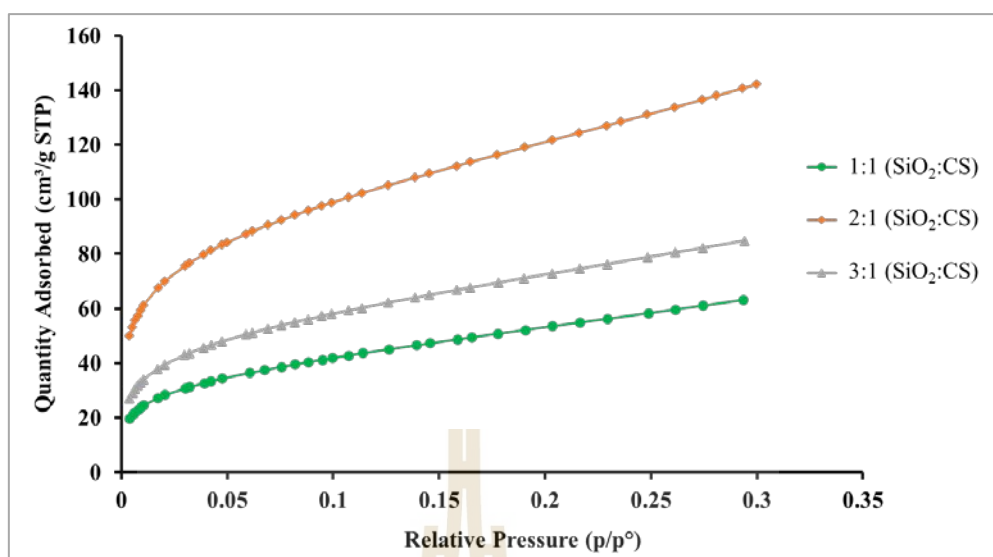


Figure 4.11 The Brunauer-Emmett-Teller (BET) isotherm for the SiO₂-CS hybrid materials.

Table 4.3 The surface characteristics of SiO₂-CS hybrid materials.

Sample SiO ₂ -CS	BET surface area (m ² /g)	Total pore volume (cm ³ /g)	Average pore diameter (nm)	Average particle size (nm)
1:1	196	0.27	5	31
2:1	441	0.60	5	14
3:1	265	0.49	7	23

4.4 Effect of *in situ* SiO₂ content on the properties of NR composites

4.4.1 The SiO₂ content in *in situ* SiO₂/NR composites

The SiO₂ content was investigated by Thermogravimetric analysis (TGA). Percentage of remainder was assumed to be SiO₂ content that occurs in NR composites. The highest temperature of the analysis can decompose NR thus, the remainder is only SiO₂. TGA curves and results are shown in Figure 4.12 and Table 4.4. The thermal decomposition temperature at 25%, 50%, and 75% mass loss. It can be seen that mass loss temperatures of *in situ* SiO₂/NR composites are higher than neat NR. The higher thermal stability of *in situ* SiO₂/NR composites due to the SiO₂ can absorb heat energy and retard the heat transfer to the rubber chains (Poompradub et al., 2014).

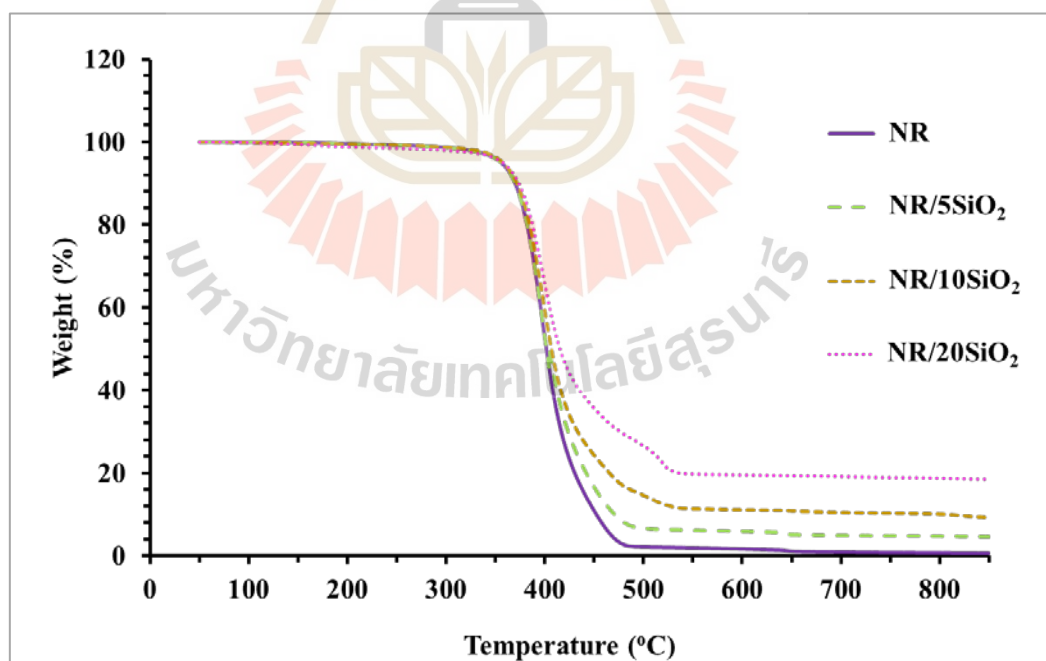


Figure 4.12 TGA curve of NR and *in situ* SiO₂/NR composites at various SiO₂ contents.

Table 4.4 Thermal decomposition temperatures of NR and *in situ* SiO₂/NR composites.

Sample	T _{25%} (°C)	T _{50%} (°C)	T _{75%} (°C)	Remainder (%)	
				Expected	Actual
NR	386.0	401.5	422.5	-	0.70
NR/5SiO ₂	391.5	409.5	440.5	4.76	4.09
NR/10SiO ₂	389.0	406.5	447.9	9.09	9.21
NR/20SiO ₂	392.0	415.0	509.0	16.67	18.55

T_{25%}, T_{50%}, T_{75%} = temperatures correspond to the weight loss of 25%, 50%, and 75%, respectively.

4.4.2 Cure characteristics

Cure characteristics at 150°C of *in situ* SiO₂/NR composites at various *in situ* SiO₂ contents including the minimum torque (ML), maximum torque (MH), torque difference (ΔM) scorch time (t_{s1}), 90% of cure time (t_{c90}), and cure rate index (CRI). Figure 4.13 shows ML and MH of NR and NR composites. The value of ML indicates the initial viscosity of rubber compounds. ML of the composites increased with increasing *in situ* SiO₂ content thus, the mobility of rubber chains was hidden by *in situ* SiO₂. The physical cross-link network of the NR compounds is indicated from the value of ML. The value of MH and ΔM as well, the enhancement of MH and ΔM are attributed to a chemical cross-link network and degree of cross-linking of NR composites, respectively. The enhancing of NR compound viscosity by the addition of *in situ* SiO₂. Moreover, the reinforcing potential of filler in NR composites was evaluated by α_f . Table 4.5 shows the α_f value of *in situ* SiO₂/NR composites. At 5 phr of *in situ* SiO₂ presents the highest filler reinforcing potential (Tabaei et al., 2015).

Scorch time (t_{s1}) and 90% of cure time (t_{c90}) are shown in Figure 4.14. Scorch time of *in situ* SiO₂/NR composites is shorter than unfilled NR. However, the increase of *in situ* SiO₂ content increases scorch time of NR composites.

On the other hand, cure time of *in situ* SiO₂/NR composites is also shorter than unfilled NR but it decreases when increasing *in situ* SiO₂ content. Generally, the surface chemistry of SiO₂ was explained that its surface contains acidic hydroxyl, siloxane, and silanol groups which can reduce the efficiency of accelerator and curing agent leading to increased cure time. In the case of *in situ* SiO₂, the enhancement of ML indicates the formation of physical network increased which can changes the accessibility of the surface groups. Thus, the adsorption of accelerator on the surface of *in situ* SiO₂ is less. It can speed up the vulcanization (short cure time) and increases the chemical crosslinking as well.

Cure rate index (CRI) of NR and *in situ* SiO₂/NR composites is shown in Figure 4.15. The CRI value indicates the speed of curing reaction. The CRI value of *in situ* SiO₂/NR composites higher than NR except NR composites filled *in situ* SiO₂ at 5phr due to it had the most difference of t_{c90} and t_{s1} . This can be concluded that the surface of *in situ* SiO₂ at 5 phr can adsorb the accelerator and curing agent thus extended the vulcanization time and decelerated the rate of vulcanization.

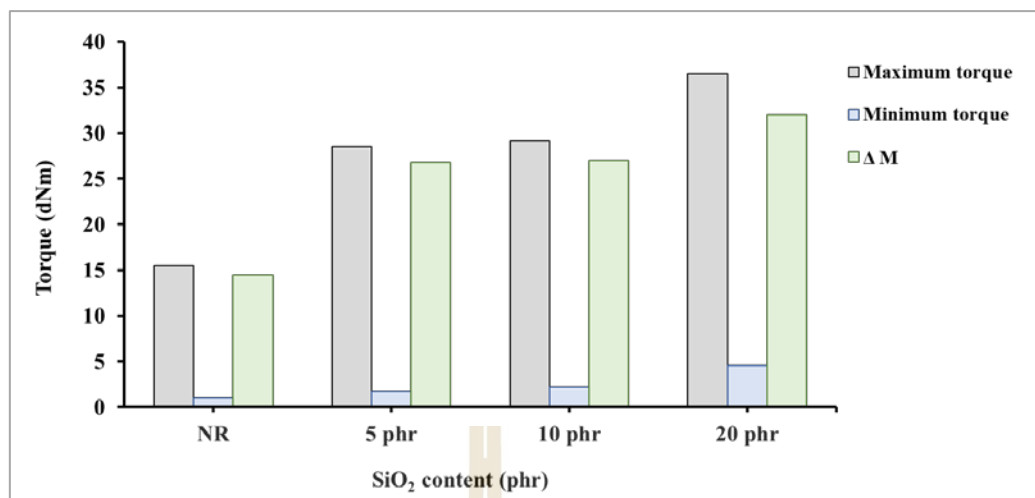


Figure 4.13 Effect of *in situ* SiO₂ content on maximum, minimum torque, and torque difference of *in situ* SiO₂/NR composites.

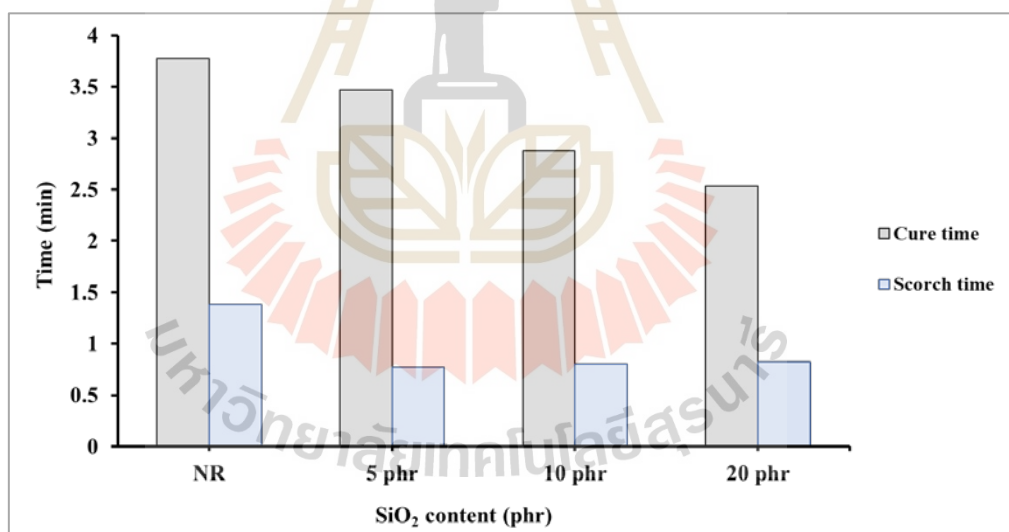


Figure 4.14 Effect of *in situ* SiO₂ content on cure time and scorch time of *in situ* SiO₂/NR composites.

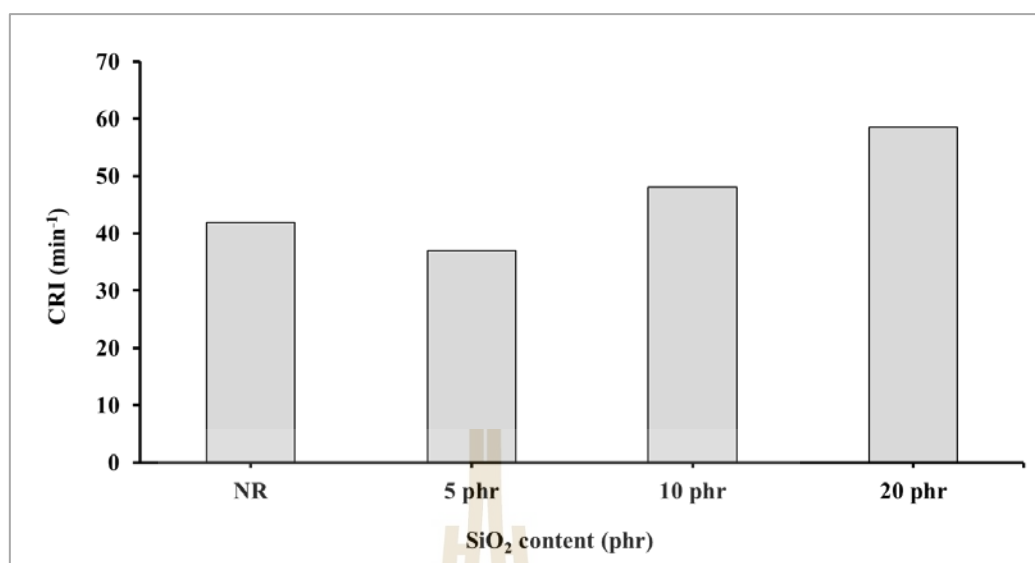


Figure 4.15 Effect of *in situ* SiO₂ content on cure rate index of *in situ* SiO₂/NR composites.

Table 4.5 Cure characteristics of NR and *in situ* SiO₂/NR composites.

Sample	ML (dNm)	MH (dNm)	ΔM (dNm)	α_f	t_{s1} (min)	t_{c90} (min)	CRI (min ⁻¹)
NR	1.02	15.50	14.48	-	1.38	3.77	41.84
NR/5SiO ₂	1.77	28.54	26.77	19.56	0.77	3.47	37.03
NR/10SiO ₂	2.19	29.18	26.99	10.38	0.80	2.88	48.08
NR/20SiO ₂	4.55	36.56	32.01	7.88	0.82	2.53	58.48

4.4.3 Mechanical properties

Stress-Strain curves and tensile properties of NR and *in situ* SiO₂/NR composites including tensile strength, %elongation at break, modulus at 100% elongation (M100), and 300% elongation (M300) are shown in Figure 4.16, 4.17, 4.18, 4.19, and 4.20, respectively. Tear strength and hardness of NR and *in situ* SiO₂/NR composites are shown in Figure 4.21 and Figure 4.22. Tensile strength and tear strength of *in situ* SiO₂/NR composites increased with increasing *in situ* SiO₂ content up to 10 phr. Therefore, the optimum loading of *in situ* SiO₂ is 10 phr. At 20 phr of SiO₂, its tensile strength decreased due to the intense SiO₂ caused poor interaction between matrix and filler. Elongation at break of *in situ* SiO₂/NR composites was decreased by the addition of *in situ* SiO₂. This suggested that the addition of *in situ* SiO₂ into NR can be enhanced the rigidity of the composites. Due to the fact that the mobility of NR molecular chains was restricted by SiO₂ particles. Hence, it can resist the stretching of NR. M100, M300, and hardness of *in situ* SiO₂/NR composites increased with increasing *in situ* SiO₂ content. The results indicate that the stiffness of the composites increase because the elasticity of NR molecular chains was restricted by SiO₂ particles.

4.4.4 Morphological properties

The morphology of NR and *in situ* SiO₂/NR composite fractured surface are shown in Figure 4.23. The fractured surface of unfilled NR shows smooth surface. On the other hand, the fractured surface of NR composites at 5, 10, and 20 phr of SiO₂ showed rough surface and the SiO₂ particles were observed especially at 5 phr of SiO₂. NR composites were prepared by the latex mixing method. So, the mixture was contained by water from solution depend on solution content that was added into the mixture. The mixture of 5 phr of SiO₂ has the least water content compared with

10 and 20 phr thus, the system that has fewer water forms larger particles quickly than systems that have a lot of water. In addition, the crystals of the residual sodium acetates may be observed in the composites. However, EDX mapping represents the good distribution of SiO_2 particles in all composites. It can be observed well distributed SiO_2 particles (white spot).

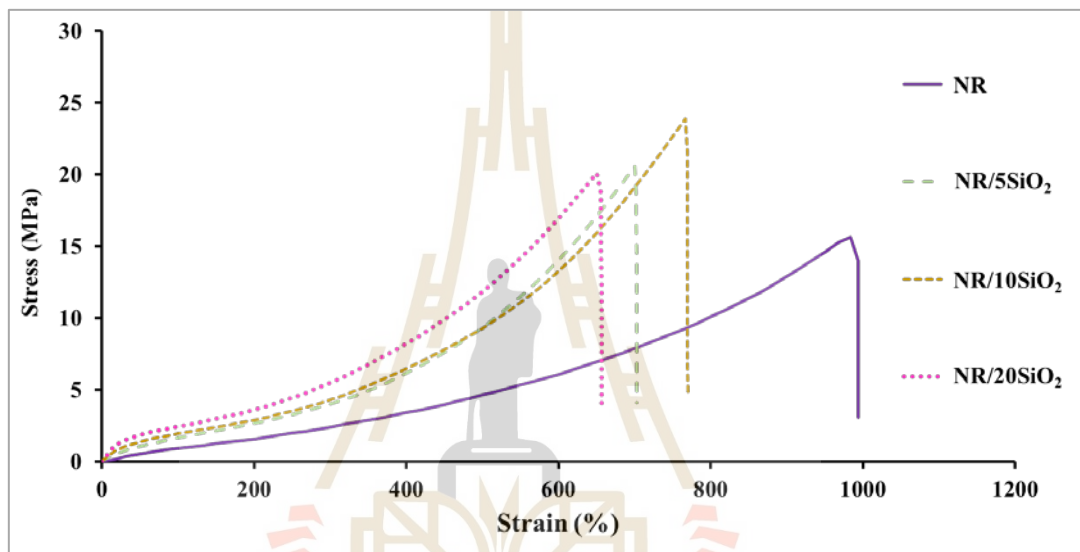


Figure 4.16 Stress-Strain curves of NR and *in situ* SiO_2 /NR composites at various SiO_2 contents.

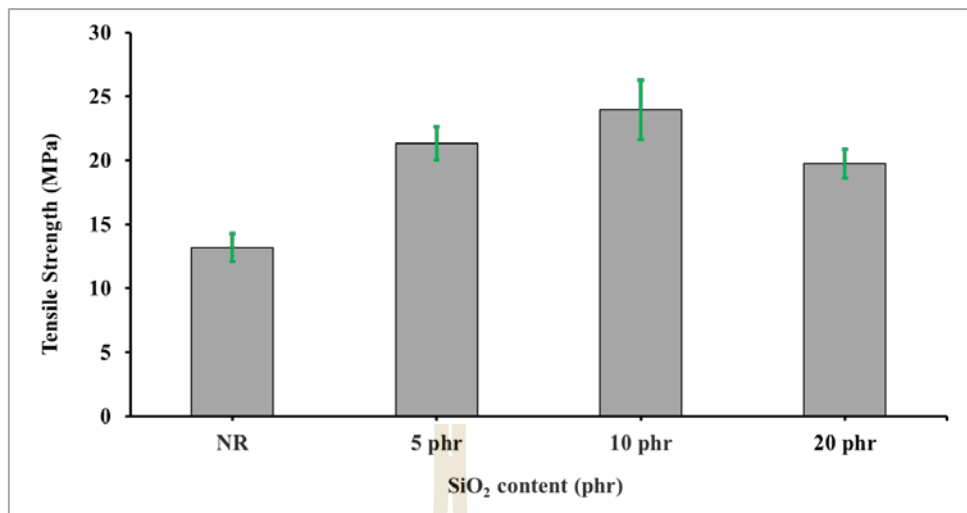


Figure 4.17 Effect of *in situ* SiO₂ content on tensile strength of *in situ* SiO₂/NR composites.

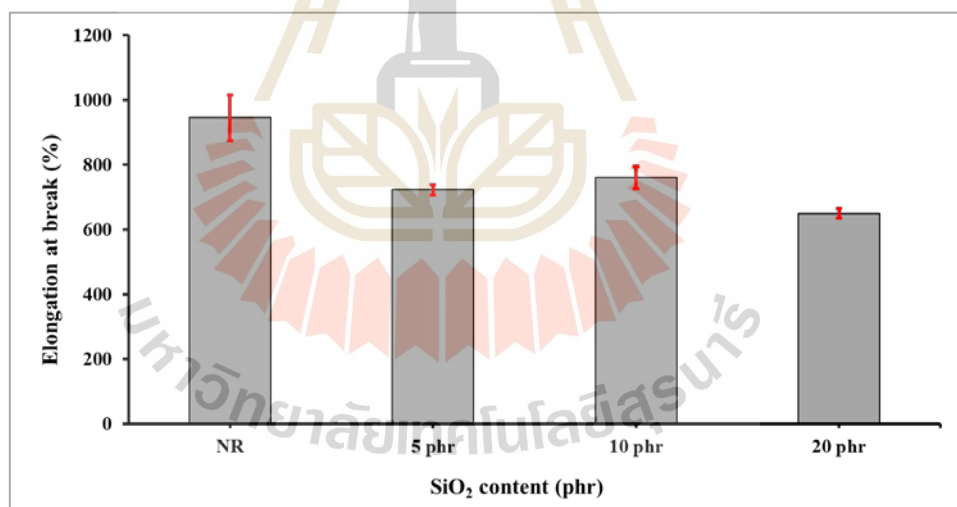


Figure 4.18 Effect of *in situ* SiO₂ content on elongation at break of *in situ* SiO₂/NR composites.

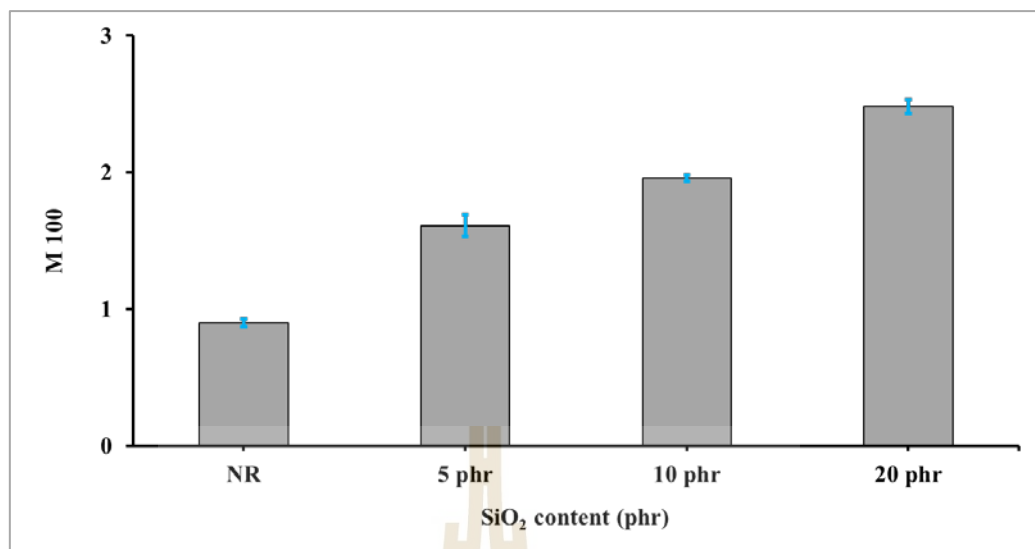


Figure 4.19 Effect of *in situ* SiO₂ content on M100 of *in situ* SiO₂/NR composites.

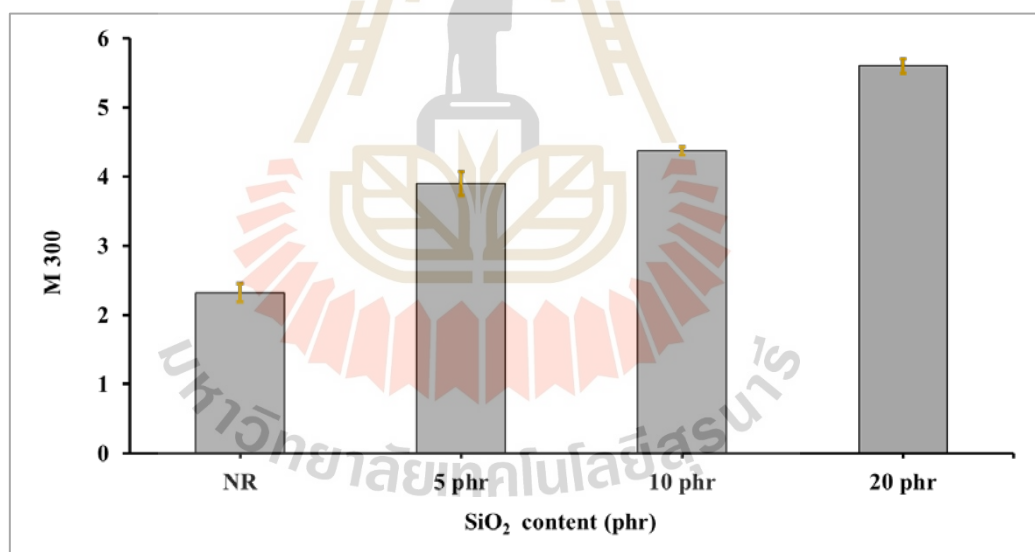


Figure 4.20 Effect of *in situ* SiO₂ content on M300 of *in situ* SiO₂/NR composites.

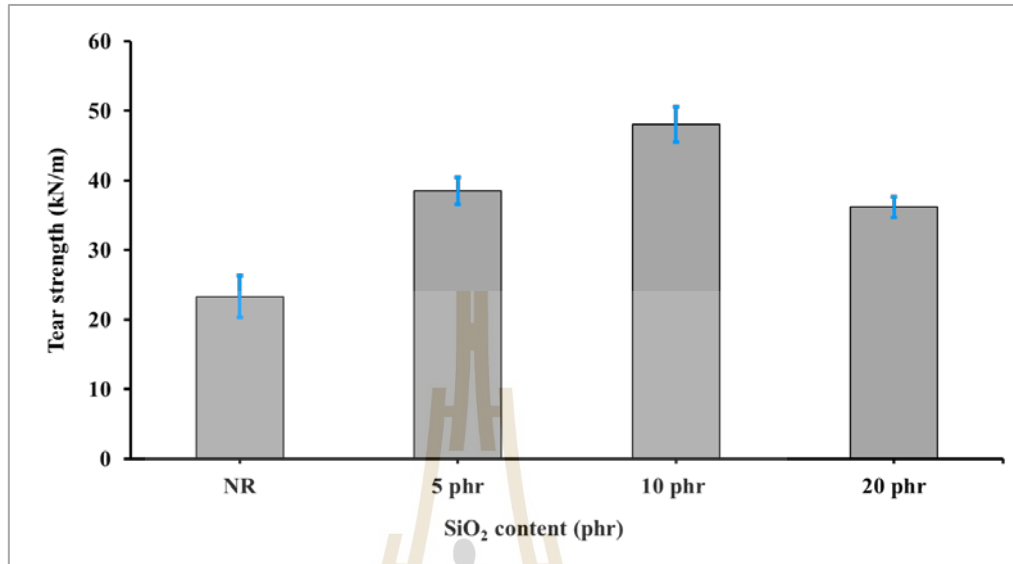


Figure 4.21 Effect of *in situ* SiO₂ content on tear strength of *in situ* SiO₂/NR composites.

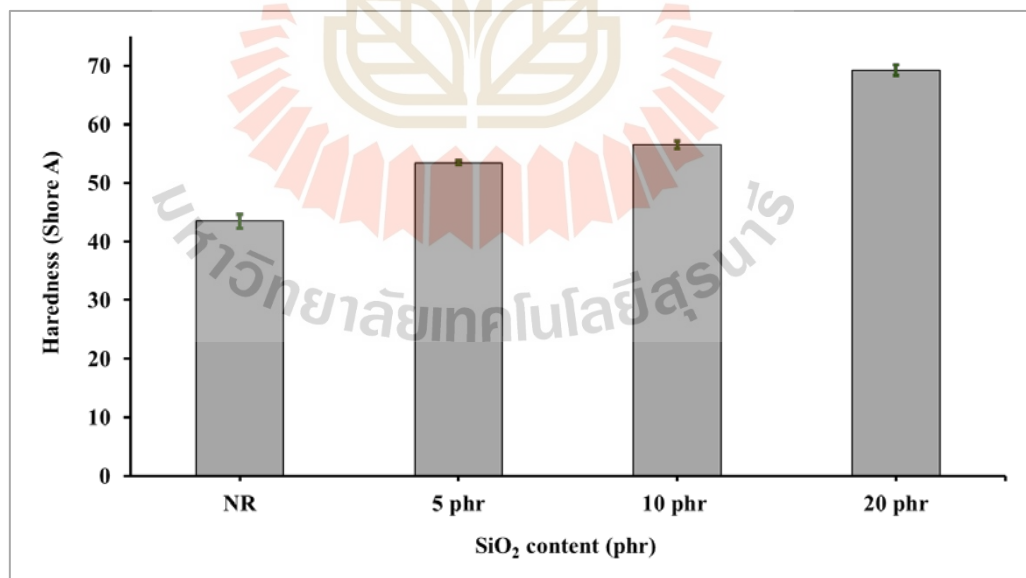


Figure 4.22 Effect of *in situ* SiO₂ content on hardness of *in situ* SiO₂/NR composites.

Table 4.6 Mechanical properties of NR and *in situ* SiO₂/NR composites.

Sample	Tensile strength (MPa)	Elongation at break (%)	M100 (MPa)	M300 (MPa)	Tear strength (kN/m)	Hardness (Shore A)
NR	13.21±1.07	944.60±70.00	0.90±0.03	2.32±0.13	23.32±2.96	43.47±1.68
NR/5SiO ₂	21.33±1.31	722.50±16.68	1.61±0.08	3.90±0.17	38.48±1.94	53.47±0.31
NR/10SiO ₂	23.95±2.33	760.39±34.10	1.96±0.02	4.37±0.06	48.03±2.54	56.53±0.67
NR/20SiO ₂	19.74±1.14	649.36±14.91	2.48±0.05	5.60±0.10	36.17±1.49	69.23±0.91

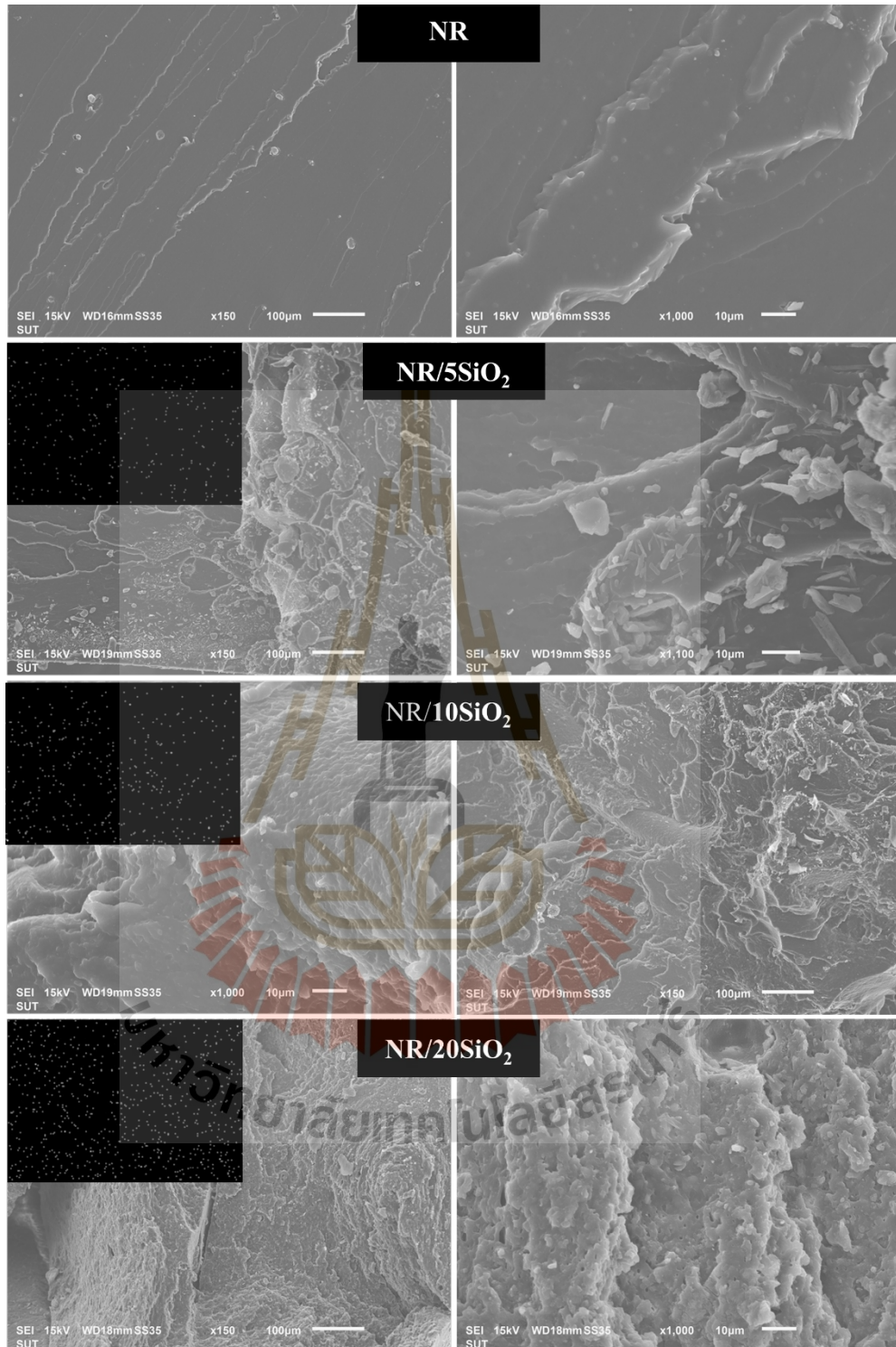


Figure 4.23 SEM micrographs of NR and SEM micrographs and their EDX mapping (left top of each micrograph) of *in situ* SiO₂ NR composite fractured surface at 150X (left) and 1000X (right) magnification.

4.5 Effect of *in situ* SiO₂-CS hybrid filler at various SiO₂ content on the properties of NR Composites

4.5.1 The SiO₂ content in *in situ* SiO₂-CS/NR composites

Similar to 4.4.1 section, the SiO₂ content was investigated by Thermogravimetric analysis (TGA). The remainder was assumed to be SiO₂ content that occurs in NR composites. The highest temperature of the analysis can decompose NR thus, the remainder is only SiO₂. TGA curve and results are shown in Figure 4.24 and Table 4.7. The thermal decomposition temperature at 25%, 50%, and 75% mass loss. 50% and 75% mass loss, it can be seen that mass loss temperatures of *in situ* SiO₂-CS/NR composites are higher than unfilled NR. The higher thermal stability of *in situ* SiO₂-CS/NR composites due to SiO₂ can adsorb heat energy and retard the heat transfer to the rubber chains (Poompradub et al., 2014). However, the thermal decomposition temperature at 25% of *in situ* SiO₂-CS/NR composites is lower than neat NR because the weight loss of CS is fast in the beginning due to the thermal stability of CS is low (Johns and Rao, 2008).

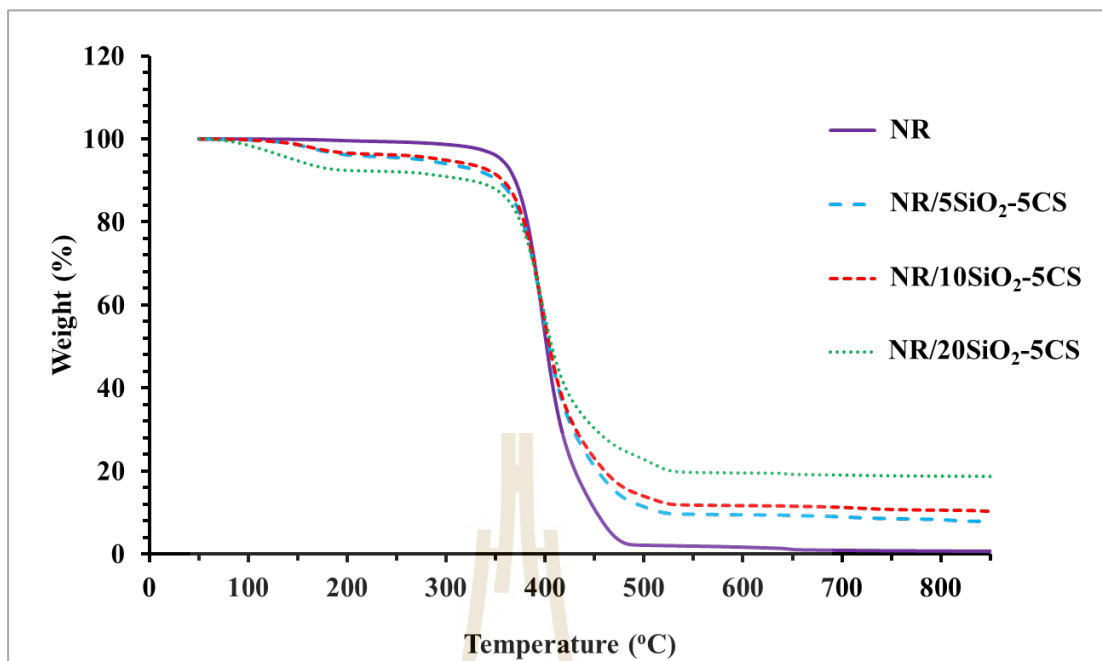


Figure 4.24 TGA curve of NR and *in situ* SiO₂-CS/NR composites at various SiO₂ contents.

Table 4.7 Thermal decomposition temperatures of NR and *in situ* SiO₂-CS/NR composites.

Sample	T _{25%} (°C)	T _{50%} (°C)	T _{75%} (°C)	Remainder (%)
NR	386.0	401.5	422.5	0.70
NR/5SiO ₂ -5CS	383.5	404.0	431.5	5.54
NR/10SiO ₂ -5CS	384.0	404.5	443.5	10.20
NR/20SiO ₂ -5CS	382.5	407.0	479.0	18.67

T_{25%}, T_{50%}, T_{75%} = temperatures correspond to the weight loss of 25%, 50%, and 75%, respectively.

4.5.2 Cure characteristics

Cure characteristics at 150°C of *in situ* SiO₂-CS/NR composites at various *in situ* SiO₂-CS contents including minimum torque (ML), maximum torque (MH), torque difference (ΔM) scorch time (t_{s1}), 90% of cure time (t_{c90}), and cure rate index (CRI). The summarized of NR and *in situ* SiO₂-CS/NR composites

cure characteristics in Table 4.8. Figure 4.25 shows ML, MH and ΔM of NR and *in situ* SiO₂-CS/NR composites. The ML value of NR composites increased with increasing *in situ* SiO₂-CS content due to the mobility of rubber chains was hidden by *in situ* SiO₂-CS. This is similar to section 4.4.2. The MH and ΔM values of *in situ* SiO₂-CS/NR composites are higher than unfilled NR. However, the increase of *in situ* SiO₂-CS content reduced the MH and ΔM values of *in situ* SiO₂-CS/NR composites. This may be due to the curing agent was deactivated by more filler content. This can greatly reduce torque level. Table 4.8 shows the α_f value of *in situ* SiO₂-CS/NR composites. At 5-5 phr of *in situ* SiO₂-CS presents the highest filler reinforcing potential (Tabaei et al., 2015).

Scorch time (t_{s1}) and 90% of cure time (t_{c90}) are shown in Figure 4.26. Scorch time and cure time of *in situ* SiO₂-CS/NR composites is shorter than unfilled NR. However, the increase of *in situ* SiO₂ content does not significantly affect scorch time of the NR composites.

Cure rate index (CRI) of NR and *in situ* SiO₂-CS/NR composites is shown in Figure 4.27. The CRI value indicates the speed of curing reaction. The CRI value of *in situ* SiO₂-CS/NR composites is higher than NR except NR composites filled *in situ* SiO₂ at 10 phr and CS at 5 phr due to it had the most difference of t_{c90} and t_{s1} . This can be concluded that the surface of *in situ* SiO₂ and CS can adsorb the accelerator and curing agent thus extended the vulcanization time and decelerated the rate of vulcanization.

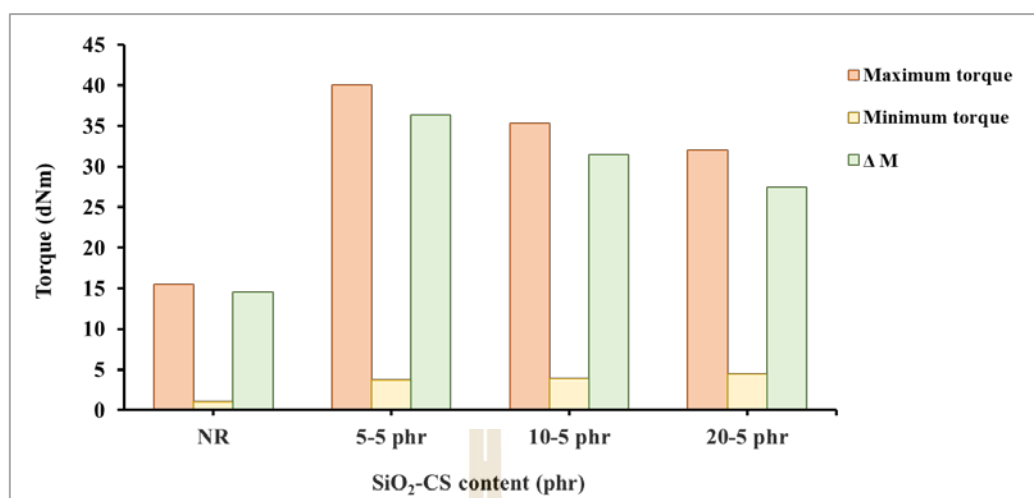


Figure 4.25 Effect of *in situ* SiO₂ content on maximum, minimum torque, and torque difference of *in situ* SiO₂-CS/NR composites.

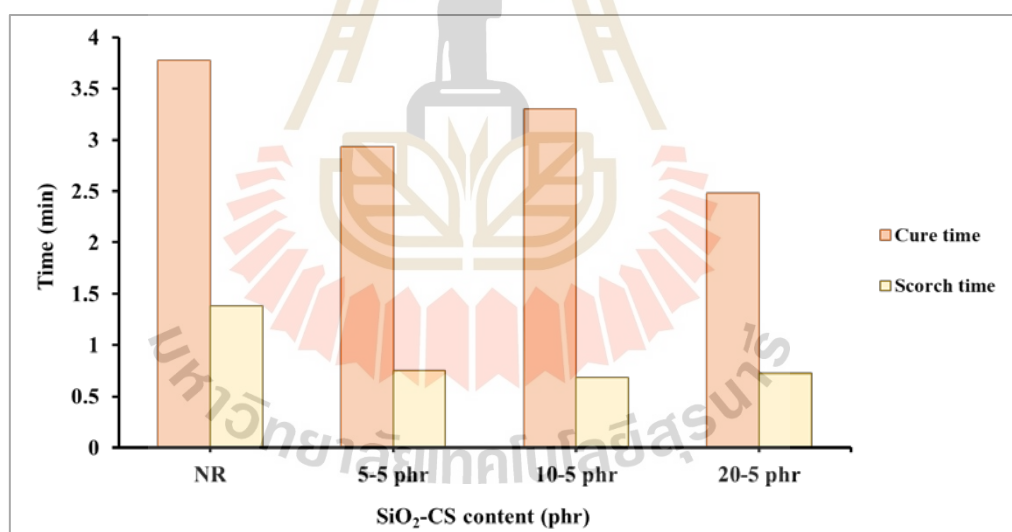


Figure 4.26 Effect of *in situ* SiO₂ content on cure time and scorch time of *in situ* SiO₂-CS/NR composites.

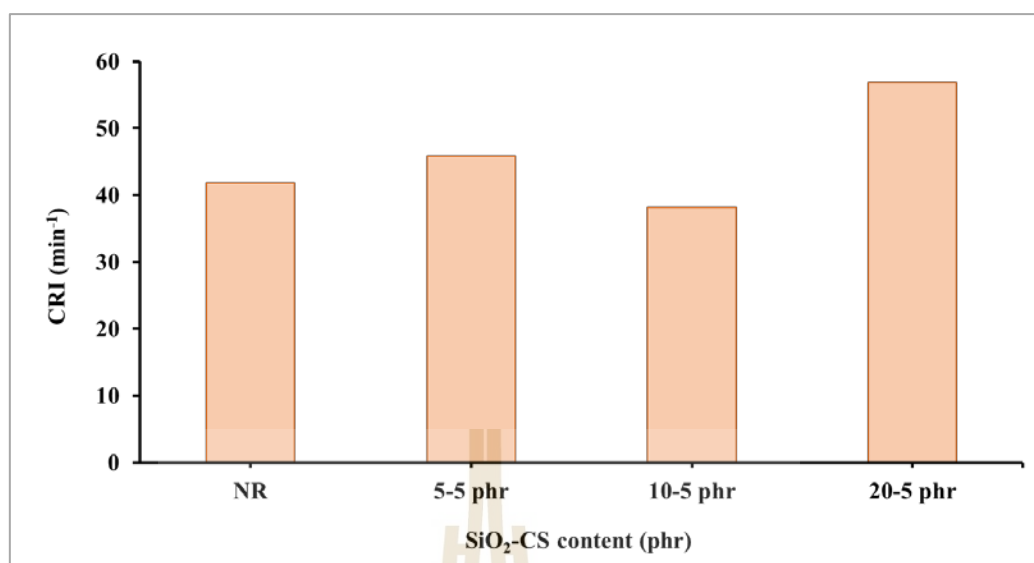


Figure 4.27 Effect of *in situ* SiO₂ content on CRI of *in situ* SiO₂-CS/NR composites.

Table 4.8 Cure characteristics of NR and *in situ* SiO₂-CS/NR composites.

Sample	ML (dNm)	MH (dNm)	ΔM (dNm)	α_f	t_{s1} (min)	t_{c90} (min)	CRI (min ⁻¹)
NR	1.02	15.50	14.48	-	1.38	3.77	41.84
NR/5SiO ₂ -5CS	3.72	40.05	36.33	18.14	0.75	2.93	45.87
NR/10SiO ₂ -5CS	3.86	35.36	31.50	9.81	0.68	3.30	38.17
NR/20SiO ₂ -5CS	4.49	31.98	27.49	4.86	0.72	2.48	56.82

4.5.3 Mechanical properties

Figure 4.28 and Figure 4.29 represent stress-strain curves and tensile strength of NR and NR composites with various *in situ* SiO₂-CS contents. Tensile strength increased from 13.21 to 22.06 MPa by adding 5-5 phr of *in situ* SiO₂-CS. However, tensile strength at 10-5 and 20-5 phr of *in situ* SiO₂-CS decreased when compared with 5-5 phr of *in situ* SiO₂-CS. This was due to poor interaction between matrix and filler caused by high filler–filler interaction. From Figure 4.35 was observed obviously that 10-5 and 20-5 phr have fine layer surface from more filler content which was confirmed the result of poor interaction. Moreover, tensile strength at 20-5 phr of *in situ* SiO₂-CS lower than unfilled NR. This may be due to the result of more rigid phase that caused NR composites more brittle. Tear strength of NR and NR composites are shown in Figure 4.33. The highest tear strength increased from 23.32 to 55.97 kN/m by adding 10-5 phr of *in situ* SiO₂-CS while its tensile strength slightly less than 5-5 phr of *in situ* SiO₂-CS.

Elongation at break of NR composites with various *in situ* SiO₂-CS contents is shown in Figure 4.30. Elongation at break decreased with increasing *in situ* SiO₂-CS content. Elongation at break of *in situ* SiO₂-CS/NR composites was decreased from 866.53% for 5-5 phr of *in situ* SiO₂-CS to 381.16% for 20-5 phr of *in situ* SiO₂-CS. This was due to the flexibility of NR chains were reduced by the presence of filler network throughout NR matrix.

Modulus at 100% elongation (M100), 300% elongation (M300), and hardness of NR and *in situ* SiO₂-CS/NR composites are shown in Figure 4.31, 4.32, and 4.34, respectively. M100, M300, and hardness of *in situ* SiO₂-CS/NR composites were

higher than unfilled NR and increased with increasing *in situ* SiO₂-CS content. This was because of the increment of rigid phase from the addition of *in situ* SiO₂-CS.

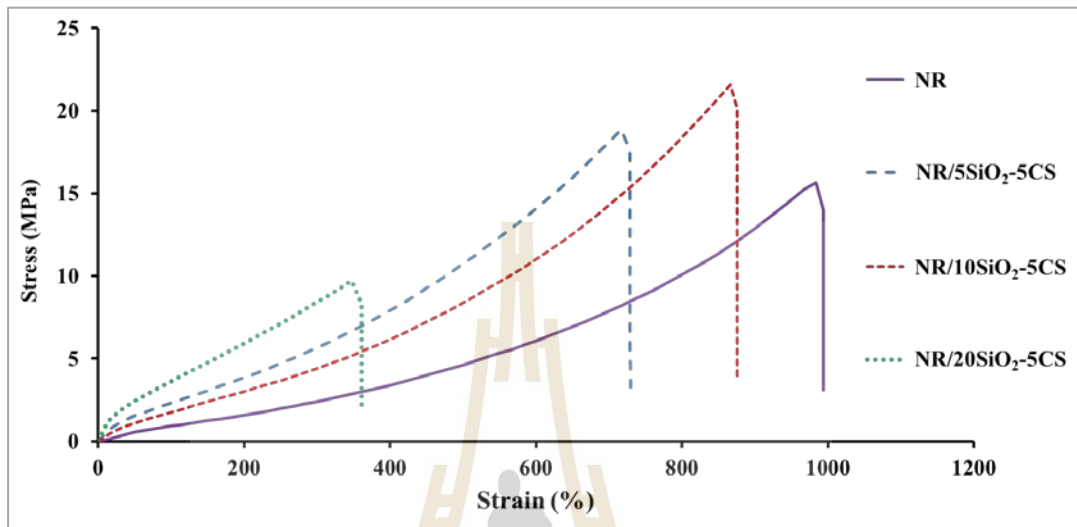


Figure 4.28 Stress-Strain curves of NR and *in situ* SiO₂-CS/NR composites at various SiO₂ contents.

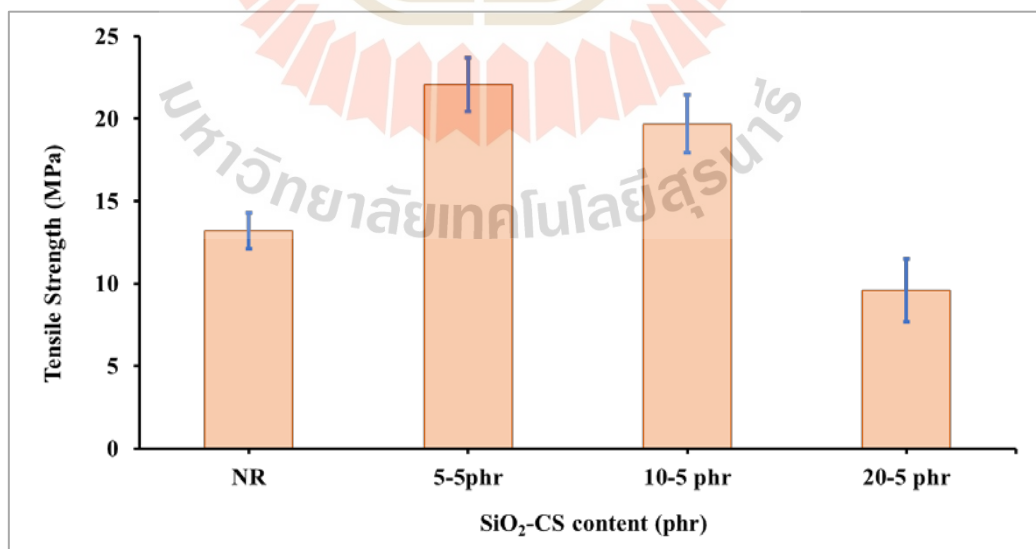


Figure 4.29 Effect of *in situ* SiO₂ content on tensile strength of *in situ* SiO₂-CS/NR composites.

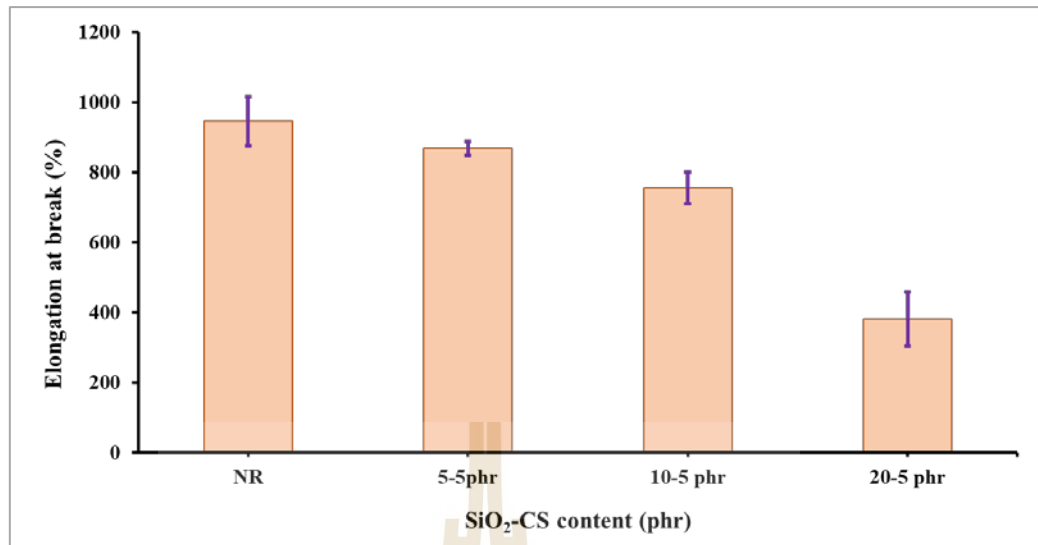


Figure 4.30 Effect of *in situ* SiO₂ content on elongation at break of *in situ* SiO₂-CS/NR composites.

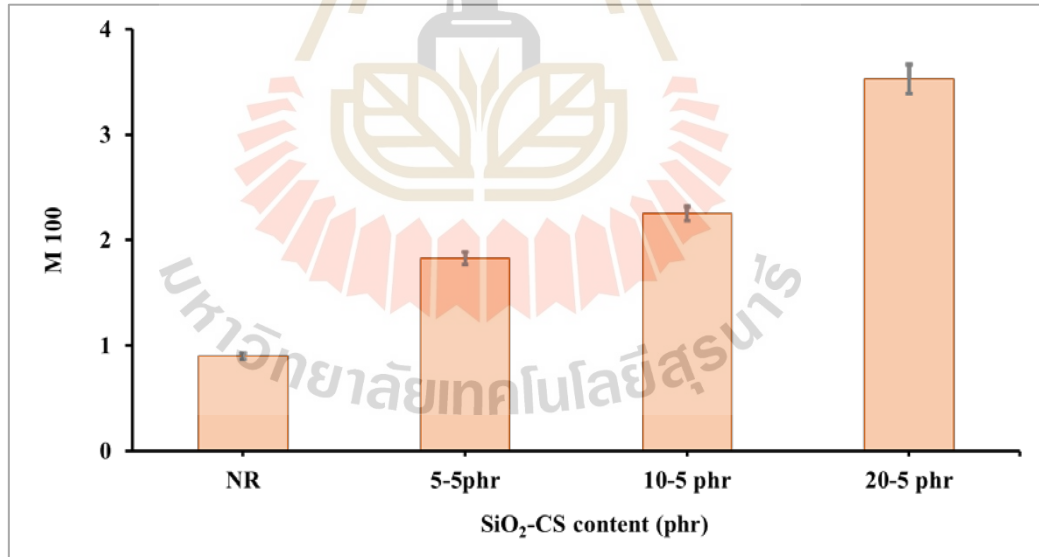


Figure 4.31 Effect of *in situ* SiO₂ content on M100 of *in situ* SiO₂-CS/NR composites.

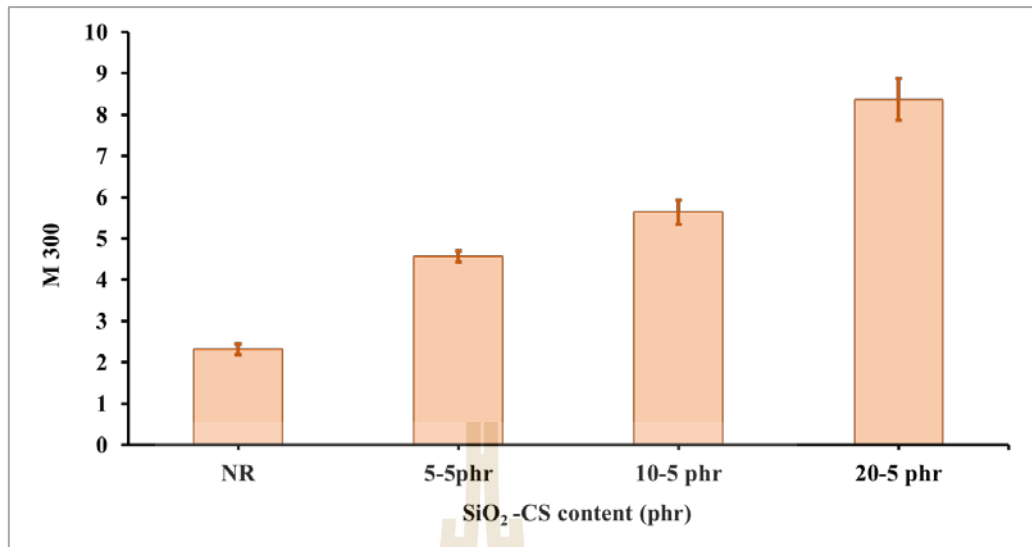


Figure 4.32 Effect of *in situ* SiO₂ content on M300 of *in situ* SiO₂-CS/NR composites.

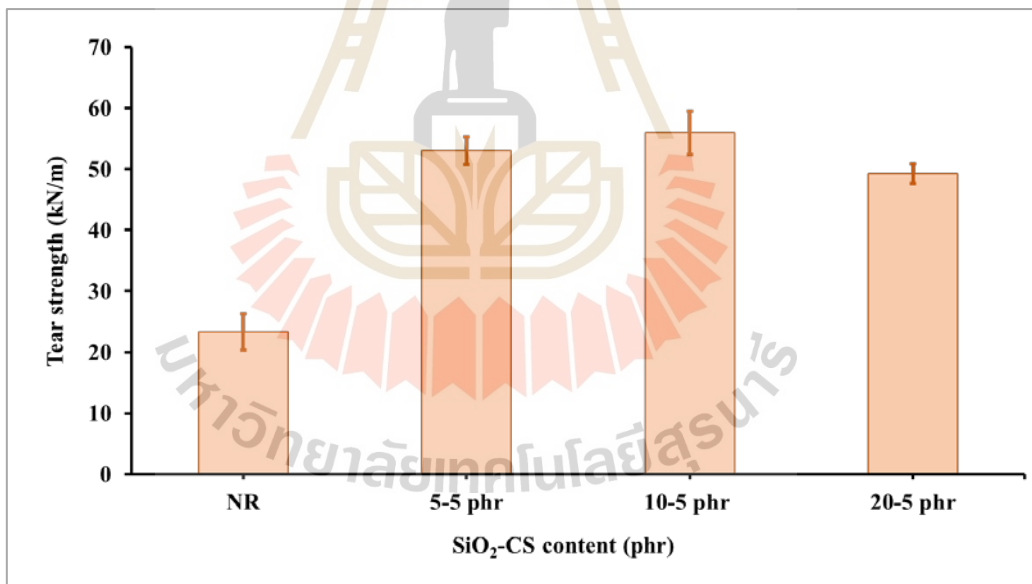


Figure 4.33 Effect of *in situ* SiO₂ content on tear strength of *in situ* SiO₂-CS/NR composites.

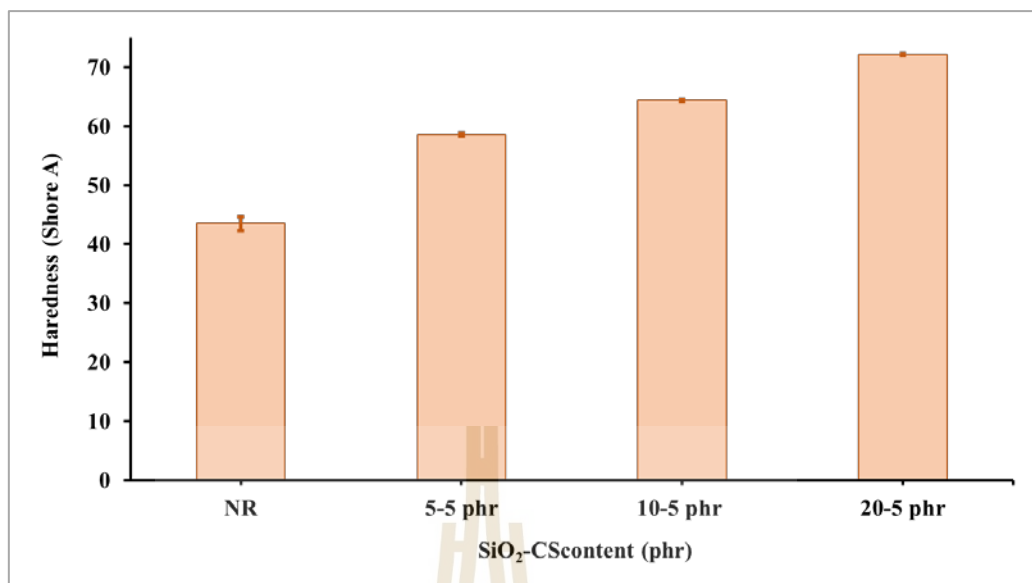


Figure 4.34 Effect of *in situ* SiO₂ content on hardness of *in situ* SiO₂-CS/NR composites.



Table 4.9 Mechanical properties of NR and *in situ* SiO₂-CS/NR composites.

Sample	Tensile strength (MPa)	Elongation at break (%)	M100 (MPa)	M300 (MPa)	Tear strength (kN/m)	Hardness (Shore A)
NR	13.21±1.07	944.60±70.00	0.90±0.03	2.32±0.13	23.32±2.96	43.47±1.68
NR/5SiO ₂ -5CS	22.06±1.64	866.53±19.39	1.83±0.06	4.56±0.16	53.04±2.24	58.53±0.25
NR/10SiO ₂ -5CS	19.69±1.78	753.93±45.40	2.25±0.07	5.64±0.29	55.97±3.54	64.37±0.15
NR/20SiO ₂ -5CS	9.59±1.92	381.16±77.39	3.53±0.14	8.37±0.51	49.25±1.60	72.10±0.20



4.5.4 Morphological properties

The morphology of NR and *in situ* SiO₂-CS/NR composite fractured surface are shown in Figure 4.35. The fractured surface of unfilled NR shows a smooth surface. On the contrary, the fractured surface of NR composites at 5-5, 10-5, and 20-5 phr of SiO₂-CS show a rough surface. At 150X magnification, each NR composite showed a similar surface. Each NR composite was observed that has many layer surfaces but the agglomeration of SiO₂ was not observed. However, the difference in their surface was observed at the higher magnification. The rough and thick layer surface of NR/5SiO₂-5CS was observed over its fracture surface while NR/10SiO₂-5CS and NR/20SiO₂-5CS have more fine layer surface than NR/5SiO₂-5CS due to more filler content caused the strong of matrix-filler interaction do not have enough. EDX mapping represents the good distribution of SiO₂ particles in all composites. It can be observed well distributed SiO₂ particles (white spot) as well as NR composites without CS.

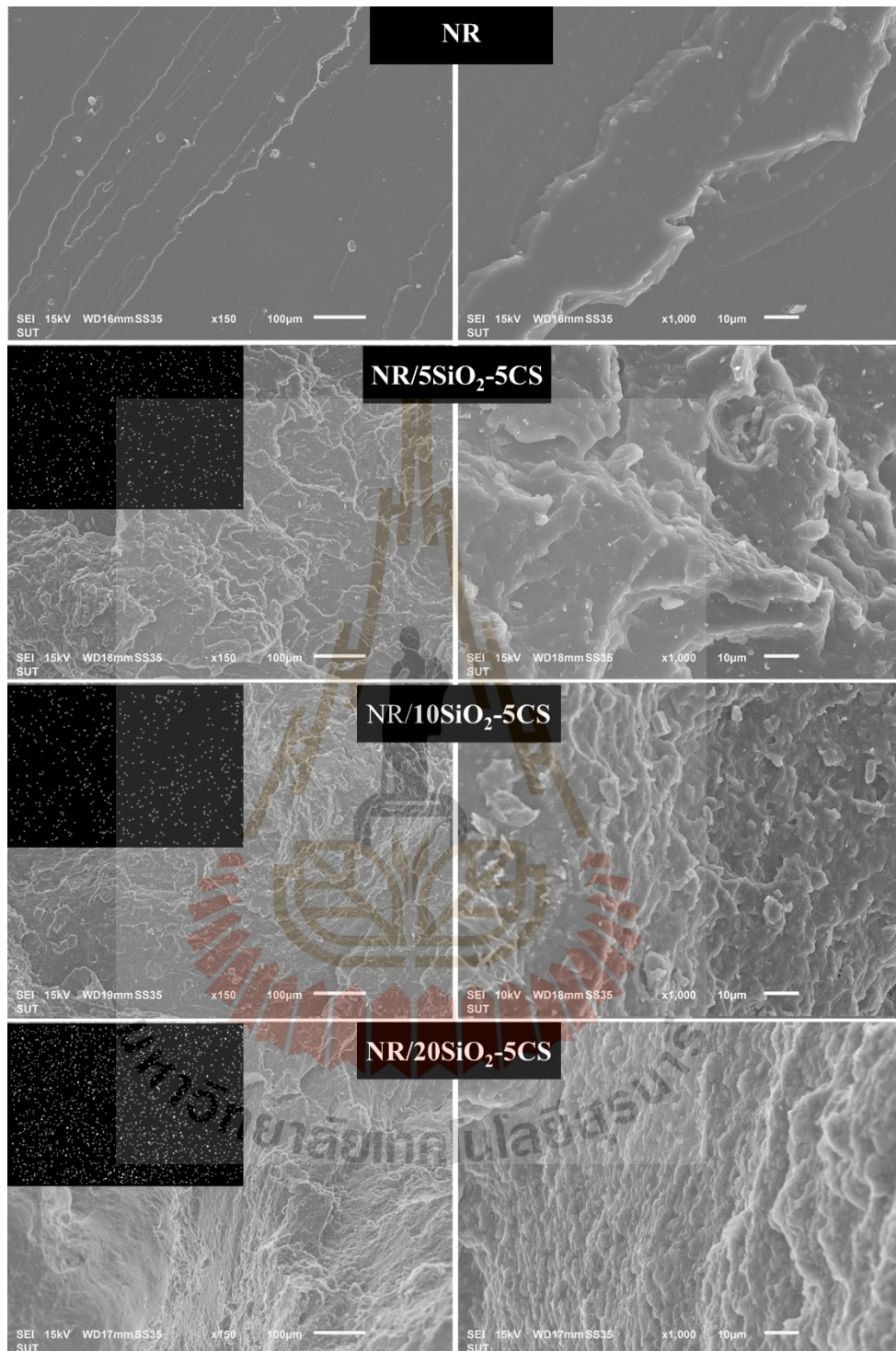


Figure 4.35 SEM micrographs of NR and SEM micrographs and their EDX mapping (left top of each micrograph) of *in situ* SiO₂-CS/NR composite fractured surface at 150X (left) and 1000X (right) magnification.

4.6 Effect of SiO₂-CS hybrid filler at various CS contents on the antimicrobial activity and absorption properties of *in situ* SiO₂-CS/NR composites

4.6.1 Antimicrobial activity

The effect of CS content on inhibition of microbial growth of the *in situ* SiO₂-CS/NR composite films are shown in Figure 4.33. The inhibition of microbial cell growth by CS was due to a positive charge of CS interferes with bacteria metabolism by stacking on the negative charge of bacterial surface (Benhabiles et al., 2012). The antibacterial activity of *in situ* SiO₂-CS/NR composite films were represented by inhibition zone or clear zone around the samples. All of composite films show the clear zone of *E. coli* inhibition and the highest diameter of the clear zone is 25 mm from NR/10SiO₂-5CS following by 20 mm from NR/10SiO₂-10CS and 12 mm from NR/10SiO₂-3CS. Although NR/10SiO₂-10CS has the most of CS content, its diameter of the clear zone was less than that of NR/S10iO₂-5CS. This may be due to the interaction of CS and other components which resulted in a decrease in its antimicrobial efficiency. For NR composites without CS, no clear zone was observed. This may be due to it does not have the active positive charge of CS. However, the antimicrobial activity of CS depends on molecular weight (MW) and degree of deacetylation (DD). Chitosan with a higher degree of deacetylation tends to have higher antimicrobial activity due to an increase in positive charges (Benhabiles et al., 2012).

Table 4.10 The diameter of inhibition zone of NR and NR composites.

Sample	CS content (phr)*	Clear zone diameter (mm)
NR	0	0
NR/10SiO ₂	0	0
NR/10SiO ₂ -3CS	3	12
NR/10SiO ₂ -5CS	5	25
NR/10SiO ₂ -10CS	10	20

*phr refer to parts per hundred rubber.

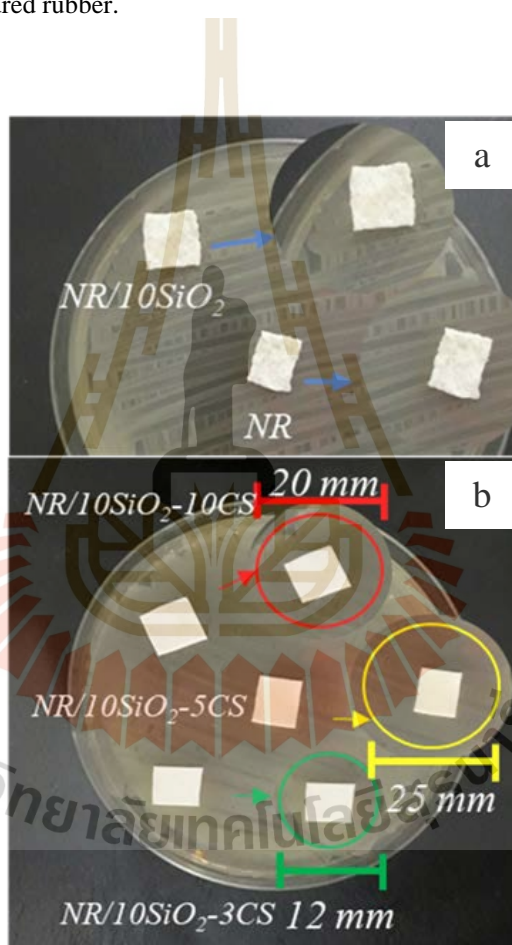


Figure 4.36 Effect of CS content on antimicrobial activity of *in situ* SiO₂-CS/NR composite films (a) without CS and (b) with CS.

4.6.2 Absorption properties

Water absorption behavior as a function of time of the *in situ* SiO₂-CS/NR composites was shown in Figure 4.37. The water absorbability of NR composites was increased with the addition of CS due to the hydrophilic nature of CS. However, water absorbability of NR/ 10SiO₂-10CS is less than NR/10SiO₂-3CS and NR/ 10SiO₂-5CS. This may be due to better interaction between NR and CS which shown by the FTIR in Figure 4.38.

FTIR spectrum of NR and the NR composites are shown in Figure 4.38. Basically, pure NR shows characteristic peak at 842 cm⁻¹ represented =CH out of plane bending. Peak at 1375 cm⁻¹ and 1432 cm⁻¹ are characteristic of CH₂ deformation and at the region between 2852-2925 cm⁻¹ represented the CH₂ symmetric stretching vibrations (Manohar et al., 2017) (Aiello et al., 2014). All of NR composites filled SiO₂ show a strong peak at 464 and 1086 cm⁻¹ that were attributed to the asymmetric bending vibration and the asymmetrical stretching vibration of Si-O-Si, respectively (Jarnthong et al., 2017) (Jembere, 2017). The region between 908-1259 cm⁻¹ of pure NR was intercepted by the asymmetrical stretching vibration of Si-O-Si in NR composites. NR composites filled CS, especially NR/10SiO₂-10CS shows a peak at 2350 cm⁻¹ that is a characteristic of N-H stretching. The height of the peak increased with increasing chitosan content. This may be due to the interaction between NR and CS or silanol groups of SiO₂ and CS (Johns and Rao, 2008). Each peak confirmed characteristic and presence of NR, SiO₂, and CS in the composites.

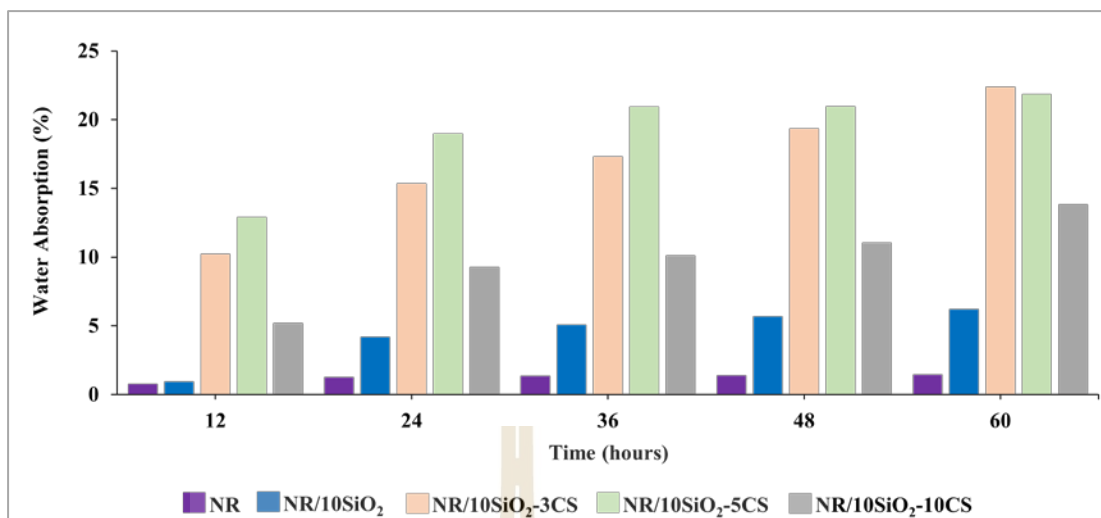


Figure 4.37 Effect of CS content on water absorption of NR composites.

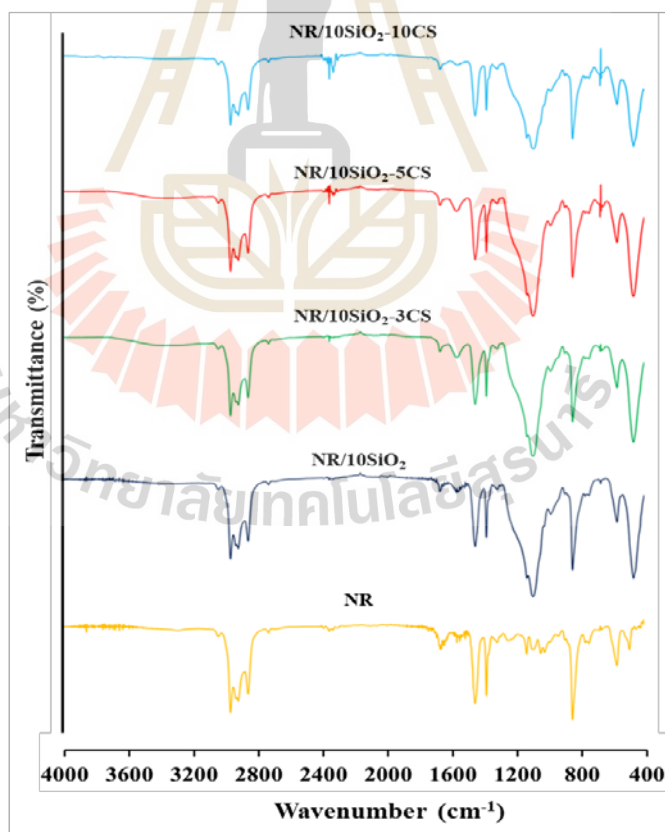


Figure 4.38 The FTIR spectrum of NR and the NR composites.

CHAPTER V

CONCLUSIONS

Agricultural waste like rice husk (RH) and shrimp shells were prepared as a filler and hybrid filler in natural rubber (NR) composites. Sodium silicate (Na_2SiO_3) solution was prepared from rice husk ash (RHA) which has 86.12% of silica (SiO_2) in the form of amorphous structure. The obtained chitosan (CS) was prepared from shrimp shells. It has only elements which are the major composition of CS. Its degree of deacetylation is 65% approximately and its average molecular weight is 642,000 Da.

Hybrid materials were prepared from the combination of RHSiO_2 and CS by sol-gel reaction of Na_2SiO_3 and CS solution at difference ratios of 1:1, 2:1, and 3:1 (SiO_2 -CS). The SiO_2 -CS ratio of 2:1 showed the optimum ratio which gave the material with the highest BET surface area and had a potential to use as a filler in composite materials.

NR composites from agricultural waste derived from RH SiO_2 and CS from shrimp shell waste were successfully prepared by a latex solution method. SiO_2 filler was added into NR matrix by sol-gel reaction of Na_2SiO_3 and acid solution then it became *in situ* of SiO_2 particles in NR phase. NR composites with *in situ* SiO_2 and *in situ* SiO_2 -CS at various contents of 0, 5, 10, and 20 phr SiO_2 were prepared. Effect of *in situ* SiO_2 content on cure characteristics, mechanical properties, and morphological properties of *in situ* SiO_2 /NR composites and *in situ* SiO_2 -CS/NR composites were investigated. The scorch time and cure time of *in situ* SiO_2 /NR composites and *in situ* SiO_2 -CS/NR composites were decreased by the addition of *in situ* SiO_2 and *in situ* SiO_2 -CS.

The mechanical properties of *in situ* SiO₂/NR composites, modulus at 100% elongation (M100), modulus at 300% elongation (M300), and hardness increased with increasing *in situ* SiO₂ content while tensile and tear strength increased with increasing *in situ* SiO₂ content up to 10 phr. Nevertheless, at 20 phr still has better properties than neat NR. Elongation at break of *in situ* SiO₂/NR composites was decreased by the addition of *in situ* SiO₂. SEM micrographs of *in situ* SiO₂/NR composites showed rough surface and many layers. The SiO₂ particles were observed from *in situ* SiO₂ at 5 phr.

The mechanical properties of *in situ* SiO₂-CS/NR composites, modulus at 100% elongation (M100), modulus at 300% elongation (M300), and hardness increased with increasing *in situ* SiO₂ content whereas elongation at break decreased. Tensile and tear strength increased with increasing *in situ* SiO₂ content up to 5 and 10 phr, respectively. SEM micrographs of *in situ* SiO₂-CS/NR composites showed rough surface and many layers same as *in situ* SiO₂/NR composites. Thick layer surface was observed at 5-5 phr of SiO₂-CS whereas, at 10-5 and 20-5 phr of SiO₂-CS have thin and fine surface.

Effect of SiO₂-CS hybrid filler at various CS contents on the antimicrobial activity and absorption properties of *in situ* SiO₂-CS/NR composites were investigated. All of the NR composites which was added CS show the clear zone of *E. coli* inhibition and the highest diameter of the clear zone is 25 mm for NR/10SiO₂-5CS following by 20 mm for NR/10SiO₂-10CS and 12 mm for NR/10SiO₂-3CS. The absorption of *in situ* SiO₂-CS/NR composites was increased by the addition of CS whereas, these properties of NR/10SiO₂-10CS is lower due to the interaction between NR and CS is better when compared with NR/10SiO₂-3CS and NR/10SiO₂-5CS.

REFERENCES

- Adams, F., Ikotun, B., Patrick, D., Mulaba-Bafubiandi, A. (2014). Characterization of Rice Hull Ash and Its Performance in Turbidity Removal from Water. **Particulate Science and Technology**. 32: 329-333.
- Aielo, P., Azevedo Borges, F., Romeira, K., Romeiro, C., Arruda, L., Lisboa-Filho, P., Herculano, R. (2014). Evaluation of Sodium Diclofenac Release Using Natural Rubber Latex as Carrier. **Materials Research**. 17: 146-152.
- Alaneme, K. K., Olubambi, P. (2013). Corrosion and wear behaviour of rice husk ash-Alumina reinforced Al-Mg-Si alloy matrix hybrid composites. **Journal of Materials Research and Technology**. 2(2): 188-194.
- Alothman, Z. (2012). A Review: Fundamental Aspects of Silicate Mesoporous Materials. **Materials**. 5: 2874-2902.
- Ameh, A. O., Isa, M. T., Mariam AYINLA, Bassey, S. O., Olatunji, B. M. (2015). Lactic acid demineralization of shrimp shell and chitosan synthesis. Available from: http://ljs.academicdirect.org/A26/get_html.php?htm=057_066
- Arayapranee, W., Na-Ranong, N., Rempel, G. L. (2005). Application of Rice Husk Ash as Fillers in the Natural Rubber Industry. **Journal of Applied Polymer Science**. 98: 34-41.
- Benhabiles, M. S., Salah, R., Lounici, H., Drouiche, N., Goosen, M. F. A., Mameri, N. (2012). Antibacterial activity of chitin, chitosan and its oligomers prepared from shrimp shell waste. **Food Hydrocolloids**. 29: 48-56.

- Boonrasri, S., Sae-Oui, P., Chaiharn, M. (2018). Effects of Chitosan Contents on Latex Properties and Physical Properties of Natural Rubber Latex/Chitosan Composites. **RMUTP Research Journal**. 12(1): 172-182.
- Budnyak, T. M., Pylypchuk, I. V., Tertykh, V. A., Yanovska, E., Kolodynska, D. (2015). Synthesis and adsorption properties of chitosan-silica nanocomposite prepared by sol-gel method. **Nanoscale Research Letters**. 10(87).
- Chen, D., Hu, M., Huang, C., Zhang, R. (2013) Preparation and properties of natural rubber composites and nanocomposites. **Natural Rubber Materials: Volume 2: Composites and Nanocomposites**. 2: 112-135
- Chen, X., Qiu, T. (2020). Natural rubber composites reinforced with basic magnesium oxysulfate whiskers: Processing and ultraviolet resistance/flame retardant properties. **Polymer Testing**. 81.
- Conradi, M. (2013). Nanosilica-Reinforcement Polymer Composites. **Materials Technology**. 47(3): 285-293.
- Da Costa, H., Visconte, L., Nunes, R. C., Furtado, C. (2002). Mechanical and dynamic mechanical properties of rice husk ash-filled natural rubber compounds. **Journal of Applied Polymer Science**. 83: 2331-2346.
- Dominic, M., Begum, P., Joseph, R., Joseph, D., Kumar, P. (2013). Synthesis, characterization and application of rice husk nanosilica in natural rubber. **International Journal of Science, Environment and Technology**. 2(5): 1027-1035.
- Ebisike, K., Okoronkwo, A. E., Alaneme, K. K. (2018). Synthesis and characterization of Chitosan-silica hybrid aerogel using sol-gel method. **Journal of King Saud University – Science**. “In press”

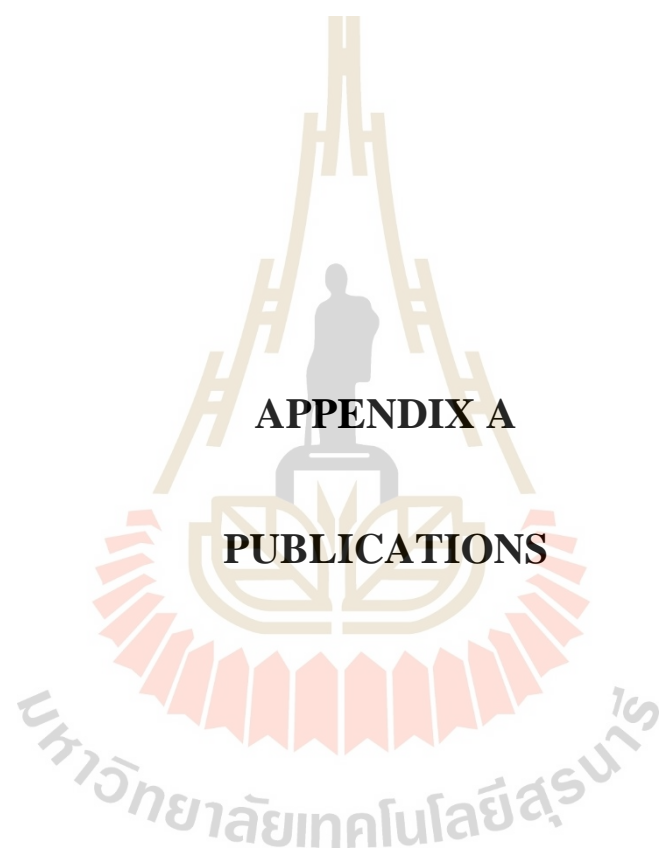
- Hajji, S., Younes, I., Ghorbel-Bellaaj, O., Hajji, R., Rinaudo, M., Nasri, M., Jellouli, K. (2014). Structural differences between chitin and chitosan extracted from three different marine sources. **International Journal of Biological Macromolecules**. 65: 298-306.
- Intom, S., Kalkornsurapranee, E., Johns, J., Kaewjaeng, S., Kothan, S., Hongtong, W., Kaewkhao, J. (2020). Mechanical and radiation shielding properties of flexible material based on natural rubber/ Bi₂O₃ composites. **Radiation Physics and Chemistry**. 172.
- Islam, S. Z., Khan, M., Alam, N. (2016). Production of chitin and chitosan from shrimp shell wastes. **Journal of the Bangladesh Agricultural University**. 14.
- Jarnthong, M., Liao, L.-S., Zhang, F.-Q., Wang, Y., Li, P., Peng, Z., Intharapat, P. (2017). Characterization of interaction between natural rubber and silica by FTIR (Vol. 1846).
- Jembere, A. (2017). Studies on the Synthesis of Silica Powder from Rice Husk Ash as Reinforcement Filler in Rubber Tire Tread Part: Replacement of Commercial Precipitated Silica. **International Journal of Materials Science and Applications**. 6.
- Jembere, A. L., Fanta, S. W. (2017). Studied on the Synthesis of Silica Powder from Rice Husk Ash as Reinforcement Filler in Rubber Tire Tread Past: Replacement of Commercial Precipitated Silica. **International Journal of Materials Science and Applications**. 6(1): 37-44.
- Johns, J., Rao, V. (2008). Characterization of Natural Rubber Latex/Chitosan Blends. **International Journal of Polymer Analysis and Characterization**. **International Journal of Polymer Analysis and Characterization**. 13: 280-291.

- Kawahara, S. (2018). Structure and Properties of Natural Rubber. **NIPPON GOMU KYOKAISHI**. 91: 143-150.
- Kickelbick, G. (2007) **Hybrid materials: Synthesis, Characterization, and Applications**. Betz-Druck GmbH, Darmstadt: Wiley-VCH.
- Knidri, H. E., Belaabed, R., Addaou, A., Laajeb, A., Lahsini, A. (2018). Extraction, chemical modification and characterization of chitin and chitosan. **International Journal of Biological Macromolecules**. 120: 1181–1189.
- Knidri, H. E., Khalfaouy, R. E., Laajeb, A., Addaou, A., & Lahsini, A. (2016). Eco-friendly extraction and characterization of chitin and chitosan from the shrimp shell waste via microwave irradiation. **Process Safety and Environmental Protection**. 104: 395-405.
- Korotkova, T. G, Ksandopulo, S. J, Donenko, A. P, Bushumov, S. A, Danilchenko, A. S. (2016). Physical Properties and Chemical Composition of the Rice Husk and Dust. **Oriental Journal of Chemistry**. 32(6).
- Kumar S., Sangwan, P., Dhankhar R., Mor V., Bidra S. (2013). Utilization of Rice Husk and Their Ash. **Research Journal of Chemical and Environmental Sciences**. 1(5): 126-129.
- Liou, T. H. (2004). Preparation and characterization of nano-structured silica from rice husk. **Materials Science and Engineering**. A (364): 313-323.
- Liou, T. H., Yang, C. C. (2011). Synthesis and surface characteristics of nanosilica produced from alkali-extracted rice husk ash. **Materials Science and Engineering**. B (176): 521-529.
- Manohar, N., Jayramudu, J., Suchismita, S., Rajkumar, K., Babulreddy, A., Sadiku, E. R., Maurya, D. J. (2017). A unique application of second order derivative FTIR–

- ATR spectra for compositional analyses of natural rubber and polychloroprene rubber and their blends. **Polymer Testing**. 62.
- Ming-zhe, L., Li-feng, W., Lei, F., Pu-wang, L., Si-dong, L. (2017). Preparation and properties of natural rubber/chitosan microsphere blends. **Micro & Nano Letters**. 12(6): 386–390.
- Moosa, A. A., Saddam, B. F. (2017). Synthesis and Characterization of Nanosilica from Rice Husk with Application to Polymer Composites. **American Journal of Materials Science**. 7(6): 223-231.
- Oyelaran, O., Tudunwada, Y. Y. (2014). Characterization of Garko and Kura Rice Husks. **American Journal of Engineering Research**. 240-244.
- Poompradub, S., Thirakulrati, M., Prasassarakich, P. (2014). In situ generated silica in natural rubber latex via sol-gel technique and properties of the silica rubber composites. **Materials Chemistry and Physics**. 144: 122-131.
- Raheem, A. A., Kareem, M. (2017). Chemical Composition and Physical Characteristics of Rice Husk Ash Blended Cement. **International Journal of Engineering Research in Africa**. 32: 25-35.
- Rambo, M., Cardoso, A., Bevilaqua, D., Rizzetti, T., Ramos, L., Korndorfer, G., Martins, A. (2011). Silica from Rice Husk Ash as an Additive for Rice Plant. **Journal of Agronomy**. 10: 99-104.
- Rao, V., Johns, J. (2008). Mechanical Properties of Thermoplastic Elastomeric Blends of Chitosan and Natural Rubber Latex. **Journal of Applied Polymer Science**. 107: 2217-2223.
- Shen, Y. (2017). Rice Husk silica derived nanomaterials for sustainable applications. **Renewable and Sustainable Energy Reviews**. 80: 453-466.

- Songsaeng, S., Thamyongkit, P., Poompradub, S. (2019). Natural rubber/reduced-graphene oxide composite materials: Morphological and oil adsorption properties for treatment of oil spills. **Journal of Advanced Research**. 20: 79-89.
- Suwandittakul, P., Montha, S., Kongkaew, C., Kongkaew, A., Phanpheng, K., Wiriyasontorn, S. (2018). Preparation of In Situ Silica filled natural Rubber by Sol-Gel Reaction of Sodium Silicate in natural Rubber Latex. **RAW MATERIALS AND APPLICATIONS**. 4: 46-53.
- Tabaei T.A, Bagheri R, Hesami, M (2015) Comparison of cure characteristics and mechanical properties of nano and micro silica-filled CSM elastomers. **Journal of Applied Polymer Science**.
- Thailand Convention and Exhibition Bureau (TCEB). TIRE AND RUBBER INDUSTRY OF THAILAND. October 24, 2019. Thailand Convention and Exhibition Bureau (TCEB).TIRE AND RUBBER INDUSTRY OF THAILAND. October 24, 2019. Available from: <https://intelligence.bussinesseventsthailand.com/en/industry/tire-and-rubber>.
- Thongpin, C., Sripethdee, C., Rodsantiea, R. (2011). Cure characteristic, mechanical properties, and morphology of in-situ silica-gel/NR composites. **ICCM International Conferences on Composite Materials**.
- Todkar, B. S., Deorukhkar, O. A., Deshmukh, S. M. (2016). Extraction of Silica from Rice Husk. **International Journal of Engineering Research and Development**. 12(3): 69-74.
- Tuan, L. N. A., Dung, L. T. K., Ha, L. D. T., Hien, N. Q., Phu, D. V., Du, B. D. (2017). Preparation and characterization of nanosilica from rice husk ash by chemical

- treatment combined with calcination. **Vietnam Journal of Chemistry**. 55(4): 455-459.
- Wei Y, Zhang H, Wu L. (2017) A review on characterization of molecular structure of natural rubber. **MOJ Polymer Science**. 1(6):197-199.
- Yasmeen, S., Kabiraz1, M. K., Saha, B., Qadir, Md. R., Gafur Md. A. and. Masum, S. Md. (2016). Chromium (VI) Ions Removal from Tannery Effluent using Chitosan-Microcrystalline Cellulose Composite as Adsorbent. **International Research Journal of Pure and Applied Chemistry**. 10(4): 1-14.
- Yeh, J.T., Chen, C.L., Huang, K.S. (2007). Synthesis and properties of chitosan/SiO₂ hybrid materials. **Materials Letters**. 61: 1292-1295.
- Yu, Z., Li, B., Chu, J., Zhang, P. (2018). Silica in situ enhanced PVA/chitosan biodegradable films for food packages. **Carbohydrate Polymers**. 184: 214-220.
- Yuvakkumar, R., Elango, V., Kannan, N. (2012). High-purity nano silica powder from rice husk using a simple chemical method. **Journal of Experimental Nanoscience**. 1: 1-10.
- Zhuravlev, L. T. (2000). The surface chemistry of amorphous silica. Zhuravlev model. **Colloids and Surfaces**. 173: 1-38.



APPENDIX A

PUBLICATIONS

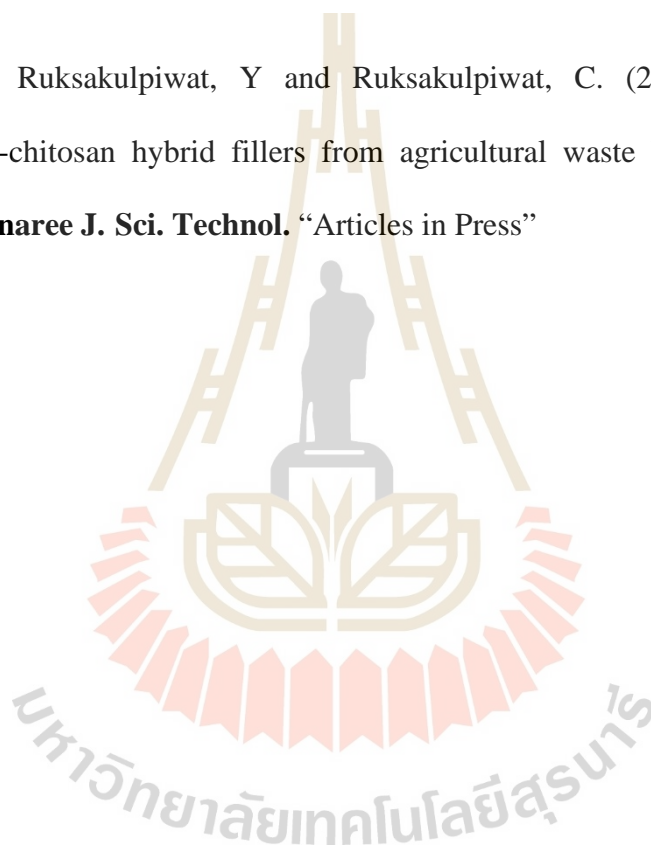
List of Publications

Injorhor, P., Ruksakulpiwat, Y and Ruksakulpiwat, C. (2020). Effect of shrimp shell chitosan loading on antimicrobial, absorption and morphological properties of natural rubber composites reinforced with silica-chitosan hybrid filler.


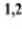

Biointerface Res. Appl. Chem. 10(3): 5656-5659.

Injorhor, P., Ruksakulpiwat, Y and Ruksakulpiwat, C. (2020). Preparation of silica-chitosan hybrid fillers from agricultural waste by sol-gel technique.

Suranaree J. Sci. Technol. “Articles in Press”



Effect of shrimp shell chitosan loading on antimicrobial, absorption and morphological properties of natural rubber composites reinforced with silica-chitosan hybrid filler

Preeyaporn Injorhor^{1,2} , Yupaporn Ruksakulpiwat^{1,2} , Chaiwat Ruksakulpiwat^{1,2,*} 

¹School of Polymer Engineering, Institute of Engineering, Suranaree University of Technology, Muang, Nakhon Ratchasima 30000, Thailand

²Center of Excellence on Petrochemical and Materials Technology, Chulalongkorn University, Bangkok 10330, Thailand

*corresponding author e-mail address: charuk@sut.ac.th | Scopus ID 57191342194

ABSTRACT

The natural rubber composites reinforced with hybrid filler between silica from rice husk and chitosan from shrimp shell were prepared by a latex solution method. The amount of shrimp shell chitosan was varied as 0, 3, 5, and 10phr with a constant amount of rice husk silica at 10phr. The natural rubber composites with hybrid filler were prepared before mixing with vulcanizing agents using conventional curing system. The antimicrobial, absorption, and morphological properties of the natural rubber composite films and cured composites were investigated by the Agar Diffusion Method, Water Absorption Test and Scanning Electron Microscopy (SEM), respectively. Using 5phr of chitosan shows the optimum properties for used as filler incorporated with silica in natural rubber composites for medical applications.

Keywords: natural rubber composites; rice husk silica; shrimp shell chitosan; hybrid filler; antimicrobial activity; water absorption; morphological properties.

1. INTRODUCTION

Chitosan is an amino-polysaccharide extracted from chitin which is the second biopolymer on earth. The sources of chitin are not only in the shells of shrimp and crab but also can be obtained in some insects and certain fungi. Chitosan is a biocompatible and biodegradable polymer. Moreover, it has antimicrobial activity [1-2]. A lot of research has focused on the utilize of chitosan as antimicrobial materials in biomedical applications [3-5]. Chitosan blended with natural rubber latex directly was shown to improve its thermal stability, mechanical, hydrophilic, and antimicrobial properties of natural rubber [6-7].

Rice husk is an agricultural waste from the rice milling process. Rice husk ash was used as a silica source that contained more than 60% of amorphous silica with high surface area, porosity and reactivity [8-11]. Silica plays an important role in some mechanical properties of natural rubber composites, not only to improve tensile strength, modulus, hardness, and wet traction but also reduce rolling resistance. To improve the ability of silica dispersion in natural rubber matrix, in-situ silica by sol-gel method was used for rubber composite preparation. Sodium silicate prepared from silica ash dissolution in sodium hydroxide was used as a precursor and it was become gel by acid solution [12-16].

Natural rubber or cis 1,4-polyisoprene is an elastomeric material that derived from the sap of rubber tree also known as natural rubber latex that contains the natural rubber hydrocarbon in a fine emulsion form in an aqueous serum [17]. It is an important economic crop in Thailand due to natural rubber products are the number one agricultural product with the highest export volume in the country. Natural rubber has the advantage namely low cost, renewable materials, and use in a variety of applications [18].

Many researchers have been prepared natural rubber composites reinforced with silica derived from rice husk or prepare natural rubber composites reinforced with chitin or chitosan that derived from shrimp shells to improve their properties [19-20]. In this work, natural rubber composites reinforced with both filler (silica-chitosan) were prepared and investigated their properties such as the antimicrobial properties, the absorption properties, and the morphological properties.

The aim of this work is to investigate the effect of shrimp shell chitosan on antimicrobial properties, absorption properties and morphological properties of natural rubber composites reinforced with silica-chitosan hybrid filler. Natural rubber composites were prepared by the latex solution method.

2. MATERIALS AND METHODS

2.1. Materials.

High ammonia natural rubber latex (HA Latex) was purchased from Viroonkit Industry Co., Ltd. (Thailand). It contains 60% Dry Rubber Content (DRC) and 0.7% ammonia. Shrimp shell chitosan (CS) with a degree of deacetylation of 65% and average molecular weight of 181×10^3 Da were prepared in our laboratory. Sodium silicate solution was prepared by dissolving rice husk silica ash (86% of SiO₂) with 2.5% of sodium hydroxide. Other chemicals for rubber compounding such as

stearic acid, zinc oxide, N-cyclohexyl-2-benzothiazole-2-sulfenamide (CBS) and sulphur were supported by Innovation Group (Thailand) Ltd.

2.2. Preparation of natural rubber composite films reinforced by silica-chitosan hybrid filler.

10phr of silica in the form of sodium silicate solution was added into NR latex that was diluted into 30% of DRC by distilled water. They were stirred for 12 hours until obtaining a homogeneous mixture. The dissolution of shrimp shell chitosan

Effect of shrimp shell chitosan loading on antimicrobial, absorption and morphological properties of natural rubber composites reinforced with silica-chitosan hybrid filler

with 2% acetic acid was used to prepare the chitosan solution. Then chitosan solution at various chitosan contents (0, 3, 5, and 10phr) was then added to the mixture of natural rubber latex and sodium silicate in order to precipitate silica in rubber latex. The pH of the mixture was adjusted to 7 by using 2% acetic acid. The mixtures were stirred for 6 hours and cast into Petri dishes before oven-dried at 60°C for 2 days to obtain composite films.

2.3. Preparation of vulcanized natural rubber composites.

The composite films were compounded by a two-roll mill machine. The ingredients for compounding were shown in Table 1. The compounding was started by mastication of NR composite film before adding stearic acid, ZnO, CBS and sulphur. After mixing 15 min, the compound was stored for 24 hours at room temperature. Curing time of the compound was determined by Moving Die Rheometer (MDR) at 150°C. The compounds were vulcanized in a hydraulic press at 150°C with a pressure of 150 kg/cm² with the curing time from MDR testing.

2.4. Characterization of natural rubber composite films.

2.4.1 Fourier transform infrared spectroscopy (FTIR)

FTIR spectrometer was used to identify the functional groups of the composite films. The frequency range 4000 - 400 cm⁻¹ at resolution of 4 cm⁻¹.

2.4.2 Antimicrobial Activity

The antimicrobial activity of the composite films was evaluated using the agar diffusion method. *Escherichia coli*

(*E.coli*) bacteria was used for testing the antimicrobial activity. The composite films were placed on Mueller Hinton agar medium that had been seeded with 10⁵cfu/ml (Colony Forming Units/mL) of the *E.coli*. The plates were incubated at 37°C for 24 hours. The antimicrobial properties of the composite films were observed from an inhibitory effect of microbial growth by measured the diameter of the inhibition zone around the composite films and cured composites.

2.4.3 Absorption Test

The cured composite samples were cut into 10x10 mm square sheet with thickness of 1 mm. Each sample was oven dried at 80°C and they were cooled in desiccator before weighing (W_1) then placed in Erlenmeyer flasks of distilled water for 2 days at a temperature of 37°C in the oven. After that, they were taken out from the oven and wiped with a tissue paper before weighing (W_2). The water absorption was calculated as follows:

$$\% \text{ Absorption} = \frac{W_2 - W_1}{W_1} \times 100 \quad (\text{Eq. 1})$$

2.4.4 Scanning Electron Microscopy (SEM)

The surface morphology of the composite films was observed using SEM. The samples were cut into small pieces then were dried and coated with gold by a sputter coater before testing.

Table 1. Compounding formulations.

Sample	NR (phr) ^a	SiO ₂ (phr) ^a	Chitosan (phr) ^a	Stearic acid(phr) ^a	ZnO (phr) ^a	CBS (phr) ^a	Sulphur (phr) ^a
NR	100	-	-	1	5	1.2	3
NR/SiO ₂ 10	100	10	-	1	5	1.2	3
NR/SiO ₂ 10-CS3	100	10	3	1	5	1.2	3
NR/SiO ₂ 10-CS5	100	10	5	1	5	1.2	3
NR/SiO ₂ 10-CS10	100	10	10	1	5	1.2	3

^apart per hundred rubber

3. RESULTS

3.1. FTIR spectral analysis.

FTIR spectrum of NR and the composite films is shown in Figure 1.

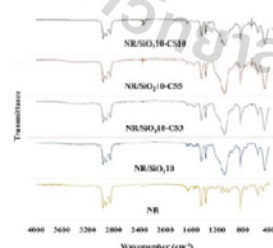


Figure 1. The FTIR spectrum of NR and the composite films

Basically, pure NR shows characteristic peak at 842 cm⁻¹ represented =CH out of plane bending. Peak at 1375 cm⁻¹ and 1432 cm⁻¹ are characteristic of CH₂ deformation and at the region 2852-2925 cm⁻¹ represented the CH₂ symmetric stretching vibrations [21-22]. All of NR composites filled SiO₂ show a strong peak at 464 and 1086 cm⁻¹ that were attributed to the asymmetric bending vibration and the asymmetrical stretching vibration of Si-O-Si, respectively [23-24].

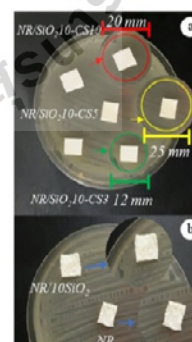


Figure 2. Effect of chitosan loading on antimicrobial activity of natural rubber composite films (a) with CS and (b) without CS.

The region between 908-1259 cm⁻¹ of pure NR was intercepted by the asymmetrical stretching vibration of Si-O-Si in NR composites. NR composites filled chitosan, especially NR/SiO₂10-CS10 show a peak at 2350 cm⁻¹ that is a characteristic of N-H stretching. The height of the peak increased with

increasing chitosan content. This may be due to the interaction between NR and chitosan or silanol groups of SiO₂ and chitosan [25]. Each peak confirmed the characteristic and presence of NR, SiO₂, and chitosan in the composites.

3.2. Antimicrobial properties.

The effect of chitosan loading on inhibition of microbial growth of the composite films and cured composites is shown in Table 2, Figure 2, and Figure 3.

The inhibition of microbial cells growth by chitosan was due to a positive charge of chitosan interferes with bacteria metabolism by stacking on the negative charge of bacterial surface [5].

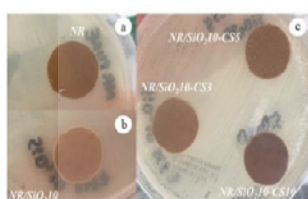


Figure 3. Effect of chitosan loading on antimicrobial activity of cured natural rubber composite (a) and (b) without CS and (c) with CS.

The antibacterial activity of the composite films and cured composites were represented by inhibition zone or clear zone around the samples. All of the composite films show the clear zone of *E. coli* inhibition and the highest diameter of the clear zone is NR/SiO₂/10-CS5 following by NR/SiO₂/10-CS10 and NR/SiO₂/10-CS3. Although NR-SiO₂/10-CS10 has the most of chitosan loading, its diameter of the clear zone was less than that of NR/SiO₂/10-CS5. This may be due to the interaction of chitosan and other components which resulted in a decrease in its antimicrobial efficiency. For cured composites, no clear zone was observed. This may be due to the unactive positive charge of chitosan. However, the antimicrobial activities of chitosan depend on molecular weight (Mv) and the degree of deacetylation (DD). Chitosan with a higher degree of deacetylation tends to have higher antimicrobial activity due to an increase in positive charges [5].

Table 2. The diameter of inhibition zone of natural rubber and natural rubber composites.

CS content (phr)	Composite Films			Cured Composites		
	3	5	10	3	5	10
Clear Zone diameter (mm)	12	25	20	0	0	0

3.3. Absorption properties.

The water absorption behavior as a function of time of the cured composites was shown in Figure 4. The water absorbability

4. CONCLUSIONS

Natural rubber composites reinforced with hybrid filler between rice husk silica and shrimp shell chitosan were successfully prepared by a latex solution method. All of NR composites that with the addition of shrimp shell chitosan show antimicrobial activity. The most efficient *E. coli* inhibition and the

5. REFERENCES

1. Sagheer, F.A.A.; Al-Sughayer, M.A.; Muslim, S.; Elsabee, M.Z. Extraction and characterization of chitin and chitosan from

of NR composite was increased with the addition of chitosan due to the hydrophilic nature of chitosan. However, water absorbability of NR/SiO₂/10-CS10 is less than NR/SiO₂/10-CS3 and NR/SiO₂/10-CS5. This may be due to better interaction between NR and chitosan which shown by the FTIR.

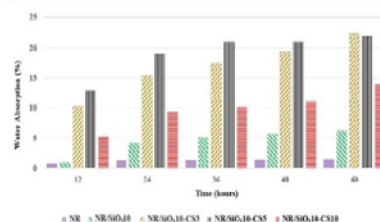


Figure 4. Graph of water absorption

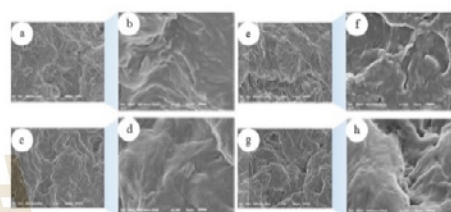


Figure 5. SEM micrographs showing the surface of natural rubber composites reinforced with silica and hybrid filler between silica and chitosan at 100X and 1000X magnification (a), (b) NR/SiO₂/10-CS3, (c), (d) NR/SiO₂/10-CS5, (e), (f) NR/SiO₂/10-CS10 and (g), (h) NR/SiO₂/10

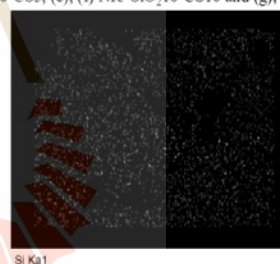


Figure 6. Energy dispersive X-ray (EDX) mapping analysis of silicon in NR/SiO₂/10 composite.

3.4. Morphological properties.

SEM micrographs of the composite films are shown in Figure 5. All of the samples show the same surface morphology and no agglomeration of silica and incompatible zone in NR matrix. Si atoms are dispersed on the surface of the composites, as shown in the SEM-EDX mapping images in Figure 6.

absorption properties suitable for use as wound dressing was obtained from NR composite with 5 phr shrimp shell chitosan. Each NR composites show the same surface morphology. The silica agglomerate was not shown.

marine sources in Arabian Gulf. *Carbohydr. Polym.* **2009**, *77*, 410-419, <https://doi.org/10.1016/j.carbpol.2009.01.032>.

Effect of shrimp shell chitosan loading on antimicrobial, absorption and morphological properties of natural rubber composites reinforced with silica-chitosan hybrid filler

2. Bastiaens, L.; Soetemans, L.; D'Hondt, E.; Elst, K. Sources of Chitin and Chitosan and their Isolation. In: *Chitin and Chitosan: Properties and Applications*. 1st ed.; Lambertus, A.M.; van den, B.; Carmen, G.B.; eds; John Wiley & Sons Ltd.; USA. 2020; pp.1-34, <https://doi.org/10.1002/9781119450467.ch1>.
3. Islam, M.M.; Masum, S.M.; Mahub, K.R.; Haque, M.Z. Antibacterial Activity of Crab-Chitosan against *Staphylococcus aureus* and *Escherichia coli*. *J Adv Scient Res*. **2011**, *2*, 63-66.
4. Mohandas, A.; Deepthi, S.; Biswas, R.; Jayakumar, R. Chitosan based metallic nanocomposite scaffolds as antimicrobial wound dressings. *J Bio Act Mat*. **2018**, *3*, 267-277, <https://doi.org/10.1016/j.bioactmat.2017.11.003>.
5. Benhabiles, M.S.; Salah, R.; Lounici, H.; Drouiche, N.; Goosen, M. F. A.; Mameri, N. Antibacterial activity of chitin, chitosan and its oligomers prepared from shrimp shell waste. *J. Food. Hyd.* **2012**, *29*, 48-56, <https://doi.org/10.1016/j.foodhyd.2012.02.013>.
6. Lv, M.; Wang, L.; Fang, L.; Li, P.; Li, S. Preparation and properties of natural rubber/chitosan microsphere blends. *Micro Nano Lett*. **2017**, *12*, <https://doi.org/10.1049/mnl.2016.0775>.
7. Boonrasri, S.; Sae-Oui, P.; Chaiham, M. Effects of Chitosan Contents on Latex Properties and Physical Properties of Natural Rubber Latex/Chitosan Composites. *RMUTP Research Journal* **2018**, *1*, 72-82, <https://doi.org/10.14456/jrmtp.2018.15>.
8. Todkar, B.S.; Deorukhkar, O.A.; Deshmukh, S.M. Extraction of Silica from Rice Husk. *Int. J. Eng. Res. Dev.* **2016**, *12*, 69-74.
9. Zarib, N.S.M.; Abdullah, S.A.; Jamil, N.H. Extraction of Silica from Rice Husk Via Acid Leaching Treatment. Proceedings of the 2018 Asia International Multidisciplinary Conference, Universiti Teknologi, Malaysia, 2018, pp. 175-183, <https://doi.org/10.15405/epsbs.2019.05.02.16>.
10. Azat, S.; Korobeinyk, A.V.; Moustakas, K.; Inglezakis, V.J. Sustainable production of pure silica from rice husk waste in Kazakhstan. *J. Clean. Prod.* **2019**, *217*, 352-359, <https://doi.org/10.1016/j.jclepro.2019.01.142>.
11. Zou, Y.; Yang, T. Rice Husk, Rice Husk Ash and Their Applications. In: *Rice Bran and Rice Bran Oil*. Elsevier Inc.; Netherlands. 2019; pp. 207-246, <https://doi.org/10.1016/B978-0-12-812828-2.00009-3>.
12. Surya, I.; Hayemasae, N. Reinforcement of natural rubber and epoxidized natural rubbers with fillers. *J. Eng. Sci. Technol.* **2019**, *1*, 12-21, <https://doi.org/10.32734/jet.v1i1.682>.
13. Moosa, A.; Saddam, B. Synthesis and Characterization of Nanosilica from Rice Husk with Applications to Polymer Composites. *Am. J. Mater. Sci.* **2017**, 223-231.
14. Poompradub, S.; Thirakulrati, M.; Prasassarakich, P. In situ generated silica in natural rubber latex via the sol-gel technique and properties of the silica rubber composites. *Mater. Chem. Phys.* **2014**, *144*, 122-131, <https://doi.org/10.1016/j.matchemphys.2013.12.030>.
15. Suwandittakul, P.; Montha, S.; Kongkaew, C.; Kongkaew, A.; Phanpheng, K.; Wiriyasontorn, S. Preparation of in situ silica filled natural rubber by sol-gel reaction of sodium silicate in natural rubber latex. *KGK Kautschuk Gummi Kunststoffe* **2018**, *71*, 46-53.
16. Maitra, S.; Mukherjee, S.; Yadav, V. Synthesis and Characterization of Nano Silica from Rice Husk Ash. *Indian Sci. Cruiser* **2018**, *32*, 25-31, <https://doi.org/10.24906/isc/2018/v32/i4/176489>.
17. Kawahara, S. Structure and Properties of Natural Rubber. *Nippon Gomu Kyokaishi* **2018**, *91*, 143-150, <https://doi.org/10.2324/gomu.91.143>.
18. Thongpin, C.; Sripethdee, C.; Rodsantiea, R. Cure characteristic, mechanical properties and morphology of in-situ silica-gel/NR composites. Proceedings of the 18th ICCM International Conferences on Composite Materials 2011, Jeju Island, Korea, 21st to 26th of August 2011.
19. Ibrahim, N.; Shokri, A.; Kamarun, D.; Faiza, M. Cure characteristic and mechanical properties of natural rubber vulcanizates with digested rice husk ash (RHA). Proceedings of the 3rd International Conference on Mechanical Engineering (ICOME 2017), Jawa Timur, Indonesia, 5th to 6th of October 2017, <https://doi.org/10.1063/1.5047188>.
20. Petchsoongsakul, T.; Dittanet, P.; Loykulnant, S.; Kongkaew, C.; Prapainainar, P. Synthesis of Natural Composite of Natural Rubber Filling Chitosan Nanoparticles. *Key Engineering Materials* **2019**, *821*, 96-102, <https://doi.org/10.4028/www.scientific.net/KEM.821.96>.
21. Manohar, N.; Jayramudu, J.; Suchismita, S.; Rajkumar, K.; Babulreddy, A.; Sadiku, E.R.; Priti, R.; Maurya, D.J. A. unique application of second order derivative FTIR-ATR spectra for compositional analyses of natural rubber and polychloroprene rubber and their blends. *Polym. Test.* **2017**, <https://doi.org/10.1016/j.polymertesting.2017.07.030>.
22. Aielo, P.; Azevedo Borges, F.; Romeira, K.; Romeiro, C.; Arruda, L.; Lisboa-Filho, P.; Drago, B.; Herculano, R. Evaluation of Sodium Diclofenac Release Using Natural Rubber Latex as Carrier. *Mater. Res.* **2014**, *17*, 146-152, <https://doi.org/10.1590/S1516-14392014005000010>.
23. Jarnthong, M.; Liao, L.-S.; Zhang, F.-Q.; Wang, Y.; Li, P.; Peng, Z.; Malawet, C.; Intharapat, P. Characterization of interaction between natural rubber and silica by FTIR. Proceedings of the 2nd International Conference on Composite Materials and Material Engineering (ICMME 2017), Chengdu, China, 17th to 19th February 2017, <http://dx.doi.org/10.1063/1.4983595>.
24. Jembere, A. Studies on the Synthesis of Silica Powder from Rice Husk Ash as Reinforcement Filler in Rubber Tire Tread Part: Replacement of Commercial Precipitated Silica. *Int. J. Mater. Sci. App.* **2017**, *6*, 37-44, <https://doi.org/10.11648/j.ijmsa.20170601.16>.
25. Rao, V.L.; Johns, J. Natural rubber latex/chitosan blends. *Int. J. Polym. Anal. Charact.* **2008**, *13*, 280-291.

6. ACKNOWLEDGEMENTS

The authors gratefully acknowledgement Suranaree University of Technology and Center of Excellence on Petrochemical and Materials Technology for their financial support.



© 2020 by the authors. This article is an open access article distributed under the terms and conditions of the Creative Commons Attribution (CC BY) license (<http://creativecommons.org/licenses/by/4.0/>).

BIOGRAPHY

Miss Preeyaporn Injorhor was born on August 1, 1990, in Nakhon Ratchasima Province, Thailand. She received her Bachelor's Degree in Science and Technology (Materials Science) from Thammasat University in 2013. After graduation, she has been worked as Quality Control staff at T. TARUTANI company. In 2014, she has been employed under the position of Quality Assurance Staff by Thainamthip Manufacturing Co., Ltd. She continued her Master's degree in Polymer Engineering at School of Polymer Engineering, Institute of Engineering, Suranaree University of Technology. During her master's degree study, she gave poster presentations and her research work was published on the topic of "Preparation of silica-chitosan hybrid fillers from agricultural waste by sol-gel technique" in the 2nd Materials Research Society of Thailand International Conference (MRS2019) in Chonburi, Thailand. This work was published in Suranaree Journal of Science and Technology (Suranaree J. Sci. Technol.) and the topic of "Effect of shrimp shell chitosan loading on antimicrobial, absorption and morphological properties of natural rubber composites reinforced with silica-chitosan hybrid filler" in the 2nd International Conference on Materials Engineering and Nanotechnology (ICMEN2019) in Kuala Lumpur, Malaysia. This work was published in Biointerface Research in Applied Chemistry (Biointerface Res. Appl. Chem.).